BIO-NANOPARTICLES AND BIO-MICROFIBERS FOR IMPROVED GENE TRANSFER INTO GLIOMA CELLS

YANG JINGYE

NATIONAL UNIVERSITY OF SINGAPORE

2009

BIO-NANOPARTICLES AND BIO-MICROFIBERS FOR IMPROVED GENE TRANSFER INTO GLIOMA CELLS

YANG JINGYE

(B. Eng.)

A THESIS SUBMITTED

FOR THE DEGREE OF DOCTOR OF PHILOSOPHY

NUS GRADUATE SCHOOL FOR INTEGRATIVE SCIENCES

AND ENGINEERING

NATIONAL UNIVERSITY OF SINGAPORE

December 2009

ACKNOWLEDGMENTS

I wish to express my sincere gratitude to Dr. Wang Shu, Associate Professor, Department of Biological Science, National University of Singapore; Group Leader, Institute of Bioengineering and Nanotechnology, who has been my supervisor since the beginning of my PhD study, for his continuous support, in-depth guidance, and constant encouragement throughout the entire course of this work.

I would like to acknowledge the outstanding research groups at the Department of Biological Sciences from National University of Singapore and Institute of Bioengineering and Nanotechnology for providing technical assistance and an inspiring and motivational research environment for my PhD studies.

I would like to specially acknowledge my colleagues: Dr. Song Haipeng, Dr. Seong Loong Lo, Dr. Zhao Ying, Dr. Emril Mohamed Ali, Dr. Andrew Wan, Dr. Zeng Jieming, Dr. Yang Jing, and Dr. Wu Chunxiao. They have all provided considerable assistance and helpful discussion during my research project. In addition, I appreciate the valuable advice and kind help offered by my lab mates: Harsh Joshi, Bak Xiao Ying, Lin Jia Kai, Dang Hoang Lam, Yukti Choudhury, Ram Roy, and Liu Fengxia, all of whom provided valuable suggestions that greatly improved the quality of this study.

I would also like to acknowledge NUS Graduate School for Integrative Sciences and Engineering for providing me a full scholarship and educational allowance over the four years of my PhD study. This research was possible because of the generous funding from Institute of Bioengineering and Nanotechnology, Agency for Science, Technology and Research (A*STAR), National Medical Research Council, Singapore (NMRC/119/2007), and Ministry of Education of Singapore (T206B3110).

Last but not least, this thesis is dedicated to my father, Yang Xianzhong, my mother, Weng Jian, and my wife, Yao Qianna, who constantly helped me to concentrate on completing this work and supported me mentally during the entire course of my PhD study. Without their help and encouragement, this study would not have been completed.

TABLE OF CONTENTS

SUMMARY

Developing effective therapeutic strategies for gliomas, a type of primary brain tumor, is one of the current focuses in cancer therapy. Gene therapy, while still at the stage of preclinical and clinical trials, has shown promise for therapeutic intervention of gliomas. To be effective, however, gene therapy requires gene transfer vehicles capable of efficiently transducing tumor cells. The research conducted for this thesis focused mainly on strategic development of gene transfer vectors with the objective of boosting gene delivery performance in glioma cells and potentially improving on current therapies for central nervous system (CNS) glioma tumors.

Non-viral magnetofection facilitates gene transfer by using a magnetic field to concentrate magnetic nanoparticle-associated plasmid delivery vectors onto target cells. In light of the well-established effects of the transactivating transcriptional activator (Tat) peptide, a cationic cell-penetrating peptide, in enhancing the cytoplasmic delivery of a variety of cargos, we tested whether the combined use of magnetofection and Tat-mediated intracellular delivery would improve transfection efficiency. Through electrostatic interaction, bio-nanoparticles were formed by mixing polyethyleneimine (PEI)-coated cationic magnetic iron beads with plasmid DNA, followed by the addition of a bis(cysteinyl) histidine-rich Tat peptide. These ternary magnetofection complexes provided a four-fold improvement in transgene expression over the binary complexes without the Tat peptide, and transfected up to 60% of cells *in vitro*. Enhanced transfection efficiency was also observed *in vivo* in the rat

spinal cord after lumbar intrathecal injection. Moreover, the injected ternary magnetofection complexes in the cerebrospinal fluid responded to a moving magnetic field by shifting away from the injection site and mediating transgene expression in a remote region. Thus, bio-nanoparticles could potentially be useful for effective gene therapy treatments of localized diseases.

Insect baculovirus (BV)-based vectors were recently introduced as potential viral gene delivery vectors to overcome obstacles inherent in commonly used animal viral systems. Upon *in vivo* administration, however, BVs are easily inactivated following exposure to serum complements. We hypothesized that the problems of serum inactivation could be avoided by assembling bio-nanoparticles through the interaction of PEI-coated cationic magnetic iron beads, Tat peptide, and therapeutic BVs, rather than plasmid DNA. Our preliminary *in vitro* studies indicate positive results.

More importantly, our studies show that BV particles can be encapsulated inside bio-microfibers, which may offer an innovative material engineering approach to protecting BVs against serum complement inactivation. We established the generation of fibers through self-assembly of polyelectrolytes comprising plasmid DNA and a set of specially designed amphiphilic peptides of alternating Leucine, Alanine, and Arginine residues. The positively charged Arginine peptide units can interface with plasmid DNA through electrostatic interactions. Additionally, the hydrophobic nature of Leucine and Alanine strengthens the connections between peptide molecules, thus facilitating fiber formation at high concentrations. Our findings suggest that BVs retain their

activity after emerging in the fiber, and the fibers provide a sustained release of the BV over a period of 48 hours by inducing sufficient transgene expressions in a glioma cell line. Of particular note is that BVs encapsulated inside the fiber have shown resistance to human serum complement both *in vitro* and *in vivo*, which indicates a promising opportunity to protect BVs against serum inactivation during systemic administration.

In summary, we have devised and implemented a strategy to use complexation procedures to form bio-nanoparticles and bio-microfibers. The findings in this study should enrich the development of gene therapies for CNS diseases, particularly in glioma tumors, and should advance virus, material engineering, and gene delivery-related studies.

LIST OF PUBLICATIONS

Publications

1. Yi Yang, Seong-Loong Lo, **Jingye Yang**, Jing Yang, Sally Goh, Chunxiao Wu, Si-Shen Feng, and Shu Wang. Polyethylenimine coating to produce serum-resistant baculoviral vectors for *in vivo* gene delivery. *Biomaterials.* 2009;30(29):5767–5774.
2. Hai Peng Song, **Jingye Yang**, Soong Loong Lo, Yi Wang, Weimin Fan, Xiaosheng Tang, Jun Min Xue, and Shu Wang. Gene transfer using self-assembled ternary complexes of cationic magnetic nanoparticles, plasmid DNA and cell-penetrating Tat peptide. *Biomaterials.* 2010;31(4):769–778.

Revisions

Xiao Ying Bak, **Jingye Yang**, and Shu Wang. Baculovirus-transduced bone marrow mesenchymal stem cells for systemic cancer therapy. *Human Gene Ther.* 2010.

Manuscripts

Jingye Yang, Harsh Joshi, Seong-Loong Lo, and Shu Wang. Encapsulation of BV with biocompatible polyelectrolyte fibers for improved resistance against serum complement inactivation. 2010.

The experiments in the above noted publications and manuscripts were performed during my PhD study. The major findings were presented in this thesis.

LIST OF FIGURES AND TABLES

Figure **Page**

Table **Page**

ABBREVIATIONS

AAV	adeno-associated virus
AcMNPV	*Autographa californica* multiple nucleopolyhedrovirus
BV	baculovirus
CAG	cytomegalovirus enhancer/chicken β-actin promoter
CMV	cytomegalovirus
CNS	central nervous system
DAF	decay-accelerating factor
DMEM	dulbecco’s modified eagle’s medium
EGFP	enhanced green fluorescent protein
FBS	fetal bovine serum
FESEM	field emission scanning electron microscopy
GCV	ganciclovir
HSV	herpes simplex virus
IPC	interfacial polyelectrolyte complexation
LDH	layered double hydroxides
Luc	luciferase
MOI	multiplicity of infection
PBS	phosphate buffered saline

PEI	polyethylenimine
PFU	plaque-forming units
RLU	relative light unit
SEM	scanning electron microscopy
Tat	transactivating transcriptional activator
TEM	transmission electron microscope
TK	thymidine kinase
VSV-G	vesicular stomatitis virus G

CHAPTER 1

INTRODUCTION

1.1 General Introduction

Gliomas are a type of primary central nervous system (CNS) tumor that arise from glial cells and have a tendency to aggressively invade the brain. Gliomas originate predominantly from astrocytes, and are graded from I to IV with increasing level of malignancy. Grade IV gliomas, also termed glioblastoma multiforme, comprise nearly half of all gliomas and are the most frequent primary brain tumors in adults. Even with complete surgical excision, radiation therapy, and chemotherapy, high-grade gliomas almost always grow back and patients usually die within a year, with only a few patients surviving longer than 3 years (Ohgaki *et al.*, 2004; Ohgaki and Kleihues, 2005). In this study, we proposed to adopt gene therapy with both viral and non-viral vectors and putative anti-tumor genes that have been used successfully for other cancers, along with various gene regulatory elements, to treat gliomas.

1.1.1 Introduction to Gene Therapy

Gene therapy is a disease treatment that involves the addition into an individual's cells of foreign genetic materials that reconstitute or correct missing or aberrant genetic functions or interfere with disease-causing processes. In the case of a hereditary disorder, the gene therapy will replace a defective mutant allele with a functional one (Factor, 2001). On September 14, 1990, the first approved gene therapy procedure was performed by Brandon Rogers at the U.S. National Institutes of Health on a 4-year old patient born with severe combined immunodeficiency, a rare genetic disease that made her extremely vulnerable to infections. White blood cells from the patient were collected and grown up in the lab. The missing gene was

inserted and the white blood cells were then infused back into the patient's bloodstream. The genetically modified cells functioned for a few months and then the process had to be repeated. Laboratory tests showed that the genetically modified blood cells strengthened the patient's immune system; she no longer suffers recurrent colds, she has been allowed to attend school, and she was immunized against whooping cough. Gene therapy is one of the most rapidly advancing fields in biotechnology, with hundreds of clinical trials underway worldwide (Verma and Somia, 1997). Accelerated by recent scientific breakthroughs in genomics and an understanding of the important role of genes in disease, gene therapy holds great promise for treating both inherited and acquired diseases.

Gene therapy involves three essential components: a therapeutic gene; a regulatory element, usually a promoter; and a delivery vehicle, also known as a vector (Russell, 1997). Therefore, three central issues have emerged as this technology advances: gene identification, gene expression, and gene delivery. The therapeutic gene is selected according to the target disease. Originally, the therapeutic gene was used as a substitute for the mutant gene. However, this replacement was complex and difficult in the disease-treating process. The therapeutic gene is now more commonly and practically used to alleviate diseases, either inherited or acquired, by enhancing, reducing, or altering a particular gene expression in the target cells (Mountain, 2000). Therapeutic genes must be controlled by a regulatory element, usually a promoter that is functionally active in the respective cell type. The expression level and specificity of the therapeutic gene is determined primarily by the activity of the

promoter at the transcriptional level, and the type of promoter can also influence the duration of transgene expression. The gene delivery vector, which carries and transfers the gene of interest into the nuclei of the host cell as part of its replication cycle, is another key player in gene therapy. The tropism of the vector can essentially decide the cell type specificity of the transgene expression at the transductional level, and the transduction efficiency of the vector will largely determine the expression level. More importantly, the status of the transferred gene—integrated or episomal—will decide the transient or long-term duration of the transgene expression. For glioma gene therapy, both the promoter and vector must be carefully selected, combined, and sometimes properly modified for the treatment of a particular condition.

1.1.2 Overview of Gene Delivery Vectors

Potential gene transfer vectors for mammalian cells are classified into physical, non-viral, and viral vectors. Physical delivery modalities, such as needle-free injection, which is often referred to as “gene gun” or “Jetgun,” make use of high-pressure power to deliver DNA. Electroporation, which transfers DNA to cells using an electric field to transiently break down the cell membrane, has been used for many years (Mathei *et al.*, 1997; Tacket *et al.*, 1999). However, due to their poor *in vivo* performance and low efficiency, physical vectors are not extensively employed for gene therapy applications and are rarely used for gene delivery to the CNS.

Non-viral and viral vectors are the most common gene delivery vehicles. Numerous studies have demonstrated the capability of non-viral materials such as cationic polymers, lipids, proteins, and peptides as vectors to mediate gene delivery (Lungwitz *et al.*, 2005; Martin *et al.*, 2005; Gupta *et al.*, 2005). The advantages of a non-viral system, including ease of manipulation, delivery flexibility, large transfer capacity, and low pathogenic risk, have made it an attractive research area. However, this system has the drawback of low transfection efficiency.

On the other hand, viral vectors can achieve high transduction efficiencies that seem unreachable for non-viral gene delivery systems. Six main types of viral vectors have been developed for CNS gene delivery purposes. (1) Herpes simplex virus (HSV) type 1, a common human pathogen carrying a double-stranded DNA of 152 kb, has a high infectivity in neurons, glial cells, and several other cell types. HSV type 1 can be delivered by rapid retrograde transport along neurites to the cell body (Bearer *et al.*, 1999; Sodeik *et al.*, 1997), offering a means of targeted gene transfer to neuronal cells that is otherwise difficult to reach. However, the cytotoxicity and short-term gene expression mediated by HSV type 1 has hampered its application for gene therapy of CNS disorders. (2) Adeno-associated virus (AAV) is a non-pathogenic small virus that contains a single-stranded DNA genome. AAV-based vectors can transfer a 4.5 kb transgene to host cells (Muzyczka, 1992), and inverted terminal repeat elements in the AAV genome can promote random or site-specific extra-chromosomal replication and genomic integration into the human chromosome (Balagúe *et al.*, 1997; Kotin *et al.*,

1990; Walther and Stein, 2000; Weitzman *et al.*, 1994; Yang *et al.*, 1997) of the transgene (Xiao *et al.*, 1997), providing an opportunity to achieve sustainable expression of foreign genes. The drawbacks of AAV as a gene delivery vector are its small packaging capacity and the inconvenience of large-scale preparation of viral stock (Rabinowtz and Samulski, 1998). (3) Adenovirus is another well-established gene delivery vector. Initially, the replication-defective adenovirus vectors had limitations for gene therapy because of a strong host immune response to the viral antigens (Dai *et al.*, 1995; Yang *et al.*, 1994). Recently, high-capacity “gutless” or “mini-chromosome” adenovirus vectors have been developed that retain only the sequences necessary for packaging and replication of the viral genome, but lack all structural genes (Fisher *et al.*, 1996; Hardy *et al.*, 1997; Kochanek *et al.*, 1996). These modified vectors have shown increased transgene cloning capacity and safer high-titer propagation methods by means of a Cre-lox-based recombinase system instead of helper adenovirus (Hardy *et al.*, 1997). *In vivo* studies have indicated prolonged expression of transgenes delivered by these vectors, with less host inflammatory response (Kumar-Singh and Farber, 1998; Lieber *et al.*, 1997; Morsy *et al.*, 1998). Despite the fact that new generations of adenoviruses have been created with decreased toxicity profiles in animals, the fatality report from an E1/E4-deleted adenovirus infused into the hepatic artery of a young man with partial ornithine transcarbamylase deficiency has become a severe obstacle in the application of adenoviruses for human gene therapy (Lusky *et al.*, 1998; Schiedner *et al.*, 1998; Raper *et al.*, 2003). (4) Retrovirus vectors, derived primarily from Moloney murine leukemia virus (Mulligan, 1993), are enveloped RNA viruses

that can transfer genes to a wide range of dividing cell types. Retrovirus vectors can mediate long-term gene expression by chromosomal integration and are well suited for on-site delivery to neural precursors for lineage studies (Cepko *et al.*, 2000), to tumor cells for therapeutic intervention, and for ex vivo gene transfer. The use of retrovirus vectors for gene delivery to the CNS, however, has been hampered by their ability to activate some pro-oncogenes by random insertion (VandenDriessche *et al.*, 2003). Moreover, their inability to infect non-dividing cells and the possibility of causing immunodeficiency has also restricted the application of retrovirus vectors for gene delivery to the CNS (Coffin *et al.*, 2000). (5) Lentivirus is a well-known member of the retrovirus family. Lentivirus-based vectors have the potential to integrate into the host genome of both dividing and non-dividing cells, establishing the possibility of developing a delivery system with stable expression even in postmitotic neurons (Naldini *et al.*, 1996). The limited host range, low titers, and pathogenic characteristics of the vector itself, however, hinder its utility as a gene delivery system for the CNS. (6) Baculovirus (BV) is a type of large, rod-shaped virus that belongs to the *Baculoviridae* family. Accumulated reports have demonstrated that a wide spectrum of cells and tissues are susceptible to BV infection, resulting in relatively high transgene expression levels and suggesting the strong potential of BV vectors in gene delivery, which will be used to establish proof of concept in the proposed study and reviewed in detail in the following section.

1.1.2.1 Polyethylenimine as a Powerful Non-viral Vector

Polyethylenimine (PEI), a type of cationic polymer and one of the most commonly used non-viral vectors, has demonstrated high transfection efficiency in both *in vitro* and *in vivo* gene transfer studies (Abdallah *et al.*, 1996a; Boussif *et al.*, 1995; Goula *et al.*, 1998). PEI can be linear or branched. The branched form is synthesized by cationic polymerization from aziridine monomers via a chain-growth mechanism. The linear form of PEI also originates from cationic polymerization, but from a 2-substituted 2-oxazoline monomer instead. The product is then hydrolyzed to yield linearized PEI (Godbey *et al.*, 1999). Because PEI polymers are able to effectively complex even large DNA molecules (Campeau *et al.*, 2001), they mediate transfection by condensing DNA into homogeneous spherical nanoparticles or PEI/DNA complexes of 100 nm or less. This protects DNA from enzymatic degradation and facilitates cell uptake and endolysosomal escape of the PEI/DNA complex, thereby enabling efficient cell transfection *in vitro* as well as *in vivo*. The branched form of PEI can achieve much higher cell transfection efficiency than does linear PEI, and has therefore attracted considerable attention for gene delivery to mammalian cells. The most frequently used gene delivery vehicle is highly branched PEI with the molecular weight of 25 kDa (Fischer *et al.*, 1999). Gene delivery into primary central and peripheral neurons has been successfully realized by antisense oligonucleotide shuffles conjugated to PEI (Lambert *et al.*, 1996). Moreover, the *in vivo* transfection capability of PEI was documented when gene expressions were detected in mature mouse brain by using PEI/DNA complex with PEI of different molecular weights (Abdallah *et al.*, 1996).

1.1.2.2 Baculovirus-mediated Gene Transfer

BVs constitute a group of double-stranded DNA viruses that cause lethal diseases in arthropods. A member of the BV family, *Autographa californica* multiple nucleopolyhedrovirus (AcMNPV)-based vectors were recently recognized as a type of promising viral gene delivery vectors. This AcMNPV BV is a large enveloped virus with a double-stranded, circular DNA genome of ~130 kb (Ayres *et al.*, 1994). The viral envelope protein GP64 interacts with cell surface molecules to facilitate BV uptake. Following receptor binding, the BV is transported into the cytoplasm via endolysosomal maturation and endosomal escape, after which the BV capsids are carried to the nuclear pore with the assistance of actin filaments. They are then transferred through the nuclear pore into the nuclear lumen to carry out the subsequent gene expression functionality (van Loo *et al.*, 2001). Studies have shown that recombinant vectors derived from this BV can efficiently transduce a variety of cell types, such as hepatic, pancreatic, kidney, and neural cells from different species including rodents, primates, and humans. High expression levels of the delivered genes were readily detected after successful transductions (Boyce and Bucher, 1996; Condreay *et al.*, 1999; Sarkis *et al.*, 2000). These observations revealed that recombinant BV could be a powerful vector with application for various types of gene therapies. BVs are non-replicative in mammalian cells, making the gene deliveries mediated by BV vectors controllable. The large DNA size of BV provides large cloning capacity. In addition, production and manipulation processes of recombinant BVs are scalable, allowing for large-scale preparation of the vectors (Ghosh *et al.*,

2002; Kost and Condreay, 2002). Furthermore, the lack of obvious pathogenicity and the inability to express any viral gene in mammalian cells make BV the safest viral vector for humans. These intrinsic advantages highlight BV vectors as a very enabling technology for various gene delivery applications.

Despite encouraging transduction performance achieved by BV vectors, certain problems remain. Recombinant BV performance in gene deliveries is promoter dependent to a large extent. Highly active promoters are necessary to ensure the transgene expressions of recombinant BV vectors engineered to deliver genes of interest to mammalian cells and tissues. Strong promoters derived from infective viruses, such as cytomegalovirus (CMV), simian virus, and CMV enhancer/chicken β-actin promoter (CAG), have been commonly used. As a result of the relative uncontrollability of such strong promoters, a wide range of cells and tissues will be affected when subjected to such recombinant BV transduction. Furthermore, the application of BV in clinical gene therapy could be obstructed by unspecific side effects, including possible immune responses and complement attack. Hence, engineered recombinant BV vectors equipped with suitable targeting apparatus are highly desired to realize the specific delivery and expression of the transgene in target cells, while minimizing unspecific transgene expression.

Another major disadvantage of BV as a gene delivery vector is its poor *in vivo* delivery performance in the CNS, which is considered an immune privileged site (Ghosh *et al.*, 2002; Lehtolainen *et al.*, 2002; Li *et al.*, 2004; Merrihew *et*

al., 2004; Kost and Condreay, 2002; Li *et al.*, 2005; Sandig *et al.*, 1996) due to the vulnerability of BV in the presence of serum factors (Hofmann *et al.*, 1998; Hofmann *et al.*, 1999). The susceptibility of BV to inactivation by complement exposure possibly resulted from the fact that BV, derived from insects, was not subjected to the human complement system during evolution. As a result, BV did not evolve a defensive mechanism to tolerate an attack from the human complement system (Hofmann *et al.*, 1999; Kost and Condreay, 2002; Sandig *et al.*, 1996; Hofmann *et al.*, 1998). Virus particle surface modification is one of the effective strategies to enhance BV's *in vivo* gene delivery performance. Previous reports show that the surface display method can be used to improve BV resistance to serum complement inactivation (Hüser *et al.*, 2001). However, complicated cloning work is required for such biological modifications. In addition, BV production yield is restricted by adding foreign protein sequences on the surface, making it extremely difficult to obtain BV solutions with titers high enough for *in vivo* study. Effective and flexible modification approaches are still required to overcome the problem of serum complement inactivation.

A main limitation of BV-mediated transgene expression is its short expression period, which is particularly unsuitable for gene therapy of CNS glioma (Kost and Condreay, 2002). Raymond performed the first detailed analysis of BV integrants within mammalian cells, highlighting the importance of considering long-term transgene stability, especially for studies designed to correct genetic defects *in vivo* (Merrihew *et al.*, 2001). Studies using periodic assays over a 5-month period showed no loss of green fluorescent protein (GFP)

expression for at least two of the clones. These results strengthened the potential application of BV to deliver single copies of stably integrated genes into mammalian genomes. Since the illegitimate mode of integration and long-term stability of reporter gene expression is similar to that observed for transfected DNA and other viruses, recombinant BVs should provide a superior alternative for DNA transfer into mammalian cells. Indeed, in recent studies with several different cell lines, stable clones have already been obtained from any cell line that is successfully transduced transiently, independent of the transduction efficiency.

Another concern is that preparing large volumes of high-titer vectors is time-consuming and laborious. Producing BV particles is relatively simple in comparison with other types of viral vectors, such as lentivirus, which requires co-transfection of a set of plasmids for each batch of virus production, or AAV, which requires a complicated process for purification. Nevertheless, the large-scale production of high-quality BV particles is necessary when they are used as gene delivery vectors, especially for *in vivo* application. Hence, feasible purification and concentration methods need to be established to facilitate large-scale preparation of BV particles, while minimizing the detrimental effect on virus bioactivity.

Little is known about the transduction mechanisms of BVs in mammalian cells. Several investigators have demonstrated the pathways of BV entry and transduction with different mammalian cell lines, yet the studies show conflicting data, implying that the mechanism for virus–cell interactions may

vary for different cell types. It is generally assumed that the escape from the endosomes blocks the BV transduction of some mammalian cells. However, the detailed mechanisms of intracellular movement and nuclear entry of the virus are still largely unknown. Moreover, to devise and optimize experimental treatment strategies, researchers need a method to non-invasively assess BV delivery to the target cells or tissues of interest using experimentally and clinically relevant imaging methodologies. At present, reports of *in vivo* imaging of BV in target tissues are limited to bioluminescence imaging. BV capsid display, which fuses enhanced GFP (EGFP) into the N-terminus or C-terminus of the major capsid protein vp39, offers a useful tool for transduction imaging. Yet tiring cloning work is still required for such applications. Therefore, it is imperative to develop a novel transduction imaging technology that efficiently reveals the transduction route of BV in mammalian cells to allow researchers to follow or even modify the intracellular fate of BV and also monitor BV-mediated gene delivery in a relevant clinical context.

1.1.2.3 Nanoparticle-mediated Gene Delivery

Drug and gene delivery have traditionally been achieved through oral or intravenous routes, both of which are inefficient, non-specific, and expensive. Innovative gene delivery approaches have recently been inspired by new findings in the field of nanotechnology. Non-viral gene delivery vectors have drawn increasingly more attention due to their ability to overcome the safety issues of their viral counterparts. Nanoparticles are one of the most well studied non-viral gene delivery vectors because of their attractive characteristics, including small particle size, large surface area, and the ability

to change their surface properties. Nanoparticles offer numerous advantages to promote gene transfection efficiency compared with other gene delivery systems. Gold, carbon nanotubes, fullerenes, layered double hydroxides (LDH), biodegradable nanoparticles made from biocompatible polymers such as poly(D,L-lactide-co-glycolide) (PLGA) or polylactide (PLA), and several oxide nanoparticles have all been used to facilitate cellular delivery of therapeutic genes. Nanoparticles enable much greater control over the delivery process, targeting to specific tissues or even some specific cell types with higher stability and delivery efficiency. This merit allows for lower gene or drug dosing to avoid cytotoxicity. Moreover, nanoparticles can be fabricated in large quantities at lower cost. Nanoparticles composed of natural polymers are desired over synthetic ones because of their greater biocompatibility and biodegradability.

Nanoparticles offer significant promise as efficient non-viral gene delivery vectors. In one study, functionalized nanoparticles of calcium phosphate were synthesized by controlled precipitation from aqueous solution followed by DNA coating and transfecting human endothelial cells. The results showed that nanoparticles are capable of transferring DNA into the nucleus of transformed human endothelial cells (T. Welzel *et al.*, 2004). Another study demonstrated that modified gold nanoparticles with thiolated oligonucleotides can be used as effective non-viral DNA delivery vectors (Jen *et al.*, 2004). Internalization of LDH nanoparticles into cells has also been reported, and great progress has been made in developing LDH nanoparticles as efficient cellular delivery vectors for both *in vitro* and *in vivo* applications (Ladewig *et*

al., 2009). In most cases, nanoparticle-mediated gene delivery offers rapid transfection and, as indicated by more recent work, excellent overall transfection levels. Attaching the gene of interest to nanoparticles may improve both uptake by cells and the escape of the particles from lysosomes, which typically degrade gene carriers and prevent them from delivering their DNA payload to the cell nucleus, the target site for gene therapy.

1.1.3 Introduction to Self-assembled Polyelectrolyte Microfibers

1.1.3.1 Mechanism of Microfiber Formation

To understand the principles of this work, it is crucial to explain in detail the self-assembly approach, defined as an integration process in which the components assemble in a spontaneous manner, usually by bouncing around in a solution or gas phase until a steady architecture of minimum energy is reached. Self-assembly is one of the most important methods for the assembly of biological molecules, and is thus a promising method for integrating and precisely engineering macromolecules such as proteins and nuclear DNA as well as biological particles such as viruses. In nature, one the most fundamental examples of biomolecular self-assembly occurs when two single strands of DNA assemble into the infamous double helix, where base pairing allows the specific assembly of the double helix to be stabilized by relatively strong hydrophobic interactions between the aromatic bases within the center of the helix. Components in self-assembled structures are automatically located to their specific sites based only on their structural properties, physical properties, or chemical properties, in the case of atomic or molecular self-assembly. Self-assembly is by no means restricted to

nanoscale molecules and can be achieved on almost any scale, where the powerful bottom-up approach is frequently used to construct macro and nano structures of biological functions from molecular building blocks (Tu and Tirrell, 2004; Zhang, 2003). Self-assembled macromolecules use proteins and nuclear DNA as their building blocks. The advantage of the bottom-up design is that the interactions holding together a single component—such as covalent bonds, van der Waals forces, and electrostatic interactions—are far stronger than the weak interactions that hold more than one molecule together.

One promising approach to forming self-assembled structures is to attach single-stranded DNA encoding biological information to the small particles that one wishes to assemble. These components could range from diamondoid manifolds to metallic clusters that function as quantum dots. DNA stores genetic information, but is not known to play any structural roles and is therefore unlikely to interfere with the final structure. However, the precise base-pairing of nucleic acids offers the possibility of programmable self-assembly in two and three dimensions. In addition, DNA can be coupled to other materials to allow controllable and thermally reversible assembly over a range of length scales (Payne, 2007). Upon receiving an external stimulus, these self-assembly systems will spontaneously bring together biomimetic arrangement with biological functionalities and organized structural properties. It is a challenging task, however, to design small particles or molecules that hold together biologically meaningful components without losing their biological functions. The ultimate objective is to associate components of different natures, such as organic and mineral, or synthetic and biological.

Clearly, success with this approach would have huge impacts on applications in material science, nanotechnology, and bioengineering.

Amphiphilic peptides comprising alternating hydrophobic and hydrophilic blocks are another commonly used raw material to form self-assembly structures. Alanine and Leucine amino acids are often recruited as hydrophobic domains, while Lysine and Arginine are regularly used as the hydrophilic counterparts. Depending on the alignment of these building blocks in the sequence and also the surfactant number, various self-assembled formations can be realized (Hartgerink *et al.*, 2002; Fairman and Åkerfeldt, 2005), such as micelles (Yim *et al.*, 2006), nano and microfilaments (Papapostolou *et al.*, 2007), and hydrogels (van den Beucken *et al.*, 2006).

There are certain forces responsible for the self-assembly formation and stability of biomolecules: hydrophobic interaction, electrostatic attraction and hydrogen bonding, specific protein-ligand interactions, and other non-bonding interactions. Hydrophobic interaction is caused by the tendency of hydrocarbons (or of lipophilic hydrocarbon-like groups in solutes) to shape intermolecular aggregates in an aqueous solution, and analogous intramolecular interactions. Amphiphilic molecules composed of both hydrophilic and hydrophobic subunits have been extensively exploited in a variety of self-assembled formations. Hydrophobic interaction leads to a facilitation of surfactant self-assembly that could cause, for example, a decrease of the critical micelle concentration. In this case it would be more appropriate to use a mixed micelle formation, since the polymer itself is able

to self-associate. The main driving force behind hydrophobic interactions is phase separation phenomena that contribute to the apparent repulsion between water and hydrocarbons. Hydrophobic interactions are often used for the assembly of supramolecules. For example, the natural concavity of cyclodextrins and cyclophanes can be employed to build inclusion complexes. In fact, the hydrophobic nature of their inner cavities can segregate apolar foreign molecules from the surrounding aqueous medium.

Electrostatic attraction is the attraction that holds two oppositely electrical-charged bodies together. Back in the 1990s, it had been conjectured that electrostatic interactions could act as an important basis for innovative self-assembly mechanisms. Electrostatic self-assembly can be manipulated, but requires two elements for this formation to work. The first element is a pair of oppositely charged colloids or macromolecules. It is possible to create a polymeric chain that carries electrostatic charges along its backbone. These chains—or polyelectrolytes—exhibit high solubility in water. Another characteristic is their strong adsorbing capacity on surfaces bearing an opposite charge. The second element of the pair is an oppositely charged nanometer-sized colloid. For example, Harada and Kataoka used a small and bulky protein, the chicken egg white lysozyme (diameter 5 nm), and Bronich used a surfactant micelle (Harada and Kataoka, 1998; Bronich *et al.*, 1997). The self-assembly process by electrostatic interaction simply requires soaking a selected substrate in alternate aqueous solutions containing anionic and cationic materials, such as complexes of polymers, metal and oxide nanoclusters, cage-structured molecules such as fullerenes, and proteins and

other biomolecules. Patterning these individual precursor molecules and controlling the order of the multiple molecular layers through the thickness of the film or fibers allows for manipulation of the macroscopic electrical, optical, magnetic, thermal, mechanical, and other properties relevant to many engineering and medical applications. The fundamental principle of electrostatic interactions is simple: two oppositely charged particles, suspended in a fluid, will be attracted to each other. It is often most convenient to generate charged microstructures using self-assembled monolayers (Krupp *et al.*, 1967; Maboudian and Howe, 1997). Electrostatic interactions have a longer range than hydrophobic or hydrogen-bonding interactions, and assemblies formed electrostatically can theoretically form by attraction of particles over substantial distances.

A hydrogen bond is defined as the appealing force between one electronegative atom and a hydrogen atom covalently connected to another electronegative atom. The connection is caused by a dipole-dipole force with a hydrogen atom bonded to nitrogen, oxygen, or fluorine. Hydrogen bonding also plays an important role in controlling the ternary structures adopted by proteins and nucleic acid where hydrogen bonding between parts of the same macromolecule causes it to fold into a specific shape, which serves to determine the molecule's physiological or biochemical functions. DNA-inspired hydrogen-bond self-assembly has been used to create supramolecular cages, helical, linear, and macrocyclic structures. It has been reported that the synthesis of new DNA-based artificial nucleosides, and their self-assembly into the first example of a DNA-analogue hexameric rosette,

can provide the basis to potentially expand the molecularity of DNA to a hexaplex (Rakotondradany *et al.*, 2005). However, hydrogen-bonding-associated self-assembly is usually difficult to quantify since it is based on the chemical ingredients and angle of the atoms involved.

1.1.3.2 Applications of Self-assembled Polyelectrolyte Microfiber

One of the cornerstones of this study is the formation of self-assembled microfiber driven by the interface self-assembly phenomenon of polyelectrolytes. In this study, we attempted to use both general mechanisms and specific effects. With regard to the general interfacial behavior, it is important to note the charge regulation of both polyelectrolyte complexes; the interplay between the two charge-modulating effects is the key to understanding the rationale of our observations. Oppositely charged polyelectrolytes could interact with each other to organize into multilayer architectures by sequential layering, which has been widely studied for application in drug delivery vectors and coatings. These arrangements can be formed at micro and nanoscale to assemble into ordered materials such as polyionic films and fibers. Polyelectrolyte multilayer assemblies have promising application potential as antireflection coatings, light-emitting diodes, and microcapsules.

Interfacial fibers formed via interface assembly have also been explored, though not as extensively. Three types of biostructural units have been successfully assembled using the process of fiber formation by interfacial polyelectrolyte complexation (IPC): protein-encapsulated fiber, ligand-

immobilized fiber, and cell-encapsulated fiber units (Wan *et al.*, 2004b). Indeed, previous research on fiber formation between synthetic polymers (Morgan *et al.*, 1959), and between chitosan and alginate fibers (Liao *et al.*, 2005) has confirmed the feasibility of such interfacial self-assembly systems. This approach offers the advantage of controlling the drug or gene concentration by varying the ratio of modified to non-modified polyelectrolyte used for fiber fabrication. Even fragile and highly resorbable fibers can be created, while their poor physical properties would preclude “post-fiber” modification. Fibers are produced in aqueous-based conditions that enable the inclusion of various biomolecules in the design. The usefulness of this approach has also been demonstrated by the flexibility of fiber formation. Polyelectrolyte fibers are fabricated at room temperature and do not require the denaturing of solvents needed for conventional fiber fabrication methods, making it simple to form scaffolds for tissue engineering and other medical applications.

The fibers are fabricated by placing two droplets of oppositely charged solutions in close proximity and bringing them in contact using a needle or sharp tweezers. Fibers are formed from the interface of the two solutions until either one of the polyelectrolyte phases is exhausted. This process is compelled by the formation of a polyelectrolyte complexation as a result of electrostatic interplay at the interface. Various research groups have used this process to produce IPC fibers and have demonstrated the use of the fibers as biostructural units for tissue engineering, with the possibility of encapsulating

proteins, drug molecules, DNA, and cells to provide local and sustained delivery of therapeutic agents.

Wan and colleagues have hypothesized the mechanism for the formation of polyelectrolyte fibers (Wan *et al.*, 2004a). According to their theory, a four-step process leads to fiber formation by IPC.

1) Formation of a polyionic complex film

The two components in IPC are dissolved in water solutions. Fibers are drawn from the interface of the two aqueous solutions. Free mixing of oppositely charged polyelectrolytes must be avoided to maintain an interfacial phenomenon. A polyelectrolyte complex film forms at the interface, which functions as a viscous barrier to limit exchange of the polyelectrolytes.

2) Nucleation

Upon drawing up, the interface falls apart into many individual, complexed fields acting as nucleation sites for added fiber formation. The continuous upward movement of fiber causes these complexation points to promote further nucleation.

3) Growth of nuclear fibers

The viscosity of the free extra component outside the fibers decreases as a result of the increased size of nuclear fibers, due to the continuous drawing up. Therefore, the upward drawing motion contributes to the consecutive complexation of the two oppositely charged materials at the interface.

4) Coalescence of nuclear fibers

Finally, the fibers produced from nucleation coalesce and the leftover polyelectrolytes consolidate into gel droplets along the fiber axis. The characteristic morphology of the fibers resulting from this coalescence produces a primary fiber comprising a number of secondary nuclear fibers wrapped together and scattered with gel-like beads.

The fiber formed through the IPC process can be used to encapsulate materials at surrounding temperatures and under aqueous conditions, an attribute that is especially useful for the encapsulation of biologics such as DNA and viruses. The mode of IPC fiber formation by progressing thin fiber nucleation empowers the fiber to go “around” the particles’ fiber, which enlarges both the cross section and the mechanical strength of the fiber encapsulations. IPC fiber has been proposed as a building block and biological construct unit to create scaffolds or structures via a bottom-up approach for tissue engineering applications due to its novel feature of incorporating proteins, drug molecules, DNA nanoparticles, viruses, and cells. The assembly of biostructural units into the fiber constructs has been achieved by using human mesenchymal stem cell-encapsulated fiber units (Wan *et al.*, 2004b). Cells in the resulting assembly could be successfully stimulated to differentiate along chondrogenic and osteogenic lineages, suggesting the active biological functions of such fibers. The encapsulating capability of this type of fiber has drawn increasing attention and this technique is expected to be used extensively in the future, not only because

of the uniqueness of the fiber formation phenomenon, but also for its potential application for therapeutic tissue engineering.

1.2 Objectives of This Study

In this study, we intended to develop strategies to fabricate novel bio-nanoparticles by conjugating functional polymer-coated magnetic nanoparticles with plasmid DNA and coupling the binary complex with biological active peptide through simple but stable electrostatic interactions with the purpose of enhancing the transfection efficiency. In terms of BV vectors, we established bio-nanoparticles by coating BV particles with magnetic nanoparticles that can be used to facilitate magnetically guided transduction to the surface of the cells. Moreover, we intended to engineer a process to assemble innovative bio-microfibers through the self-assembling behavior of macromolecules, including amphipathic and functional peptides with plasmid DNA and BV in order to protect BV vector from being inactivated by serum complement proteins.

Non-viral magnetofection facilitates gene transfer by using a magnetic field to concentrate magnetic nanoparticle-associated plasmid delivery vectors onto target cells. In light of the well-established effects of the transactivating transcriptional activator (Tat) peptide, a cationic cell-penetrating peptide, in enhancing the cytoplasmic delivery of a variety of cargos, we proposed to test whether the combined use of magnetofection and Tat-mediated intracellular delivery improves transfection efficiency. We expected the plasmid DNA-based bio-nanoparticles to enhance gene transfer efficiency both *in vitro* and

in vivo under the control of polymer-coated magnetic nanoparticles with the assistance of a functional peptide. We planned to apply the same approach to BV vectors to investigate the synergistic effect of magnetofection and Tat peptide on viral vector-mediated gene transfer.

On another note, this study also addressed the subject of gene delivery through a structural route. We attempted to explore the self-assembling phenomenon of three biological molecules: plasmid DNA, BV, and a set of short peptides. Polyelectrolyte fibers composed of these molecules have been characterized extensively. There is evidence that virus particles are uniformly incorporated in the fiber structure itself upon successful encapsulation. These fibers, rich in amphipathic peptide residues, cover virus particles and mediate a sustained release when they dissolve in cell culture conditions, inducing transgene expression comparable with that of naked BV. Our primary goal was to ensure that BV retained almost complete transductional activity after encapsulation. Preliminary evidence also suggests that fiber encapsulation may prevent straightforward exposure of the virus to serum complement and thus protect it from inactivation by the complement components, which is a main barrier blocking the effective *in vivo* application of BV-mediated gene delivery. This evidence illustrates the advantage of using fiber encapsulation to deliver BV to mammalian cells both *in vitro* and *in vivo*.

BV-based bio-nanoparticle and bio-microfiber vectors are expected to show better resistance to complement inactivation and therefore their potential applications for *in vivo* gene delivery would be greatly broadened. These

modular approaches could also offer new possibilities for further advancement of plasmid and BV-based vectors, in terms of improved gene expression efficiency, passive tumor targeting, augmentation of biosafety profiles, prolonged gene expression duration, immune response shielding, and the introduction of new cellular targeting moieties, all of which are essential to strengthen BV particles and improve their performance at the transductional level. Modified BV complex vectors should replicate the advantages and circumvent the disadvantages of both non-viral and viral gene delivery systems, thereby offering improved gene delivery. In addition, the magnetic nanoparticle has led to the introduction of therapeutic BV, not just into the patient's body, but to reach specific target sites.

In this study, we concentrated on investigating the gene delivery performance in tumors originated from CNS with a particular focus on glioma cells, with the objective of providing useful gene delivery vector systems for the potential treatment of glioma tumors in the CNS. Luciferase and EGFP reporter genes were used to evaluate transgene expression profiles in human-glioma-derived cell lines. In addition, different gene delivery systems were used to deliver therapeutic genes to specific target cells in experimental animal models. We hoped to temporally and spatially regulate their expression patterns given the proper regulatory elements, to test the potential application of these systems to treat neurological diseases in the CNS.

Our objective with this research was to establish an innovative bioengineering approach to overcome the major obstacles to the systemic delivery of plasmid

DNA and BV vectors. We hoped the platform technology generated in the project will be valuable in establishing effective and safe gene therapy vectors. Significant economic benefits may also emerge from the opportunity to develop advanced gene delivery vectors that can be potentially patented and commercialized. The project may further contribute to enhanced quality of life by improving the efficacy of gene therapy for CNS tumors.

1.2.1 Specific Goals

To establish appropriate delivery systems for gene therapy of neurological diseases in the CNS, vectors should be carefully selected and properly modified. One of the basic hypotheses underlying this study was that functional polymer-coated magnetic nanoparticles can interact with therapeutic plasmid DNA or BV vectors coupled with bio-active peptide to form bio-nanoparticle complexes, and the assembled bio-nanoparticles can potentially be applied for gene therapy of glioma tumors. Another fundamental assumption of this study was that polyelectrolyte fibers assembled through the interaction between positively charged amphipathic peptides and negatively charged plasmid DNA can be used to encapsulate BV to form bio-microfibers, and that the resulting complex vectors can achieve sustained release of BV, retaining transduction efficiency while offering improved therapeutic efficacy in the presence of serum complement proteins.

These hypotheses were based on the following observations. First, the insect BV AcMNPV is a promising and established viral gene delivery vector (Boyce and Bucher, 1996; Condreay *et al.*, 1999; Sarkis *et al.*, 2000) and was used

as reference in the study. Second, when employed in systemic administration, these viruses are easily inactivated after exposure to serum complements (Hofmann *et al.*, 1998; Hofmann *et al.*, 1999). Thus, our bio-nanoparticle and bio-microfiber design might protect the viruses against serum inactivation. Third, cationic polymers such as PEI can condense DNA into nanoparticles by electrostatic interaction, make it susceptible to degradation, and enhance cellular uptake via endocytosis. Although *in vitro* transduction with cationic polymers is efficient, *in vivo* results have not been encouraging, probably due to the large size formation of DNA condensed with cationic polymers, which is inefficient for cellular uptake by most cell solid tissues (Davis, 2002). Fourth, magnetic nanoparticle-aided gene delivery shows promise, based on the physical principle of magnetic separation and the ability to pull the employed gene expression vector toward the target cells or tissues, thereby accomplishing enhanced transfection level (Xenariou *et al.*, 2006). Fifth, it has been well-established that the Tat peptide can be used to greatly enhance the cytoplasmic delivery of a variety of cargos, which could be used to improve the transduction efficiency of non-viral gene delivery vectors. Sixth, amphiphilic peptides have been established as versatile building blocks for self-assembled arrangements, while interfacial interactions of polyelectrolyte solutions, such as peptides, and polyelectrolyte fibers are an effective structure to drive self-assembly for biological applications.

The main investigations of this study can be categorized into three parts:

1. Studying the Possibility of Coupling Magnetic Nanoparticle-conjugated DNA with Tat Peptide for Improved Gene Cellular Delivery

Peptides derived from the Arginine-rich basic domain of the HIV Tat have recently been introduced to massively increase the efficiency of gene cellular delivery. However, no study to date has valued the potential application of this approach on DNA-shuffled gene transfer. In this study, cationic polymer (PEI 25 kDa)-coated superparamagnetic nanoparticles were used as carriers for DNA, which can magnetically guide transduction *in vitro* and *in vivo* for the purpose of further increasing cell uptake of the gene transfer vector, and thus the transduction efficiency.

A. Synthesis and Characterization of Tat Peptide-coupled Bio-nanoparticles

This study introduced both histidine and cysteine residues to the Tat peptide to facilitate the escape of gene vectors from endosome, with the objective of achieving higher efficiency of the magnetically guided transduction. We associated the modified Tat peptide to the DNA and magnetic particle complex and examined the enhancing effect of Tat on the transfection capability of bio-nanoparticles.

B. Gene Transfer Performance of Tat-associated Magnetic Nanoparticle Complexes

The gene transfer performance of the bio-nanoparticle complex was assessed in terms of transduction efficiency to appraise the influence of Tat on the DNA, both *in vitro* and *in vivo*. We also investigated the magnetically guided transduction achieved by the magnetic particles upon application of an external magnetic field.

2. Exploring the Protective Effects of Functional Polymer PEI-coated Magnetic Nanoparticles Against Viral Inactivation Triggered by Serum Complement by Forming Bio-nanoparticles

Complement inactivation is a major obstacle affecting the gene transfer efficiency of BV *in vitro* in serum-containing medium conditions, and *in vivo* during systemic administration.

A. Fabrication of Bio-nanoparticles

In these studies, we presented a new method to generate bio-nanoparticles with PEI-coated magnetic nanoparticles comprising BV vectors carrying a reporter gene. Through simple and stable electrostatic interactions, we incorporated PEI or magnetic nanoparticles to the surface of a BV vector on the basis that BVs are negatively charged on the surface and can interact with the positively charged PEI or PEI-coated magnetic nanoparticles.

B. Characterization of Assembled Bio-nanoparticles

Surface charge and particle size measurements were carried out to characterize the charge and dimensional properties of the bio-nanoparticles to evaluate the strength and mechanism of interaction between BV and PEI or magnetic nanoparticles, respectively. The knowledge obtained from this study should establish the basis for subsequent optimization and assembly conditions.

C. Assessment of *In Vitro* and *In Vivo* Gene Delivery Performance

This study focused on the effects on gene transfer efficiency, mainly reporter gene expression levels, in cultured glioma cells and other tumor cell lines in the presence of serum, shortly after viral transduction. Similarly, in animals this could be assessed after intracranial and intravenous injection to characterize the transductional activities of PEI or magnetic nanoparticle-modified BV vectors.

D. Investigation of Magnetically Guided Transduction

These studies evaluated the effect of magnetic force on the transduction efficiency of bio-nanoparticles upon the application of an external magnetic field.

3. Investigating the Potential of Using Fiber to Protect BV against Serum Complement Inactivation

To address the obstacles associated with BV-mediated gene delivery from a materials engineering point of view, a new type of composite vector was

formed that incorporated the merits of existing non-viral and viral vectors while abolishing the deficiencies of both vector types. The underlying theme of this study is the interaction between positively charged polyelectrolyte, composed of functional peptides, and negatively charged polyelectrolyte solution, including plasmid DNA and BV. We attempted to use the polyelectrolyte complexation through interfacial phenomenon to create microfibers comprising peptides, DNA, and BV.

A. Assembly of Bio-microfibers

In this study, we tried to optimize the protocols and conditions for fiber formation between DNA and a set of peptides. Two types of peptides were used: Tat and Tat-derived peptides, and amphipathic peptides and a functionalized amphipathic peptide. Later, BV solution was combined with plasmid DNA solution to constitute the negatively charged polyelectrolyte for fiber formation.

B. Characterization of Bio-microfibers

Surface charge measurements were performed to characterize the charge properties of the bio-microfiber to evaluate the mode of interaction among peptide, plasmid DNA, and BV as well as the mechanism of the protective effect on BV against serum inactivation. Fluorescence labeling, confocal imaging, scanning electron microscopy (SEM), and light microscope imaging were performed to visualize the structural properties of the bio-microfibers.

C. Appraisal of Gene Delivery Performance

BV-encapsulating fibers were used to perform transduction experiments in glioma cell lines in the presence of human serum complement to evaluate the transductional capability and protective ability of the bio-microfiber. Experimental animal models, where gene delivery vectors were exposed to high-concentration serum complement, were employed to investigate the therapeutic effect of the hybrid gene transfer vector.

CHAPTER 2

PRODUCTION, CHARACTERIZATION, AND EVALUATION OF BIO-NANOPARTICLES

2.1 Introduction

2.1.1 Magnetofection: Magnetically Guided Nucleic Acid Delivery

Magnetofection is a gene delivery method that uses an externally applied magnetic field to direct the accumulation of magnetic nanoparticle-modified gene transfer vectors in targeted cells and regions (Scherer *et al.*, 2002; Dobson, 2006; Plank *et al.*, 2003; McBain *et al.*, 2008; Mykhaylyk *et al.*, 2007). For example, PolyMag, a commercially available magnetofection vector, is produced by the conjugation of magnetic iron oxide nanobeads with positively charged, 25 kDa branched PEI. The PEI polymers are capable of binding to negatively charged plasmid DNA, enabling the whole complex to respond to an applied magnetic force. Magnetofection speeds up the sedimentation of gene transfer vectors to the cell surface and often shortens the time span of gene delivery to minutes of incubation, as opposed to the hours required for standard *in vitro* gene transfer procedures. Magnetofection also allows for the use of lower doses of vectors to deliver transgenic expression at a functional level, thus minimizing the toxic risk caused by high concentrations of gene delivery vectors. In addition to improving gene delivery into cultured cells, this method can be used to control *in vivo* gene delivery in the body to achieve magnetic field guided organ targeting. However, magnetofection facilitates only the diffusion process of vectors. Once the vector reaches the cell, overcoming membrane barriers—including the plasma membrane, endosomal membrane, and nuclear envelope—may still pose a challenge. For non-viral magnetofection to deliver plasmid nanoparticles, active functions that can overcome these membrane barriers are particularly important to promote plasmid entry into the cell nucleus for gene expression.

2.1.2 Tat Peptide-based Gene Delivery

Tat is a highly cationic peptide derived from HIV-1 Tat protein, with a linear sequence of 13 amino acids (Brooks *et al.*, 2005; Berry, 2008). This specific sequence carries a transmembrane and a nuclear localization signal. The membrane absorption is primarily promoted by ionic interaction between the cationic charge of the Tat peptide and anionic charge of the phospholipid heads in biomembranes. Benefiting from its cell membrane-penetrating properties, the Tat peptide is capable of mediating intracellular delivery of many different types of cargos (Brooks *et al.*, 2005; Berry, 2008), including magnetic nanoparticles (Lewin *et al.*, 2000).

We developed an endosomolytic Tat peptide-based gene delivery vector by fusing the peptide with histidine residues (Lo and Wang, 2008). The imidazole group of histidine has a pKa of ~6.0 and can thus absorb protons in the acidic environment of the endosomes (pH 5–6.5), leading to osmotic swelling, membrane disruption, and eventually DNA escape. We also included two cysteine residues that contain the thiol group at both ends of the peptide. The cysteine amino acids can then interact with the cysteine residues of other peptides to form interpeptide disulfide bonds that stabilize peptide–DNA complexes. As covalent disulfide bonds are broken down, mainly under reducing conditions, plasmid DNA held within the complexes will not be released until it is introduced into the reducing environment of the endosomes, thus effectively protecting the DNA in the extracellular environment. Polymerization of the peptide through interpeptide disulfide bond formation

may also enhance the association of the small Tat peptides with DNA complexes.

2.1.3 Objectives

In this study, we hypothesized that the combination of magnetic field enhanced cell surface accumulation of magnetofection vectors and Tat peptide-mediated effective transmembrane function would provide an opportunity for high-efficiency gene transfer. To test this hypothesis, we generated ternary complex of PolyMag, plasmid DNA, and the endosomolytic Tat peptide through electrostatic interaction and examined its gene transfection efficiency in cultured human and mouse cells and in the spinal cord of rats. We also explored the protective effects of PolyMag on BV against the viral inactivation triggered by serum complement by forming bio-nanoparticles, given that complement inactivation is a major obstacle affecting the gene transfer efficiency of BVs *in vitro* under serum-containing medium conditions, and *in vivo* during systemic administration.

2.2 Materials and Methods

2.2.1 Preparation of Magnetofection Complexes and Other Gene Transfer Vectors

Magnetic nanoparticles coated with PEI 25 kDa (PolyMag) were purchased from Chemicell (Postfach, Germany). Bis(cysteinyl) histidine-rich, endosomolytic Tat peptides (Lo and Wang, 2008) were prepared using a conventional solid-phase, chemical synthetic method (GL Biochem, Shanghai, China) with a purity greater than 98%. The study used a plasmid DNA

encoding a firefly luciferase (Luc) gene under the control of the CAG promoter (pCAG-Luc, kindly provided by Yoshiharu Matsuura, National Institute of Infectious Diseases, Tokyo, Japan) and a plasmid DNA with a gene encoding an EGFP under the control of the CMV promoter (pFastBac-CMV.EGFP) (Zeng J *et al.*, 2007a). To prepare magnetofection complexes, plasmid DNA and PolyMag were diluted in separate solutions of Milli-Q water mixed at a weight/weight ratio of 1 and incubated for 15 minutes at room temperature. The endosomolytic Tat peptides were then added to the PolyMag/DNA complexes in an N/P ratio as stated in the text and immediately mixed by vortexing for 30 seconds. The ternary mixtures were incubated for 30 minutes at room temperature. Oxidization of the endosomolytic Tat peptides was performed by air-bubbling of pure oxygen gas flow for 30 seconds, followed by shaking for 30 minutes in an Eppendorf Thermomixer®. This procedure was performed twice to ensure covalent bonds were formed between peptides.

Other gene delivery systems tested in this study included two non-viral gene delivery systems: PEI/DNA complexes and Lipofectamine 2000/DNA complexes; and two viral vectors: recombinant BV and AAV type 2 (AAV-2) vectors. To prepare non-viral DNA complexes, plasmid DNA pCAG-Luc was mixed with PEI 25 kDa (Sigma-Aldrich, San Diego, CA, USA) at an N/P ratio of 15, or Lipofectamine 2000 (Invitrogen, Carlsbad, CA, USA) at a ratio of plasmid DNA (in µg) to Lipofectamine 2000 (in µL) of 1:3. Recombinant BV vectors (Wang *et al.*, 2006b) were constructed using the transfer plasmid pFastBac1 of the Bac-to-Bac® BV expression system (Gibco BRL, Life Technologies, USA) with a luciferase cDNA under the control of the human

CMV enhancer/promoter. Recombinant AAV-2 vectors (Wang *et al.*, 2005a) were constructed by cotransfection of HEK293 cells using pAAV-CMV E/P-Luc containing a luciferase reporter gene under the control of the human CMV enhancer/promoter, the AAV-2 packaging plasmid pAAV-RC, and the adenovirus helper plasmid pHelper purchased from Stratagene (La Jolla, CA, USA).

2.2.2 Preparation of Baculovirus-based Bio-nanoparticles

BV vectors that can express luciferase under the control of a CMV promoter, namely BV-CMV-Luc, were constructed using the Invitrogen Bac-to-Bac® system. To summarize, the expression cassette CMV-Luc was inserted into the pFastBacTM1 vector, which was used to transform DH10αBac competent cells, followed by the isolation of Bacmid plasmids containing the virus genome and expression. Sequentially, Bacmid was used to transfect host *Spodoptera frugiperda* (Sf9) insect cells to produce recombinant BVs. Budded viruses were then harvested and further amplified in the Sf9 cells. Virus stocks were stored at 4°C until use. Virus infectious titers were determined by plaque assays with Sf9 cells. In this study, cationic polymer (PEI 25 kDa)-coated superparamagnetic nanoparticles (PolyMag) were used to interact with BV particles. PolyMag nanoparticles were dissolved in water. BV particles and PolyMag were first adjusted to desired concentrations and then incubated separately for 5 minutes at room temperature to reach equilibrium, at which point they were shaken on the vertex machine for 1 minute to detach the particles remaining on the bottom and sides of the containers. Then the PolyMag solution and BV solution were mixed according to the desired

PolyMag concentration for interaction, shaken on the vertex machine for 1 minute to ensure uniform dispersion of the particles, and then incubated at room temperature for 40 minutes to allow the formation of PolyMag-BV bio-nanoparticles.

2.2.3 Serum Complement Inactivation of Bio-nanoparticle Vectors

After the formation of complex vectors, fetal bovine serum (FBS, Hyclone) and rat serum complements (Sigma) were applied to the particles for inactivation treatment. Serum complements were incubated with bio-nanoparticle solutions at a volume ratio of 1:1 at 37°C for 30 minutes. Heat inactivated (56°C for 30 minutes) serum complement from the same serum was used for the control.

2.2.4 Characterization of Gene Transfer Vectors

Particle sizes were determined by dynamic light scattering and zeta potentials were measured electrophoretically using Zetasizer Nano-ZS (Malvern Instruments, Malvern, UK). For TEM imaging, samples were prepared by dipping carbon-coated copper grids into sample solutions followed by drying at room temperature. TEM images of gene transfer particles were taken on a JEOL 100CX instrument operated at 200 kV.

2.2.5 *In Vitro* Magnetofection

Human U87, H4, and T98G glioma cell lines and human NT2 (Ntera-2/D1) neural stem cells were purchased from American Type Culture Collection (Manassas, VA, USA) and the U251 astrocytoma cell line was purchased from

the Chinese Academy of Science (Shanghai, China). The cell lines were maintained in Dulbecco's Modified Eagle's Medium (DMEM) supplemented with 10% FBS and 1% penicillin-streptomycin. Mouse C17.2 cells were kindly provided by Professor E. Arenas, Department of Medical Biochemistry and Biophysics, Karolinska Institute, Stockholm, Sweden, and were maintained in DMEM supplemented with 10% FBS (Gibco) and 5% horse serum (Gibco).

For magnetofection, cells were seeded in 96-well plates at a density of 20,000 cells per well in 50 µL of growth medium. Immediately prior to magnetofection, 100 µL of fresh growth medium was used to replace the old medium. The complexes with 1 µg of plasmid DNA were then added to each well. MagnetoFACTOR plate (Chemicell), a permanent magnet, was placed under the cell culture plate and created a permanent magnetic field at the cell layer location with a field strength and gradient of 70 to 250 mT and 50 to 130 T m^{-1}, respectively. After 15 minutes of incubation, the MagnetoFACTOR plate was removed to avoid cytotoxicity induced by overexposure to the magnetic field (Mykhaylyk *et al.*, 2007). The medium with magnetofection complexes was then replaced with 100 µL of normal growth medium. The cells were cultivated under standard conditions for 24 hours before gene expression analysis.

For luciferase gene expression analysis, the cells were rinsed with Phosphate Buffered Saline (PBS) and lysed with 50 µL of lysis buffer (Promega, WI, USA). A single freeze-thaw was performed to ensure complete lysis. Ten µL of the cell lysate was used for measurement with Luciferase Assay System (Promega). Measurements were made in a single-tube luminometer (Berthold

Lumat LB 9507, Bad Wildbad, Germany) for 10 seconds. The amount of protein in the lysate was measured by DC Protein Assay with bovine serum albumin as the standard. Results were expressed in relative light units (RLU) per mg total protein.

For EGFP gene expression analysis, EGFP-positive cells in the 96-well plate were imaged by fluorescent microscopy 24 hours after magnetofection. The number of transfected cells was counted in an inverted fluorescent microscope using a 10 × objective with the view field accounting for one-fiftieth of the well area. The EGFP-positive and total cells were counted in five view fields per well. Magnetofection efficiency was estimated by the average percentage of the fluorescent cells in triplicate.

2.2.6 *In Vivo* Gene Transfer

Adult male Wistar rats (200–250 g) were used for *in vivo* gene transfer. In animals anesthetized by an intraperitoneal injection of sodium pentobarbital, the lumbar injection was given using a 10-µL micro-syringe connected with a 30-gauge needle after exposing the skin around L4-L5. Slight movement of the tail reflected proper injection into the subarachnoid space. Twenty µL of magnetic complexes with 4 µg of pCAG-Luc was injected slowly into each rat over 5 minutes. The doses for other gene transfer vectors were 4 µg of plasmid DNA in non-viral PEI 25 kDa/DNA or Lipofectamine 2000/DNA complexes, 1 x 10^8 particles of AAV-2, and 1 x 10^7 particles of BV, each in 20 µL doses. After injection, the needle remained in situ for 5 minutes before being slowly withdrawn. The skin was then closed with surgical clips. An

externally applied magnetic field (NdFeB permanent magnet, 1.21 Tesla, New-Era Electro-Magnetic Int'l, Singapore) was used immediately after injection by placing the magnet on top of the injection site for 15 minutes. Alternatively, the injected magnetic complexes were moved up the spinal cord by shifting the magnet repeatedly from the injection site to the brain for 15 minutes.

For luciferase activity assays of tissue samples, animals were perfused transcardially with 0.1 M PBS 2 days after injection and the spinal cord was collected. The spinal cord was separated into cervical, thoracic, and lumbar parts. The tissue samples were homogenized with 400 µL of lysis buffer (Promega), followed by three freeze-thaw cycles. The lysate was centrifuged at 14,000 g for 5 minutes at 4°C, and supernatants were collected for luciferase activity assay as described above. For immunostaining, animals were perfused transcardially with PBS, followed by 4% paraformaldehyde/0.05% glutaraldehyde in PBS. The lumbar spinal cord was removed and sections were cut at 30 µm thickness. The sections were transferred to gelatin-coated slides and fixed with acetone. A goat anti-luciferase (1/200, Dako, Carpinteria**,** CA**,** USA) and a fluorescein isothiocyanate-conjugated anti-goat polyclonal antibody were used as the primary and secondary antibodies, respectively. After antibody incubation and washing, the sections were mounted in FluorSave™ (Calbiochem, San Diego, CA, USA) and photographed.

2.2.7 Statistical Analysis

All data are represented as the mean ± SD. The statistical significance of differences was determined by the two-factor analysis of variance (ANOVA) with replication followed by Tukey post hoc analysis or unpaired Student's t-test. A *P* value of <0.05 was considered statistically significant.

2.3 Results

2.3.1 Formation of Ternary Magnetofection Complexes

The amino acid sequence, chemical structure, and 3D structure modeling of our endosomolytic Tat peptides are shown in Figure 2.1A. The bulky imidazole groups of histidine residues are oriented on both sides of the peptide backbone in a spiral pattern to minimize steric hindrance. The rigid backbone of the peptide suggests that an interpeptide disulfide bond will form only between two cysteine residues from two peptides. To form stable and active complexes, the reversible polymeric forms of the Tat peptide with terminal cysteine residues were prepared by oxidative polymerization via the terminal thiol groups by simple infusion of pure oxygen gas into the mixtures. After 1 hour of incubation under oxidative conditions, the zeta potential and size of the complexes were measured. As shown in Figure 2.1B, PolyMag iron particles had a particle size of approximately 10 nm as determined by dynamic light scattering analysis. When PolyMag and plasmid DNA complexes were prepared at a magnetic nanoparticle iron-to-DNA ratio of 1:1 (wt/wt), the size of the binary complexes was approximately 120 nm. The zeta potential of PolyMag iron particles was 50 mV, while the zeta potential of the PolyMag/DNA complexes decreased to 30 mV, suggesting that some of the

negatively charged plasmids were exposed on the surface of the complexes. Including the endosomolytic Tat peptides into the complexes, at an N/P ratio between peptide and plasmid DNA of 3:1, reversed the zeta potential from 30 mV for the PolyMag/DNA binary complexes to approximately 50 mV for PolyMag/DNA/Tat ternary complexes, whereas the complex size remained approximately 120 nm. These results demonstrate the surface coating of positively charged Tat peptides. Further increasing the Tat peptide from an N/P ratio of 3:24 did not result in any obvious change in zeta potential and complex size (Figure 2.1B).

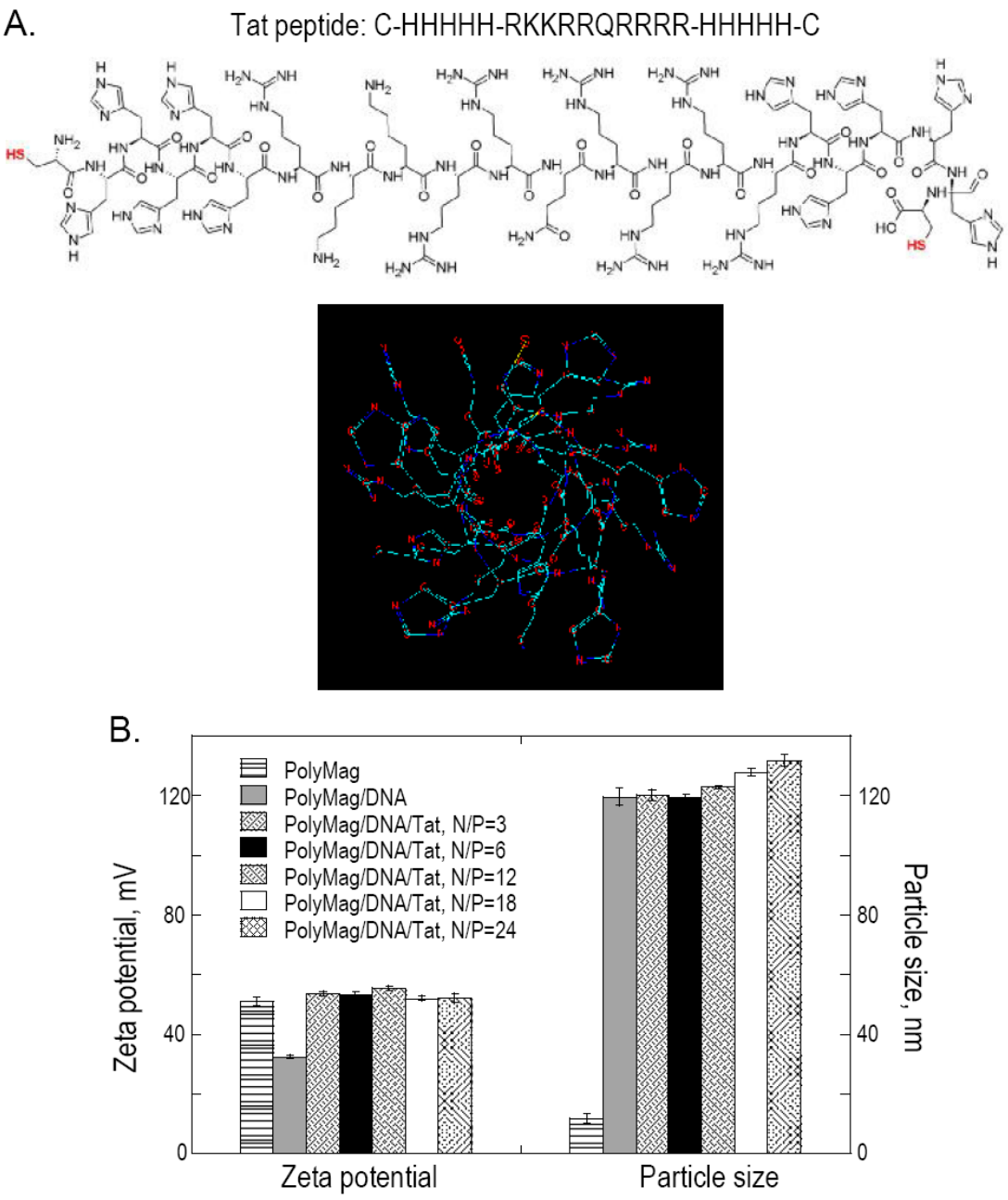

Figure 2.1 - Endosomolytic Tat peptide and ternary magnetofection complexes. (a) The amino acid sequence, chemical structure, and 3D modeling of the endosomolytic Tat peptide. The 3D modeling was based on "3D structure optimization" in ACD/ChemSketch freeware v10. The 3D structure was rotated to achieve a viewing angle from one end of the peptide. (b) Particle size and zeta potential measurements of various types of complexes (n = 3). To prepare binary complexes, PolyMag and plasmid DNA were mixed at a ratio of 1 (wt/wt). To prepare ternary complexes, various amounts of the Tat peptide were incubated with the binary complexes at an N/P ratio between peptide and plasmid DNA as indicated previously. Tat, transactivating transcriptional activator.

2.3.2 Electron Microscopic Analysis of Bio-nanoparticles

TEM images of PolyMag, PolyMag/DNA binary complexes, and PolyMag/DNA/Tat peptide ternary complexes are shown in Figure 2.2. The PolyMag nanoparticles (Figure 2.2A) displayed a smooth, spherical morphology with an average particle diameter of 10 nm, a size consistent with that obtained by dynamic light scattering analysis (Figure 2.1B). After mixing PolyMag with plasmid DNA, the particles tended to aggregate together (Figure 2.2B). The TEM image showed two phases: crystalline and amorphous, corresponding to PolyMag and plasmid DNA, respectively, suggesting electrostatic interaction between cationic PEI polymer-coated PolyMag and negatively charged plasmid DNA. After adding Tat peptides to the PolyMag/DNA binary complexes, the amorphous phase outside PolyMag nanoparticles, as well as the crystal lattice of PolyMag, was still clearly observed (Figure 2.2C). These TEM findings demonstrate the successful formation of PolyMag/DNA and PolyMag/DNA/Tat complexes. The corresponding schematic illustration of the structure of PolyMag/DNA/Tat peptide ternary complexes is shown in Figure 2.2D.

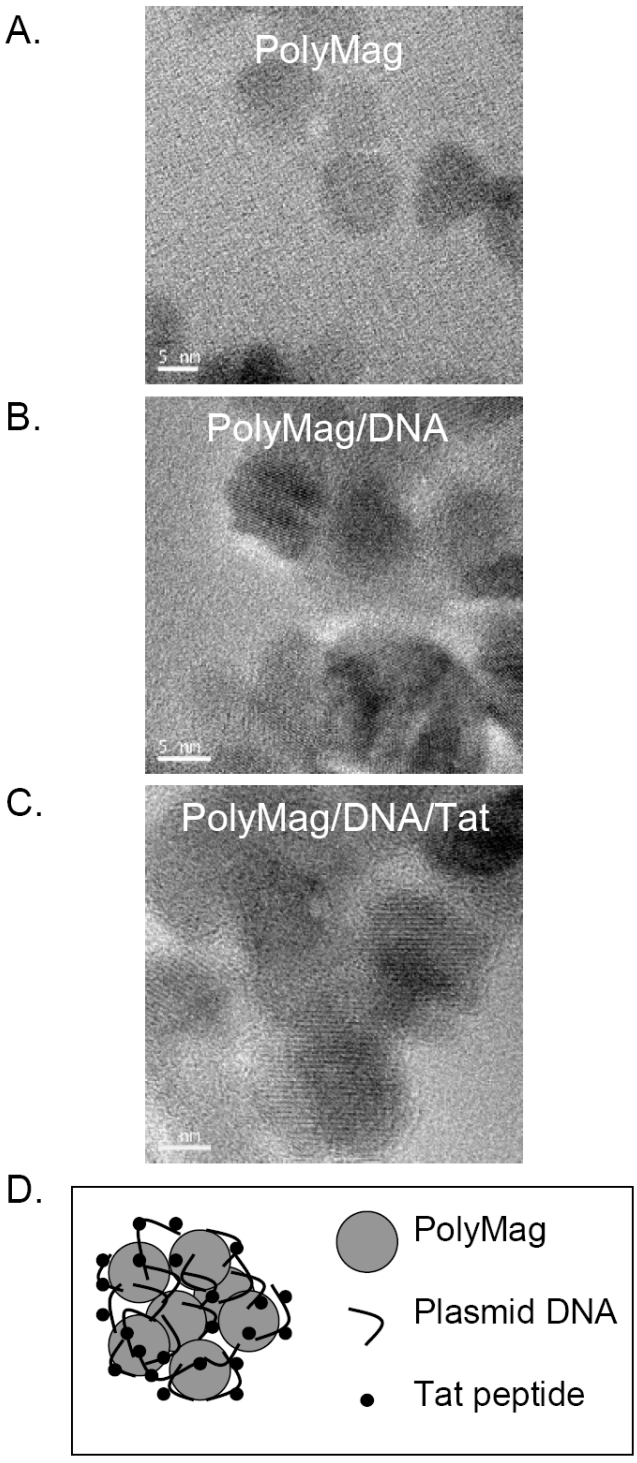

Figure 2.2 - Electron microscopic analysis of PolyMag nanoparticles, binary, and ternary magnetofection complexes. PolyMag nanoparticles are shown in (a). PolyMag/DNA binary complexes (b) were prepared at a weight ratio of 1 and PolyMag/DNA/Tat peptide ternary complexes (c) at a weight ratio of 1 plus an N/P ratio of 12. Note the outside amorphous phase wrapping layer and the inside crystalline phase of PolyMag nanoparticles in binary and ternary magnetofection complexes. (d) The schematic illustration of the structure of PolyMag/DNA/Tat peptide ternary complexes. Tat, transactivating transcriptional activator.

2.3.3 *In Vitro* Transfection Efficiency of Bio-nanoparticles

To optimize conditions for magnetofection complex preparation to achieve effective transfection, we first determined the optimal ratio of PolyMag to plasmid DNA for transfection in human astrocytoma cell line U251. Cells were transfected with these complexes when a magnet was placed under the cell culture plate. After 15 minutes of transfection, the magnet was removed and the transfection medium was replaced with a fresh normal medium. At magnetic nanoparticle iron-to-DNA ratios ranging from 0.5 to 2 (wt/wt), maximal transgene expression was achieved at the ratio of 1 (Figure 2.3A). While the addition of various amounts of the Tat peptide during complex preparation did not obviously change the zeta potential and size of PolyMag/DNA/Tat complexes (Figure 2.1B), we did observe an alteration of luciferase transgene expression when using different complexes prepared from an N/P ratio between peptide and plasmid DNA of 3:24 (Figure 2.3B). When the Tat peptide was used at an N/P ratio of 3, we observed no improvement in gene expression compared to the gene expression level provided by PolyMag/DNA binary complexes. The Tat peptide improved gene expression after the N/P ratio was increased to 6 and provided the highest expression level, with up to four-fold improvement over the complexes without the Tat peptide, at an N/P ratio of 12. Further increasing the N/P ratio resulted in a decline in the level of transgene expression. This decrease after the addition of more Tat peptides implies a negative impact from the formation of too many interpeptide disulfide bonds, which might affect intracellular plasmid DNA release from the complexes. In a control experiment, we performed transfection of U251 cells with these PolyMag/DNA/Tat ternary complexes in

the same manner as above, but without the use of a magnet plate. We observed very low levels of gene transfer in the absence of a magnetic field, regardless of which N/P ratio was used to add Tat peptides (Figure 2.3B). This finding indicates that the addition of the endosomolytic Tat peptide alone, without the influence of a magnetic field, will not significantly improve transfection efficiency under these transfection conditions, and that the complex-bound Tat peptides play an enhancement role only after a magnetic field has pulled the complexes to the surface of the cells.

In addition to the U251 cells tested above, we also used other types of neural cell lines, including human glioblastoma U87 cells, mouse C17.2 neural stem cells, and human NT2 neural stem cells. Although the absolute values of transfection efficiency under a magnetic field varied in these cells, PolyMag/DNA/Tat ternary complexes prepared at an N/P ratio of 12 provided significantly higher levels of luciferase gene expression than PolyMag/DNA binary complexes without the Tat peptide (Figure 2.3D). A similar improvement in gene expression was observed when the EGFP reporter gene was tested in U251 cells (Figure 2.4). In this case, the transfected cells were imaged by fluorescent microscope and the efficiency of gene delivery was determined by counting the number of EGFP-positive cells (Figure 2.4A). The maximum number of EGFP-expressing cells was obtained at an N/P ratio of 12, with approximately 60% positive cells (Figure 2.4B). When the complexes prepared at N/P ratios higher than 12 were used for transfection, the efficiency of transfection was reduced significantly to a level even lower than that obtained by using PolyMag/DNA binary complexes without the Tat peptide,

suggesting again the negative effect of a high number of disulfide bonds, possibly on intracellular plasmid DNA release.

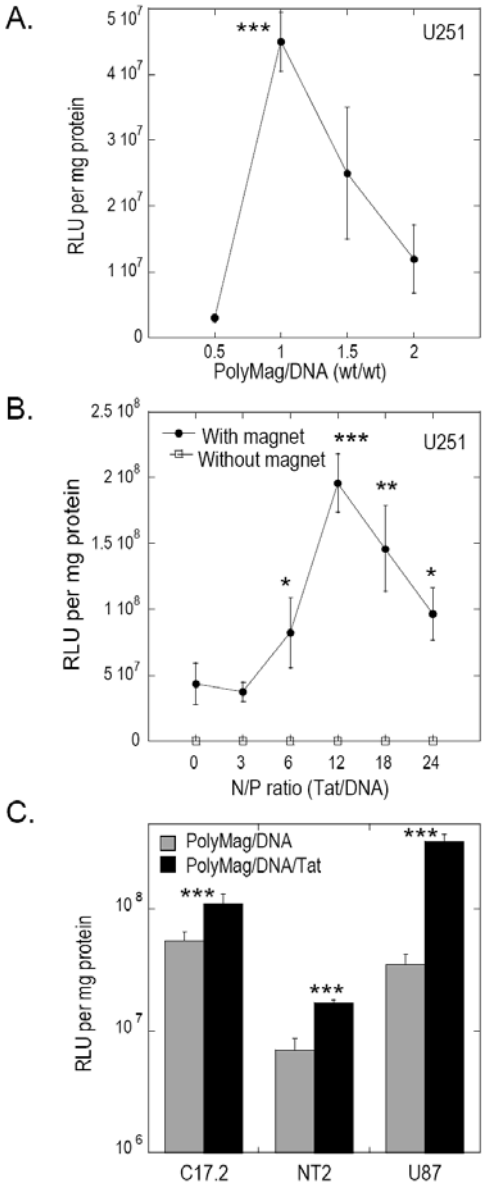

Figure 2.3 - Endosomolytic Tat peptides increase magnetofection-mediated luciferase reporter gene expression *in vitro*. (a) Effects of weight ratios between PolyMag and plasmid DNA on transgene expression. Binary complexes were prepared at ratios (wt/wt) from 0.5 to 2. Human U251 astrocytoma cells were transfected. (b) Effects of the Tat peptide. The binary complexes prepared in (a) at a weight ratio of 1 were mixed with endosomolytic Tat peptides to generate ternary complexes. The Tat peptides were added at different N/P ratios between peptide and plasmid DNA, as indicated previously. Human U251 astrocytoma cells were transfected. (c) Comparison of binary and ternary magnetofection complexes in different cell lines. Binary complexes were prepared at a weight ratio of 1 and ternary complexes at a weight ratio of 1 plus an N/P ratio of 12. Human glioblastoma U87 cells, mouse C17.2 neural stem cells, and human NT2 neural stem cells were used. The results are presented as mean RLU of luciferase activities per mg of cellular protein and standard deviations are indicated with error bars (n = 5). * P<0.05 versus the wt/wt ratio of 0.5 by ANOVA in (a), * P<0.05, ** P<0.01, *** P<0.001 versus the N/P ratio of 0 by ANOVA in (b), and ** P<0.01, *** P<0.001 versus the PolyMag/DNA group by Student's t-test in (c). RLU, relative light unit; Tat, transactivating transcriptional activator.

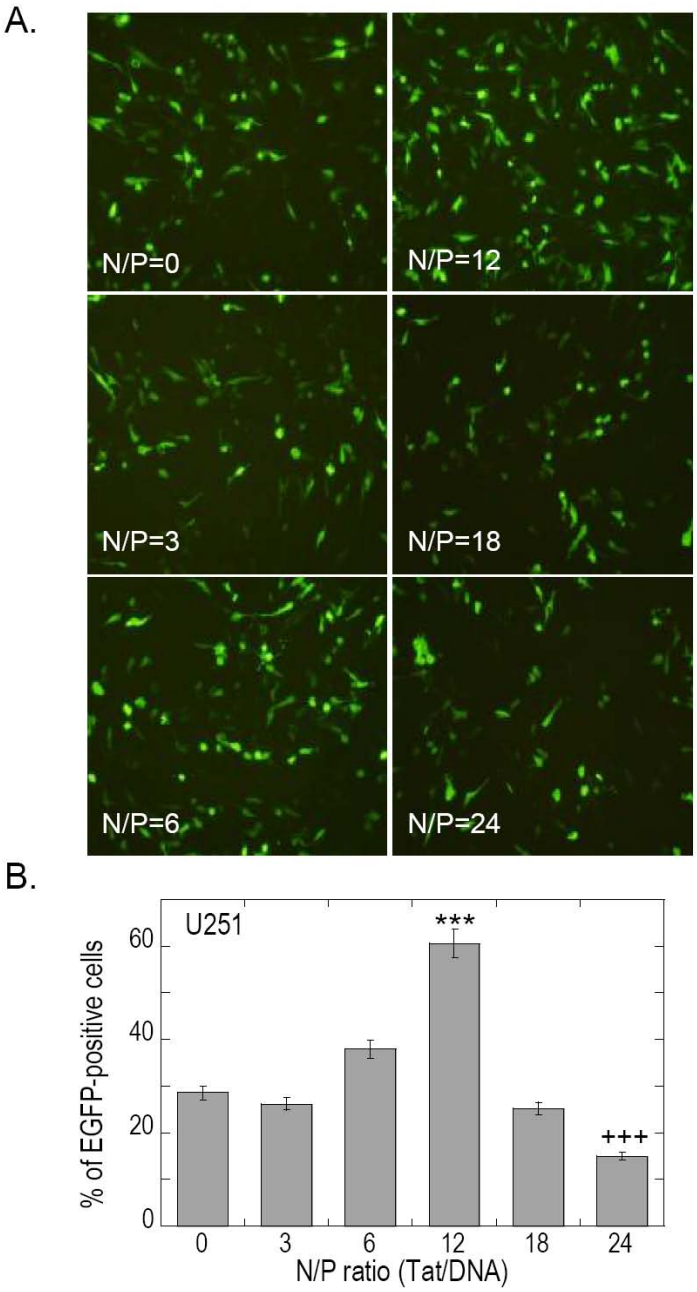

Figure 2.4 - Endosomolytic Tat peptides increase magnetofection-mediated EGFP reporter gene expression. Human U251 astrocytoma cells were transfected with binary or ternary magnetofection complexes. Binary complexes were prepared at a weight ratio of 1 and ternary complexes at a weight ratio of 1 plus different N/P ratios between peptide and plasmid DNA, as indicated previously. (a) Fluorescence microscopic images of EGFP expression. (b) Histograms summarizing the quantification of the percentage of transfected EGFP-positive cells. The mean values of triplicate experiments are presented and standard deviations are indicated by error bars. ***, significantly higher than the group with N/P ratio of 0, P<0.001 by ANOVA and +++, significantly lower than the group with N/P ratio of 0, P<0.001 by ANOVA. EGFP, enhanced green fluorescent protein; Tat, transactivating transcriptional activator.

2.3.4 *In Vivo* Gene Delivery Efficiency of Bio-nanoparticles

In conjunction with our research interest in gene delivery into the CNS, we further compared the *in vivo* gene transfection efficiencies of PolyMag/DNA binary complexes and PolyMag/DNA/Tat ternary complexes after administering the complexes into the spinal cord through lumbar intrathecal injection. A magnetic field was applied by placing a magnet on the back of the animals to prevent gene transfer complexes from being carried away by cerebrospinal fluid (CSF) flow. The level of transgene expression provided by ternary complexes was approximately two times higher than that provided by the binary complexes (Figure 2.5A). This expression level of the ternary magnetofection complexes was also higher than that provided by two commonly used non-viral gene delivery systems: PEI 25 kDa/DNA complexes and Lipofectamine/DNA complexes (Figure 2.5B). Although we made no attempt to control parameters that might affect quantitative comparison of the efficiencies between magnetofection and viral systems, it appeared that the ternary complexes mediated a level of transgene expression higher than that provided by AAV-2, but lower than that provided by BVs (Figure 2.5B). The improved magnetofection by the Tat peptide was confirmed by immunostaining of the cryostat sections of the lumbar spinal cord using luciferase antibodies (Figure 2.5C). Stronger staining, mainly in spinal meninges, was observed after injection of the ternary complexes. Several positively stained cells were observed in spinal parenchyma only when the ternary complexes were used.

We next tested whether it is possible to achieve magnetic field-guided region targeting in the spinal cord. After the intrathecal injection of the ternary magnetofection complexes, a group of animals were exposed to an external moving magnetic field. Instead of remaining immobile as in the previous *in vivo* experiment, the magnet placed on the back of this group of animals was repeatedly moved slowly along the spinal cord from the lumbar injection site to the brain. Under this moving magnetic field, the overall transfection efficiency in the spinal cord was improved by more than two-fold over that under a motionless magnetic field (Figure 2.6A). Of particular note, moving the magnet along the spinal cord effectively changed the regional pattern of transgene expression (Figure 2.6B). Using a motionless external magnetic field, luciferase transgene expression was detected mainly in the thoracic and lumbar regions that were close to the lumbar injection site. With the moving magnetic field, the peak-level expression was detected in the cervical spinal cord remote from the injection site, with the lowest level of transgene expression in the lumbar spinal cord. These findings demonstrate that magnetic guidance can be used to retarget intrathecally injected gene transfer vectors in the spinal cord.

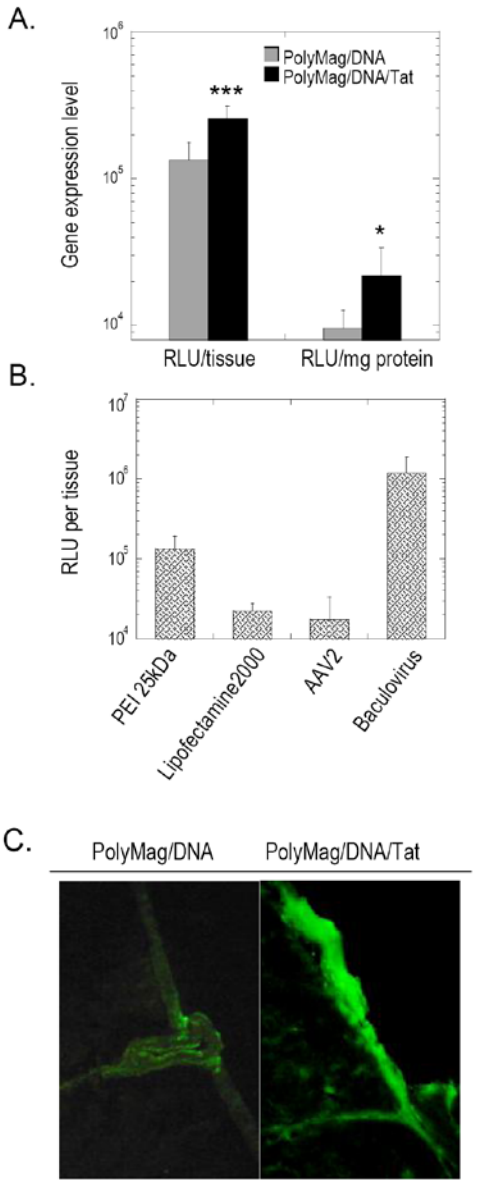

Figure 2.5 - Binary or ternary magnetofection complexes and *in vivo* luciferase reporter gene expression in the rat spinal cord. Binary complexes were prepared at a weight ratio of 1 and ternary complexes at a weight ratio of 1 plus an N/P ratio of 12. Magnetofection complexes were injected intrathecally into the lumbar spinal cord in rats, followed by placement of a magnet on the animals' backs for 15 minutes. The spinal cord was collected 2 days later for analysis. (a) Endosomolytic Tat peptides increase transgene gene expression as determined by luciferase activity assay. The mean values of five rats are presented and standard deviations are indicated by error bars. * $P<0.05$, *** $P<0.001$ versus the PolyMag/DNA group by Student's t-test. (b) Luciferase gene expression from four vectors 2 days after lumbar intrathecal injection. Results are presented as RLU per tissue and standard deviations are indicated by error bars. (c) Endosomolytic Tat peptides increase transgene gene expression as determined by immunostaining of cryostat sections of the lumbar spinal cord using luciferase antibodies. A strong staining in the meninges of the spinal cord was observed after injection of ternary magnetofection complexes. The original photographs were taken at x 200 magnification. RLU, relative light unit; Tat, transactivating transcriptional activator.

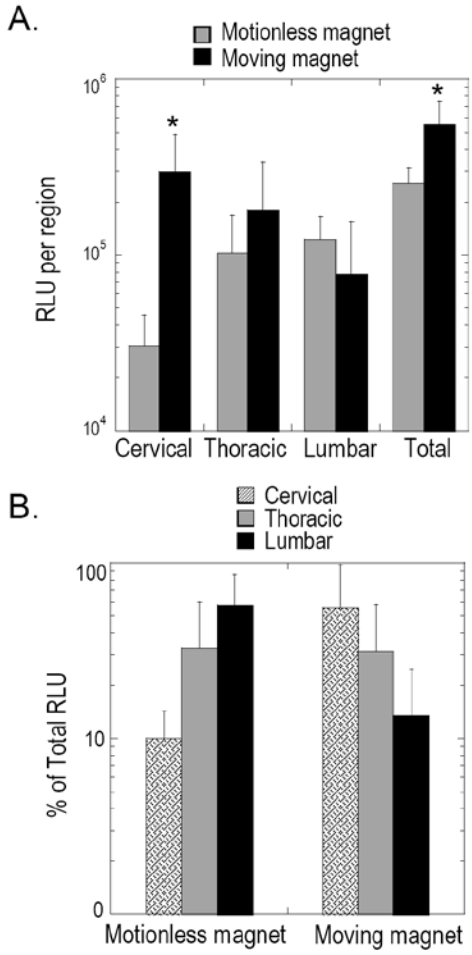

Figure 2.6 - Effects of a moving magnetic field on the distribution of transgene expression in the spinal cord. (a) Luciferase activities in the lumbar, thoracic, and cervical segments of the spinal cord under the influence of a motionless or moving magnet field. (b) Percentage of luciferase expression levels in each segment. The mean values of five rats are presented and standard deviations are indicated by error bars. * $P<0.05$ versus the group under the influence of a motionless magnet field by Student's t-test. RLU, relative light unit.

2.3.5 *In Vitro* Transduction Efficiency of Baculovirus-based Bio-nanoparticles

We further examined whether PEI 25 kDa-coated magnetic nanoparticles (PolyMag) can interact with BV and thus magnetically assist the viral-mediated gene transfer process. We performed the *in vitro* study on the U251 cell line to test this theory. As indicated in Figure 2.7, in the absence of serum, the luciferase expression level of BV vectors decreased significantly upon the application of 4 μL PolyMag per 100 μL BV solution in comparison with the group of untreated BV, revealing that strong interactions exist between negatively charged BV and positively charged magnetic nanoparticles. In contrast, the inhibitory effect of PolyMag on BV was reversed in the presence of serum as the transduction efficiency was dramatically increased with the elevation of the PolyMag concentration, which implies the significant *in vivo* application potential of PolyMag-BV bio-nanoparticles. Moreover, the transductional activity of PolyMag-BV vectors was approximately 16-fold higher than that achieved by naked BV when magnetic force was applied, an indicator that gene delivery performance in a serum-containing environment could be greatly improved by forming bio-nanoparticles with PolyMag. We noticed the trend of transduction efficiency by BV with varied concentrations of PolyMag was in opposite directions, in the absence and presence of serum. A possible explaination is that BV envalop proteins could be coated by PolyMag particles therefore preventing their interation with cell recepters. However, this shielding effect coincidentally provided protection against serum complement inactivation in the serum containing medium during the transduction process. Meanwhile, magnetic force played an important role in

enhancing the luciferase expression of the PolyMag-BV complex, as indicated by comparing the results obtained with and without a magnetic plate during transduction in the serum-containing medium. These results suggest the multifunctionality of PolyMag-BV bio-nanoparticles to simultaneously achieve magnetically guided transduction and protection of BV against serum complement inactivation.

To confirm the strength of PolyMag-BV bio-nanoparticles in terms of enhancing transduction efficiency with the existence of serum, we carried out similar transduction studies on several different cell lines, including HepG2, Hela, and NIH-3T3. As shown in Figures 2.8 to 2.10, the transduction efficiency profiles of all three cells are consistent with that of U251, although the extent to which transduction efficiency was increased varied among different cell types. These efficiency differences could arise because of the different mechanisms by which bio-nanoparticles enter cell membranes and are transported into the nucleolus, as well as the variant tolerances of different cell lines to the cytotoxicity of bio-nanoparticle vectors. We also carried out transduction experiments in the presence of rat serum, with the results (Figure 2.11) indicating that PolyMag-BV bio-nanoparticles work as well in rat serum as in FBS.

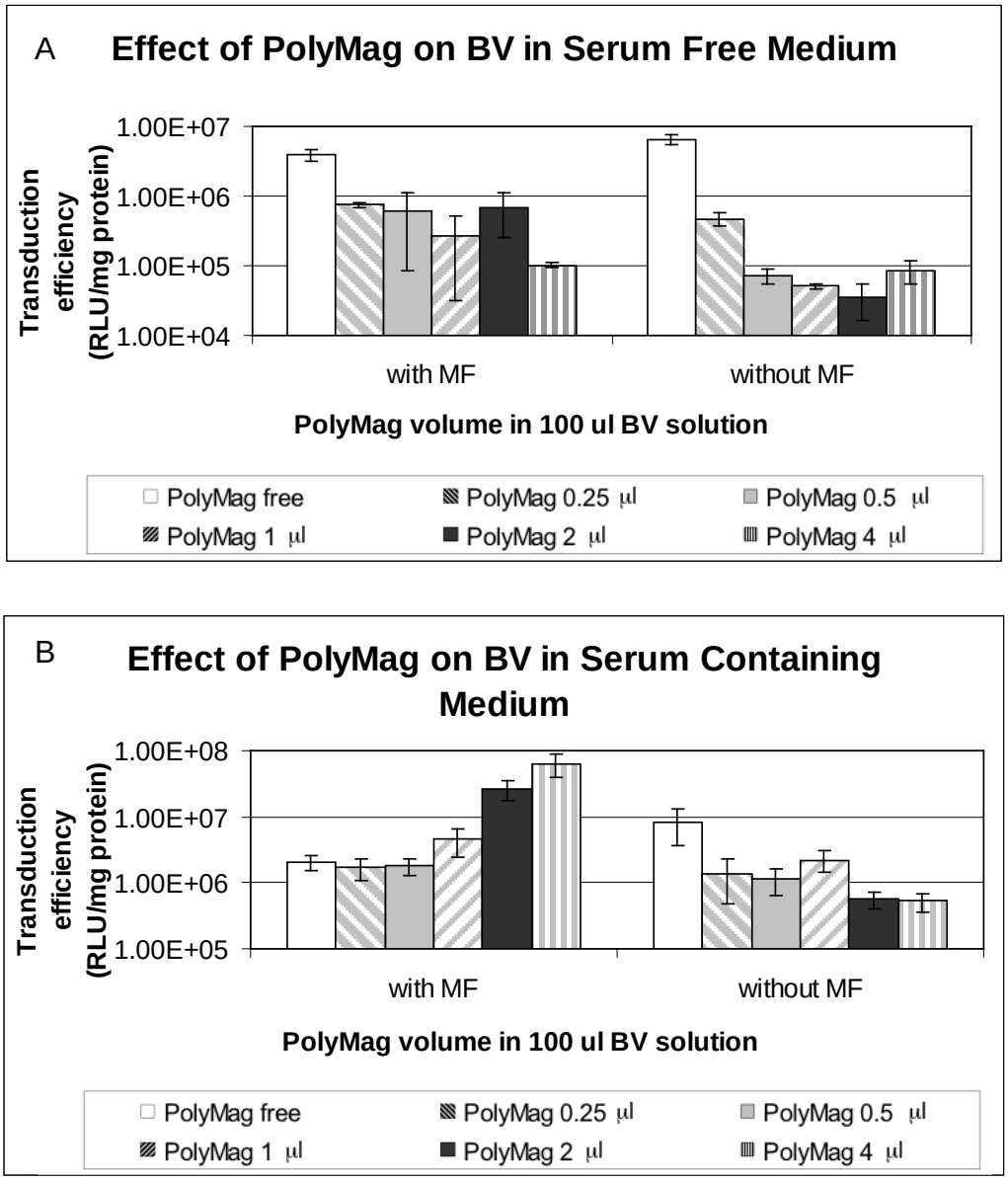

Figure 2.7 - Transduction capabilities of PolyMag-BV bio-nanoparticles in U251 cells without (a) or with (b) serum complement inactivation. PolyMag-BV complexes were used to transduce U251 cells without or with pre-treatments of serum complement inactivation. FBS was used for inactivation treatments. MOI 50 was used for transduction. Luciferase expression was quantified as RLU per mg protein. BV, baculovirus; FBS, fetal bovine serum; MF, magnetic force; MOI, multiplicity of infection; RLU, relative light unit.

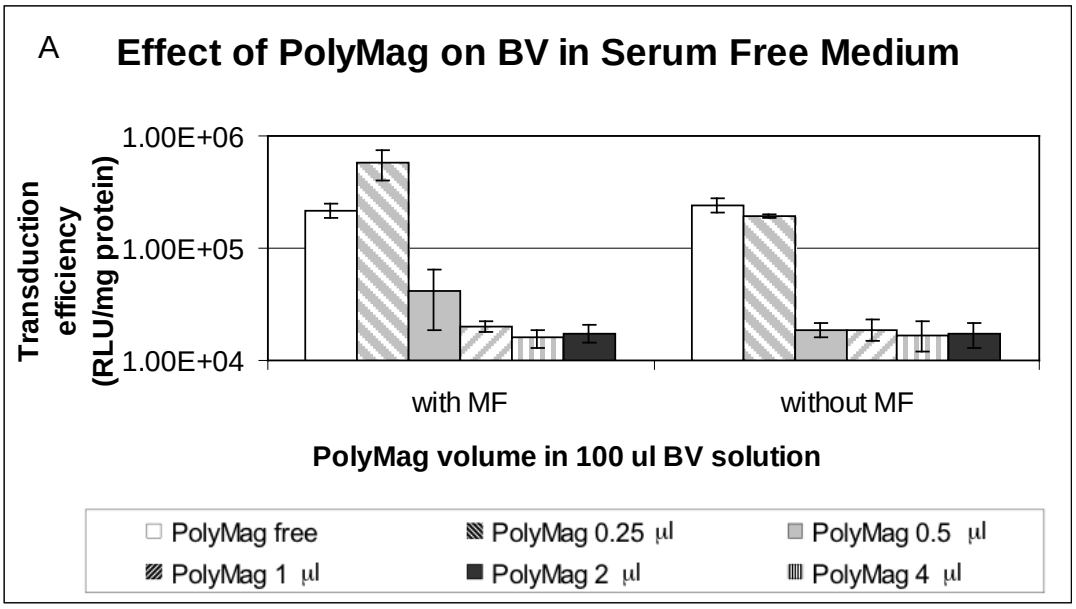

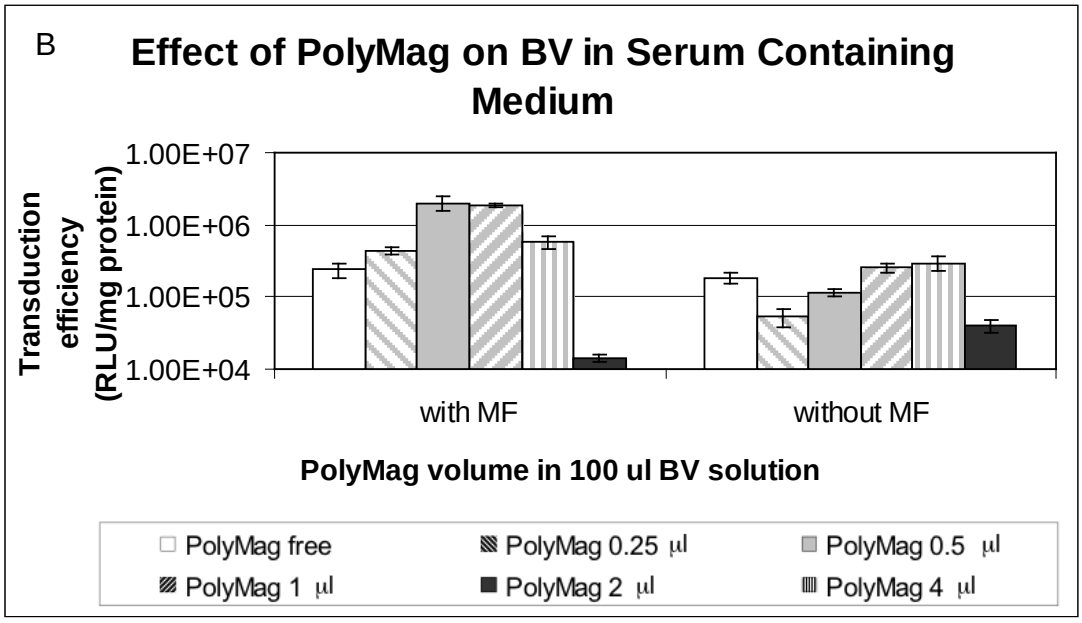

Figure 2.8 - Transduction capabilities of PolyMag-BV bio-nanoparticles in HepG2 cells without (a) or with (b) serum complement inactivation. PolyMag-BV complexes were used to transduce HepG2 cells without or with pre-treatments of serum complement inactivation. FBS was used for inactivation treatments. MOI 50 was used for transduction. Luciferase expression was quantified as RLU per mg protein. BV, baculovirus; FBS, fetal bovine serum; MF, magnetic force; MOI, multiplicity of infection; RLU, relative light unit.

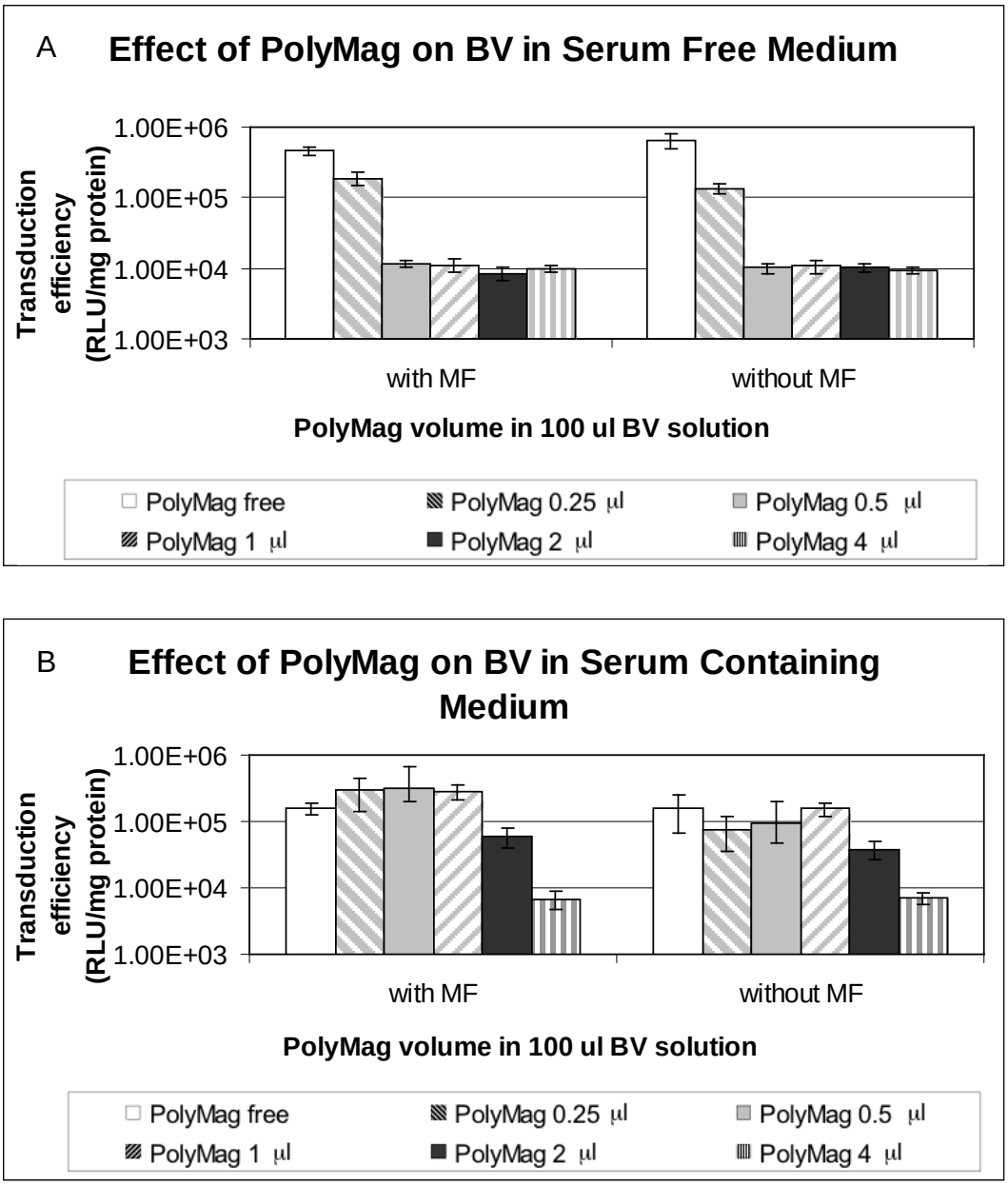

Figure 2.9 - Transduction capabilities of PolyMag-BV bio-nanoparticles in Hela cells without (a) or with (b) serum complement inactivation. PolyMag-BV complexes were used to transduce Hela cells without or with pre-treatments of serum complement inactivation. FBS was used for inactivation treatments. MOI 50 was used for transduction. Luciferase expression was quantified as RLU per mg protein. BV, baculovirus; FBS, fetal bovine serum; MF, magnetic force; MOI, multiplicity of infection; RLU, relative light unit.

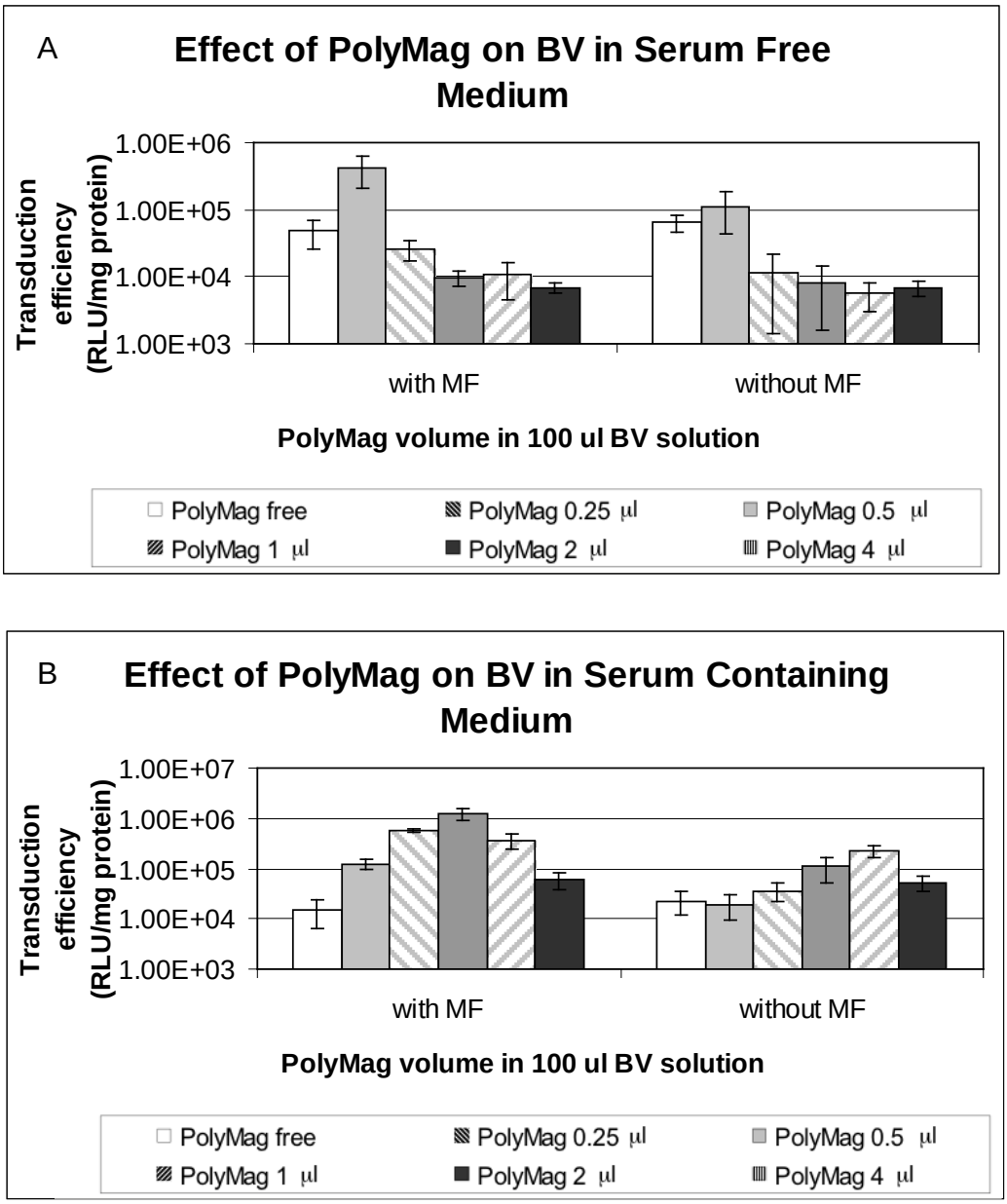

Figure 2.10 - Transduction capabilities of PolyMag-BV bio-nanoparticles in NIH-3T3 cells without (a) or with (b) serum complement inactivation. PolyMag-BV complexes were used to transduce NIH-3T3 cells without or with pre-treatments of serum complement inactivation. FBS was used for inactivation treatments. MOI 50 was used for transduction. Luciferase expression was quantified as RLU per mg protein. BV, baculovirus; FBS, fetal bovine serum; MF, magnetic force; MOI, multiplicity of infection; RLU, relative light unit.

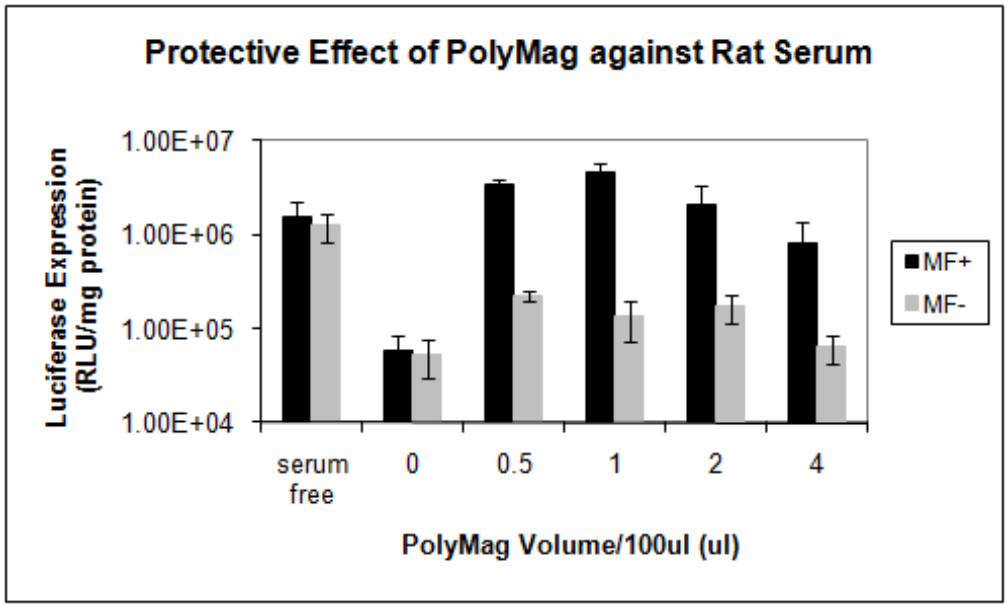

Figure 2.11 - Transduction capabilities of PolyMag-BV bio-nanoparticles in rat serum without or with serum complement inactivation. PolyMag-BV complexes were used to transduce U251 cells without or with pre-treatments of serum complement inactivation. Rat serum complement was used for inactivation treatments. MOI 50 was used for transduction. Luciferase expression was quantified as RLU per mg protein. BV, baculovirus; MF, magnetic force; MOI, multiplicity of infection; RLU, relative light unit.

2.3.6 Zeta Potential of Baculovirus-based Bio-nanoparticles

To explore the mechanism by which bio-nanoparticles protect BV against serum inactivation, we attempted to evaluate the charge properties of such complexes. Study results showed that the zeta potential of BV alone at physiological pH is -18 mV, while bio-nanoparticles have a zeta potential of approximately +25 mV at the same pH, suggesting that the negatively charged BV particles are probably coated or at least partially coated by the positively charged magnetic nanoparticles, thereby protecting BV from exposure to the serum environment (Figure 2.12).

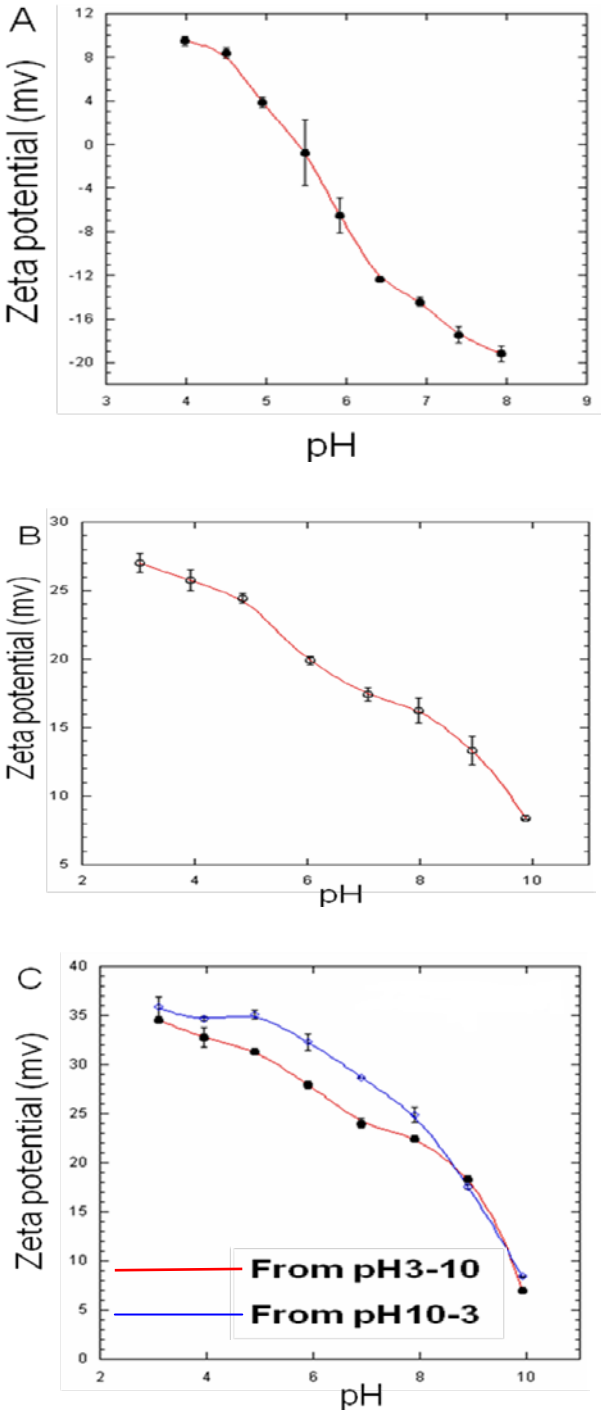

Figure 2.12 - Zeta potential measurements of various types of complexes. To prepare binary complexes, PolyMag and BV were mixed at a ratio of 4 µL/10^8 BV particles. Measurements were carried out from buffer pH 3 to pH 10 for BV particles (a) and PolyMag particles (b) alone, while for bio-nanoparticles (c) the pH movements of ascending and descending directions were applied. Results shown were averages of five independent measurements. BV, baculovirus.

2.4 Discussion

Tat peptide delivery strategy is widely used to improve intracellular delivery of various types of molecular cargos. Tat peptide function lies on its transduction domain, a small, basic, amino acid-rich stretch (RKKRRQRRR) that conveys the cell membrane penetrating property (Brooks *et al.*, 2005; Berry, 2008). Tat-mediated intracellular delivery is believed to occur directly through the plasma membrane following the inverted micelle formation. After membrane absorption, the peptide is scavenged into a hydrophilic pocket by phospholipids reorganization (Brooks *et al.*, 2005; Berry, 2008). Using a transducible Tat-Cre recombinase reporter assay on live cells, it has also been shown that after an initial ionic cell-surface interaction, Tat-fusion proteins are rapidly internalized by lipid raft-dependent macropinocytosis, and a transducible, pH-sensitive, fusogenic dTat-HA2 peptide can markedly enhance Tat-Cre escape from macropinosomes (Wadia *et al.*, 2004). The mechanisms by which the Tat peptide enables cargos to cross cell plasma membranes are effectively complementary to the functions of magnetofection, a process that improves cell surface accumulation of genetic materials. Thus, when the two approaches are used together, genetic materials effectively adhere to and then cross the cell membrane. Although it was previously reported that Tat peptide-derived magnetic nanoparticles can be efficiently internalized into stem cells for cell imaging (Lewin *et al.*, 2000), the current study documents for the first time that the Tat peptide can significantly improve the efficiency of magnetofection-based gene transfer. This new non-viral gene transfer method combines the unique features of the two well-established delivery approaches, i.e., magnetic nanoparticles-based plasmid

transfer and Tat peptide-based intracellular delivery, and is able to mediate gene transfer both *in vitro* and *in vivo*.

We previously developed a method to prepare ternary complexes of low molecular weight PEI, plasmid DNA, and a peptide derived from the nerve growth factor for targeted neuronal gene delivery (Zeng *et al.*, 2007b), which demonstrated that it is crucial to apply cationic polymers first to condense plasmid DNA to an extent that some of the negatively charged DNA molecules are still exposed on the surface for peptide binding. After using PolyMag and the Tat peptide to replace low molecular weight PEI and the neuron targeting peptide, we applied the principle of our previous study to generate self-assembled complexes in the current study. To prepare ternary magnetofection complexes, we first mixed PolyMag, a PEI 25 kDa-coated magnetic iron bead, with plasmid DNA. An appropriate amount of PolyMag was required to form complexes that provide efficient transfection. Small quantities of PolyMag beads at a wt/wt ratio of 0.5 were not sufficient for DNA binding, while large quantities of PolyMag beads might affect cell survival due to the cytotoxicity of PEI 25 kDa (Mykhaylyk *et al.*, 2007), resulting in a decrease of transfection efficiency. As suggested by the decreased zeta potential and increased particle size, binary complexes formed at the wt/wt ratio of 1 contain some negatively charged plasmid DNA molecules exposed on the surface. Positively charged endosomolytic Tat peptides were then introduced into the binary complexes through electrostatic interaction. The significant increase of zeta potential after incubation of the binary complexes with the Tat peptides suggests that the peptides had been absorbed on the

surface of the ternary complexes. No obvious change in complex size is an indication that adding the Tat peptides to the complexes did not cause further DNA condensation, probably due to the relatively small molecular weight of the peptide. Oxidation-induced polymerization of the peptide through interpeptide disulfide bond formation on the surface may prevent dissociation of the small Tat peptides from the complexes. Thus, the exposure level of the Tat peptide was assumed to be higher, consequently facilitating its membrane translocation action. This may have promoted the cellular uptake of the magnetofection complexes after a magnetic force pulled them to the cell membrane. Within the cell, both the endosomolytic Tat peptide and PEI 25 kDa can promote endosomal escape of the complexes through proton absorption in the endosomes. The nuclear localization signal of the Tat peptide may further promote plasmid DNA entry into the cell nucleus for transgene expression. In the context of the synergistic effect between PEI 25 kDa and the Tat peptide, our results are consistent with previous publications, which demonstrated that cell-penetrating peptide-modified PEI 25 kDa displayed enhanced transfection efficiency *in vivo* in the mouse lung (Kleemann *et al.*, 2005; Nguyen *et al.*, 2008).

One of the interesting findings of our study is that magnetic guidance can be used to overcome the distribution limit of intrathecally injected gene transfer vectors. Intrathecal injection in the lumbar spinal cord is a low-invasive procedure and poses little danger of injuring nerve roots, as CSF in the relatively wide subarachnoid space allows a certain degree of mobility of the nerve roots in response to needle puncture. Lumbar puncture may circumvent

the blood–brain barrier for drug delivery into the CNS and has been used as an access method for spinal anesthesia and for the introduction of therapeutic or diagnosis agents. The distribution of drugs delivered in this way is limited due to CSF flow, however. In our previous studies (Zeng *et al.*, 2007b; Shi *et al.*, 2003; Wang *et al.*, 2005b), PEI/DNA complexes delivered through lumbar intrathecal injection resulted in gene expression mainly in the lumbar and thoracic spinal cord. This distribution was not improved even when using polyethylene glycol-grafted PEI/DNA complexes (Shi *et al.*, 2003). In the current study, gene expression was redirected to the cervical spinal cord by application of a moving magnetic field. It appears that the magnetic complexes delivered through lumbar intrathecal injection responded to the externally applied magnetic field and moved within the CSF toward a location remote from the injection site. This is, to our knowledge, the first example of magnetic field guided targeting in the CNS.

In addition, our preliminary discoveries with PolyMag-BV bio-nanoparticle mediated gene transfer *in vitro* open up the possibility of achieving improved gene delivery performance *in vivo.* Following complexation between BV and PolyMag, Tat peptide could be linked to the complex for interaction to facilitate the escape of gene vectors from endosome, thereby achieving higher efficiency of the magnetically guided transduction. The gene transfer performance of the bio-nanoparticle complex can be assessed in terms of transduction efficiency to appraise the influence of Tat on the BV, both *in vitro* and *in vivo*. PolyMag-BV complex without Tat modification can be employed as a control to determine whether Tat plays a role in increasing cell uptake of

the vectors being used. More importantly, this system can be applied to investigate the potential protective effect of bio-nanoparticles on BV against serum inactivation, which is a main obstacle blocking the *in vivo* application of BV-mediated gene therapy in preclinical studies.

CHAPTER 3

ENCAPSULATION OF BACULOVIRUS WITH POLYELECTROLYTE FIBER TO FORM BIO-MICROFIBER

3.1 Obstacles of Baculovirus-mediated Glioma Therapy

Glioma is a type of primary CNS tumor originating from glial cells with the tendency to aggressively invade the surrounding brain tissue. Even when treated with complete surgical excision, radiation therapy, and chemotherapy, high-grade gliomas almost always grow back and patients usually die within a year, with only a few patients surviving longer than 3 years (Ohgaki and Kleihues, 2004; Ohgaki *et al.*, 2005). Developing effective therapeutic strategies for gliomas is one of the current focuses in cancer therapy. Gene therapy, though still at the stage of preclinical and clinical trials, has shown promise in therapeutic intervention of gliomas. It has gained sufficient efficacy to serve as a viable stand-alone treatment or at least a supplement to the conventional glioblastoma treatments. To fulfill its potential, treatment methods require gene transfer vehicles capable of efficiently transducing tumor cells. As the majority of patients undergoing adenovirus-mediated gene therapy for glioma are likely to develop a pre-existing immune response to this commonly used gene transfer vector, insect BV-based vectors have recently been introduced as promising viral gene delivery vectors to overcome obstacles inherent in the animal viral systems that are commonly used at present. Researchers have established novel methods for glioma treatment through the use of recombinant BV vectors containing the diphtheria toxin A gene (Wang *et al.*, 2006a). However, upon systemic administration, BVs often suffer the drawback of becoming inactivated following exposure to serum complement proteins. Since BV is of insect origin and was not subjected to human complement system during evolution, they likely did not evolve a

defensive mechanism to tolerate the attack from the human complement system (Hofmann and Strauss, 1998).

3.1.2 Current Approaches to Complement Inactivation

Previous reports showed that by using the surface display method, which fuses functional elements into the virus envelope proteins, it is possible to realize improved resistance of BV to serum complement inactivation (Hüser *et al.*, 2001). One example is the successful incorporation of decay-accelerating factor into the BV envelope, with the result of a BV resistant to serum complement (Guibinga and Friedmann, 2005). By analogy with recombinant retroviral vectors, BVs modified with vesicular stomatitis virus G (VSV-G) protein also displayed complement resistance. A VSV-G–modified BV effectively transduced hepatocytes after injection into the tail veins of mice (Barsoum *et al.*, 1997). Several research groups have also demonstrated that co-administration of complement inhibitors is an effective way of eliminating serum susceptibility (Hofmann *et al.*, 1999; Hoare *et al.*, 2005). Moreover, recombinant BVs displaying a polypeptide sequence of a heterologous virus were produced by a research group in Taiwan, and the authors maintain that the hybrid virus-like particles were resistant to serum complement inactivation (Ho *et al.*, 2004). These results suggest the possible use of recombinant BV vectors in combination with surface modification techniques for *in vivo* gene therapy. Although modification of the viral surface has improved the efficiency of gene transduction into various cultured cell lines, *in vivo* gene delivery efficiency of recombinant BVs is still unsatisfactory. Meanwhile, tremendously time consuming and difficult molecular cloning work is usually required for

such biological modifications. It is also difficult or even impossible to precisely control the extent of modifications, even though processes such as surface display and pseudotyping can change the surface composition of the recombinant BV. Moreover, these biological modifications are inflexible in that they can only be performed during the vector construction process, after which further modifications are extremely hard to carry out. Thus, more flexible and simple modalities that facilitate the construction of the viral vector surface by altering the composition, modifying the structure, conjugating functional components, etc., are urgently needed to broaden the application of BV vectors in brain tumor-targeted CNS gene delivery, especially when angiogenesis occurs and results in the presence of blood and serum proteins in tumor tissues.

Compared with biological modification methods such as surface display technique, the complexation approach opens up more versatile and superior possibilities of protecting BV against serum complement inactivation. It has been shown that the virus particle pegylation can be used to overcome the obstruction of complement inactivation and improve the *in vivo* gene delivery performance of BV vectors (Kim *et al.*, 2006). Also, Yang and colleagues have demonstrated that through simple but stable electrostatic interactions, PEI, a well-established gene delivery vector, can be incorporated to the surface of the BV vector. The resulting PEI-BV complex vectors showed enhanced resistance to complement inactivation, greatly amplifying their potential application for *in vivo* gene delivery (Yang *et al.*, 2009). Experimental data from our group's studies have verified the use of PEI-coated magnetic

nanoparticles to improve the transduction efficiency of BV in the presence of serum complement under the control of an external magnetic force. Meanwhile, ongoing research efforts in our group have also shown that surface conjugation of BV particles with functional peptide can effectively fight against serum destruction. Altogether, these encouraging achievements have proven the validity of generating BV-based complex vectors to protect against complement inactivation, thus improving its *in vivo* gene delivery performance.

3.1.3 Possibility of Protecting Baculovirus with Microfiber

During the course of seeking appropriate complexation methodologies, the innovative principle of fiber formation by IPC attracted our attention. The IPC fiber has been proposed as a biostructural unit for biological assembly with its ability to incorporate proteins, drug molecules, DNA nanoparticles, and cells for tissue engineering applications. A polyelectrolyte fiber can be fabricated by drawing together two droplets of high concentration solutions of oppositely charged polyelectrolytes (Wan *et al.*, 2004a). The unique feature of the IPC fiber formation process lies in its ability to encapsulate materials at room temperature and in aqueous solutions. This flexibility has enabled its application in the encapsulation of biologics. The mechanism of IPC fiber formation is supposed to create thin nuclear fibers that merge, providing a means by which biomolecules can be encapsulated within the fiber without compromising their physical properties and biological functions, making the fiber bypass the incorporated particles. Three types of biostructural units have been constructed using the process of IPC fiber formation: protein-encapsulated fiber, ligand-immobilized fiber, and cell-encapsulated fiber.

Biological substances can be released from the fiber in a controlled manner and still exert normal bioactivity (Wan *et al.*, 2004b; Liao *et al.*, 2005). Depending on the component properties, the release time of encapsulated components from these fibers can be manipulated to cater to various requirements. As a result, this promising technique can be potentially functionalized by producing drug-loaded fibers with high encapsulation efficiency, sustained release kinetics, and the ability to maintain the bioactivity of the encapsulants (Liao *et al.*, 2005).

3.1.4 Objectives

Motivated by achievements in IPC fiber formation and equipped with the knowledge offered by previous studies, we hypothesized that polyelectrolyte fiber formed by IPC could be used to encapsulate BV particles to protect them against serum complement inactivation. In this study, we evaluated the protectivity of IPC fiber on BV to assess its potential for *in vivo* applications in glioma gene therapy. The foundation of this hypothesis is the electrostatic interaction between positively charged polyelectrolyte composed of functional peptides, and negatively charged polyelectrolyte solution including plasmid DNA and BV. This proposal was clarified by initially investigating the effect of various parameters on the formation of fibers comprising a combination of plasmid and BV particles as the polyanion, and amphiphilic or Tat peptide as the polycation, and then examining the transduction efficiency and therapeutic efficacy of the fiber complex.

To test this hypothesis, we established procedures to evaluate the protective effect on BV of fibers formed through self-assembly of polyelectrolytes comprising plasmid DNA and a set of in-house designed amphiphilic peptides of alternating Leucine, Alanine, and Arginine residues or Tat peptide and its derivative. Afterward, we created a human brain tumor xenograft model in nude mice to assess the therapeutic effect of fiber-encapsulated BV vectors on glioma tumors. Fibers of polyelectrolyte complexes were synthesized by combining the peptides and plasmid DNA using the IPC process. Recombinant viruses encapsulated in such fiber not only transferred reporter genes into human glioma cell lines *in vitro*, but also effectively suppressed the tumor growth in nude mice *in vivo*. The finding of synergistic interactions of viral and non-viral vectors can assist in developing multimodal cancer gene therapies. Hopefully, the outcomes produced by this study will enrich the development of gene therapies of CNS disorders, especially glioma tumors, and will enable the advancement of BV, material engineering, and gene delivery-related studies.

3.2 Materials and Methods

3.2.1 Materials Used for Fiber Formation

Plasmid DNA

Plasmid DNA was employed as a vector backbone encoding the firefly luciferase gene (pCAG-Luc, kindly provided by Yoshiharu Matsuura, National Institute of Infectious Diseases, Tokyo, Japan). The plasmid was dissolved in Milli-Q water (Millipore, Massachusetts, USA) to required concentrations and stored at -20°C. Another plasmid DNA used to form fiber was pFastBac1

(Invitrogen), followed by the insertion of the expression cassette of CMV-EGFP or CMV-Luc.

Peptides

All of the peptides were chemically synthesized and purified by GL Biochem (Shanghai, China). They were provided in powder form and resuspended in Milli-Q water at the required concentrations and stored at -20°C. A list of peptides used in the study is as follows:

Name	Sequence	No. of Amino Acids
Tat	GRKKRRQRRRPPQC	14
C-H5-Tat-H5-C	CHHHHHGRKKRRQRRRPPQCHHHHHC	26
AR10	ARARARARAR	10
AR20	ARARARARARARARARARAR	20
LR10	LRLRLRLRLR	10
LR16	LRLRLRLRLRLRLRLR	16
LR10RGD	LRLRLRLRLRGRGDS	16

Baculovirus vectors

CMV-Luc BV with a luciferase reporter gene under the control of a CMV promoter, and CMV-EGFP BV under the control of a CMV promoter, were constructed using the Bac-to-Bac® BV expression system (Invitrogen, Carlsband, CA, USA). In summary, the expression cassette of CMV-Luc or CMV-EGFP was inserted into the pFastBac1 vector, which was then used to transform DH10Bac competent cells. After transformation, Bacmid plasmids containing the virus genome and expression cassettes were extracted and

used for the subsequent transfection of host Sf9 insect cells. Sf9 insect cells pre-adapted to Sf-900 II serum-free medium were purchased from Invitrogen, grown in spinner flasks at 27.5°C, and used to produce and propagate recombinant BV vectors. Budded viruses in the insect cell culture medium were collected and filtered through a 0.45-size filter (Millipore, Bedford, MA, USA) to remove any contamination, and concentrated by high-speed centrifugation at 28,000 g for 60 minutes. Viral pellets were resuspended in appropriate volumes of 0.1 M PBS and stored at 4°C. Virus infectious titers (plaque-forming units, PFU) were determined by plaque assays on Sf9 cells.

BV vectors harboring the HSV thymidine kinase (HSV-TK) suicide gene, under the control of a human high-mobility group box 2 (HMGB2) promoter, were constructed as previously described (Balani *et al.*, 2009). In summary, we first replaced the luciferase gene in the pGL4.11 vectors accommodating the 0.5-kb HMGB2 promoter with an HSV-TK gene obtained from pORF-TK (Invivogen) using PCR (forward primer, 5′-ATGCCTCGAGTCTT TCCTACAGCTGAGATCAC-3′ and reverse primer, 5′-ATGCTCTAGAAATGTA TCTTATCATGTCGAGCTAGC-3′). The promoter and the HSV-TK gene were then subcloned into the pFastBac Dual vector (Invitrogen) between BamH1 and Xba1. A fragment with the HSV-TK gene alone, without the promoter, was subcloned into the Not1 and Xba1 sites of the pFastBac, using Dual vector to produce a promoterless vector as the negative control. The Bac-to-Bac® BV expression system (Invitrogen) was then used to generate Bacmid DNA and subsequent BV, as previously described.

3.2.2 Fiber Formation Procedures

Aqueous solutions of peptides and plasmid DNA were prepared at 8 mg/mL concentration. To draw one fiber, 5 µL droplets each of the positive electrolyte and negative electrolyte were deposited on a plastic Petri dish in close proximity with each other; spacing between the droplets was kept at less than 50 µm. The interface of the droplets was then pulled together using a pair of tweezers, and the fiber was drawn in a continuous upward movement from the interface. There was some amount of residual solution left after each drawing due to disruption of the stable interface. Fibers can be drawn using 10 µL and even 20 µL droplets of polyelectrolytes, but the volume of residual solution increases when using larger volumes. Using 5 µL droplets for each fiber ensures minimum wastage of materials. For BV encapsulation, the concentrated virus a titer of 10^9 PFU per mL was mixed with plasmid DNA of concentration 8 µg/µL in a volume ratio of 1:3 followed by vortexing for 5 minutes. The resulting solution constituted the negative electrolyte for fiber drawing. Fibers were drawn against different peptide solutions at a concentration of 8 µg/µL.

3.2.3 Scanning Electron Microscope

DNA-peptide fibers with or without BV encapsulation were deposited onto the surface of a freshly prepared wafer holder wrapped with aluminum foil and air dried at room temperature for 4 hours. The wafer was then mounted onto an Al sample holder and sputter-coated with gold. The fiber morphology was examined using SEM (XL 30 FEG Philips, Hillsboro, OR, USA) at a magnification of 6671 x with an electron energy of 5 keV.

3.2.4 Field Emission Scanning Electron Microscope

Fiber morphology was determined using a JEOL JSM-5600 SEM. The fibers were gold-coated for imaging with a JEOL JFC-1200 fine coater using a coating current of 20 mA and sputter time of 120 seconds. The samples were imaged under high vacuum at an accelerating voltage of 10 kV.

3.2.5 Nuclear Magnetic Resonance

All samples were prepared by dissolving approximately 10 mg of materials in 1 mL of deuterium oxide (D_2O). NMR was performed with a Bruker DPX300 NMR Spectrometer at 300 MHz Ultrashield Plus and analyzed with in-house software at room temperature. The spectral width was 4789 Hz with 16 k data points. Chemical shifts were analyzed by referencing to the solvent peak (delta = 4.8 ppm for D_2O).

3.2.6 Viscosity Measurements

Viscosity measurements of the samples were performed with a HAAKE Rheoscope 1 rheometer (Karlsruhe, Germany) using a cone and plate geometry of 6 cm diameter, 0.903°C cone angle, and a measurement gap of 0.024 mm. The measurements were performed at room temperature at a constant shear rate of 10 per second for 5 minutes.

3.2.6 Fluorescence Labeling of Biomolecules

Stock solution of Bisbenzimide (Hoechst 33258) fluorescent dye (Sigma Chemical Company, Missouri, USA) was prepared by dissolving the dye in

Milli-Q water (Millipore, Massachusetts, USA) at a concentration of 1 mg/mL and storing in the dark at 4°C. The labeling solution was prepared by diluting the stock solution with water to a final concentration of 5 µg/mL. The labeling solution was mixed by vortexing with 8 µg/µL plasmid DNA using a volume ratio of 1:1. For PI labeling, Propidium Iodide (Sigma Aldrich, USA) was prepared at a concentration of 1 mg/mL. The labeling solution was prepared by diluting the stock to a final concentration of 20 µg/mL. The 10 µL of DNA was mixed with the dye and allowed to react for 2 hours in the dark. The LR10 peptide was labeled with fluorescein isothiocyanate (FITC). The 1M stock solution was diluted to 0.01 M for labeling purposes. The reaction was done at a dye to peptide molar ratio of 1:1. BV particles were labeled with a Cy5 mono-reactive dye pack (Amersham Biosciences, UK). The virus was resuspended in sodium carbonate–sodium bicarbonate buffer, mixed, and incubated with dye for 30 minutes. The labeled virus was centrifuged at 28,000g for 60 minutes followed by thorough washing with 0.1M PBS. The centrifugation and washing was repeated to ensure complete removal of unreacted dye. The virus particles were resuspended in 0.1M PBS and used for fiber formation.

3.2.8 Confocal Microscopy

The labeled fiber was visualized under a confocal microscope (Olympus, Fluoview 300, Tokyo, Japan) using a 10x objective lens. The FITC excitation and emission was 510 nm and 530 nm, respectively. The PI excitation and emission was 490 and 635 nm, respectively. The confocal imaging for EGFP expression in U251 cells was completed using an LSM 510 microscope (Carl

Zeiss, Germany). The fibers were drawn and placed on a glass coverslip inserted in 24-well plates. The cells were allowed to incubate on top of the fibers at 37°C for 48 hours to allow for EGFP expression. After 48 hours, the cell culture medium was removed and the cells were washed with 0.1M PBS. The cells were fixed using 3.7% buffered paraformaldehyde for 15 minutes at 37°C. The coverslips were then extracted from the well-plate and visualized under a confocal microscope.

3.2.9 Surface Charge Measurements

An electrokinetic analyzer (AntonPaar GmbH, Austria) was used to measure the surface zeta potential of the fibers. The fibers were prepared as previously described, air dried, and inserted in a stamp cell for measurement. The measurement was performed at pH 6.5 and 26°C. A dilute electrolyte (0.1 mM potassium chloride, pH 6.5) was circulated through the measuring cell containing the fiber sample, creating a pressure difference. The zeta potential value was calculated as the average of 5 measurements for each sample. The fiber was drawn using 5 µL droplets of both peptide solution and plasmid solution, with or without BV. The fiber containing BV was prepared with a BV and plasmid solution volume ratio of 1:3.

3.2.10 *In Vitro* Transduction and Gene Expression Assessment

For transduction assays, a human U87 glioblastoma cell line was grown in DMEM supplemented with 10% FBS, 100 U/mL penicillin, and 100 g/mL streptomycin. The cells were maintained in a humidified incubator with 5% CO_2 at 37°C. Cells at 50 to 70% confluency in 48-well plates were transduced

with CMV-Luc BVs or PEI-coated BVs for 1 hour, followed by removal of the BVs and addition of the DMEM supplemented with 10% FBS. Cells were washed 36 hours later with PBS and permeabilized with a reporter cell lysis buffer (Promega, WI, USA). Luciferase expression was measured by a single-tube luminometer for 10 seconds (Berthold Lumat LB 9507, BadWildbad, Germany).

3.2.11 Cell Transfection by DNA

Human U87 glioblastoma cells were used for this portion of the study. For the lipofectin group, 10 μg of DNA was diluted in 100 μL of Opti-MEM® I Reduced Serum Medium and 10 μL of Lipofectin® was diluted in 100 μL of Opti-MEM® I Medium. After standing at room temperature for 40 minutes, the diluted DNA was combined with diluted Lipofectin® (total volume = 200 μL), mixed gently, and incubated for 15 minutes at room temperature. For the fiber groups, 10 μg of DNA was used to form fiber with peptide or peptide and BV using the same ratio as previously described. For the mixture groups, the same amounts of plasmid DNA were mixed together with the appropriate amount of peptide or peptide and BV used previously to form the fiber. U87 cells were transfected in 24-well plates per cell by pDNA, pDNA+AR20, pDNA+AR20+BV-EGFP, pDNA/AR20 fiber, pDNA/AR20/BV-EGFP fiber, and pDNA+Lipofectin. Cells were cultivated in the growth medium for 24 hours before completing the luciferase assay. The results are shown as mean RLU of luciferase activities per mg of cellular protein (mean ± SD, obtained from five replicate assays).

3.2.12 Cell Viability Assay

Cell survival rates were measured by MTS assay (Promega) as per the manufacturer's instructions. Cells were seeded onto 24-well plates at 1×10^5 cells per well in DMEM supplemented with 10% FBS and transduced with various BV complexes at a designated MOI. The spectrophotometric assay for cell proliferation was performed 48 hours later by measuring OD at 490 nm.

3.2.13 Flow Cytometry

Fluorescence-activated cell sorting (FACS) analysis was used to quantify the transduction efficiency of BV vectors. After trypsinization to detach U87 cells from the culture plate, the cells were collected, washed in PBS, and resuspended in PBS before analysis with FACSCalibur Flow Cytometer (BD, Biosciences).

3.2.14 Serum Complement Inactivation

Human serum complement (Sigma-Aldrich) was reconstituted in 1 mL of sterile deionized water. For inactivation treatment, the human serum complement was incubated with the BVs, fiber-encapsulated BVs, or BV mixed together with plasmid DNA and peptide with designated volume at 37°C for 30 minutes.

3.2.15 Animal Studies

A nude mice tumor model was established by inoculating 1×10^6 U87 human glioblastoma cells expressing luciferase reporter genes subcutaneously on both thigh legs and tumors with the size of 2×10^7 so that a luciferase reading

could be observed after 7 days using the IVIS imaging system (Xenogen Corp., Alameda, CA). The injection procedure was performed under anesthesia by intraperitoneal injection of ketamine/xylazine (150/10 mg/kg). Intratumor injections were used for *in vivo* delivery. 100 µL of sample solution containing BV, BV in fiber, BV+pDNA+AR20, or PBS was injected into each animal on day 7 and day 14. The fiber was made as previously described. Fibers were cut into small segments and resuspended in PBS followed by vertex before injection. Each animal received 200 µL of ganciclovir (GCV) (5 mg/mL) by intraperitoneal injection daily from day 8 to day 20. IVIS images were taken and luciferase readings of tumors were measured every 2 days; animal death was recorded accordingly. Briefly, bioluminescence was measured non-invasively using IVIS. Luminescent images were taken as a 60-second acquisition 20 minutes after intraperitoneal injection of 200 µL of luciferin (5 mg/mL). During image acquisition, mice were anaesthetized continuously via inhalation of 3% isoflurane. Image analysis and bioluminescent quantification was performed using Living Image software (Xenogen Corp.). All remaining animals were sacrificed 60 days post-tumor implantation and the tumor size was recorded at that time. Tumor size was measured by a caliper and calculated as 0.5 x width^2 x length and shown as cm^3 at day 60. In the handling and care of animals, we followed the Guidelines on the Care and Use of Animals for Scientific Purposes issued by National Advisory Committee for Laboratory Animal Research, Singapore. The experimental protocols of the current study were approved by the Institutional Animal Care and Use Committee, National University of

Singapore and Biological Resource Center, and the Agency for Science, Technology and Research, Singapore.

3.2.16 Statistical Analysis

All data are represented as the mean ± SD. The statistical significance of differences was determined by the two-factor analysis of variance with replication followed by ANOVA analysis using SigmaStat 3.1 software. The statistical analysis of survival data was performed using the log rank test. A $P<0.05$ was considered statistically significant.

3.3 Results

3.3.1 Fiber Formation and Characterization

Seven types of peptides were used to form interfacial fibers with plasmid DNA. These peptides can be divided into two groups: four amphiphilic peptides including in-house designed AR10, AR20, LR10, and LR16 with alternating hydrophobic and positively charged amino acids; and two HIV-coded Tat regulatory peptides. For the cell attachment study, we also tested the fiber-forming ability of a hybrid peptide comprising LR10 and LR10 functionalized with an Arg-Gly-Asp (RGD) motif with a 1:1 molar ratio. Two droplets of oppositely charged electrolyte solutions were placed on the disc. The interface of the droplets was then pulled together using tweezers, and the fiber was drawn in a continuous upward movement from the interface (Figure 3.1A). First, we optimized the peptide and plasmid concentration required for fiber formation and found that the optimal concentration is 8 μg/μL for amphiphilic peptides and 9 μg/μL for Tat peptide and its derivative. The

optimal fiber-forming concentration of plasmid solution was 8 μg/μL for interaction with both types of peptides. Light microscopy, florescence microscopy, and confocal microscopy were used to investigate fiber morphology and prove the presence of components,. We demonstrated that all seven peptides were able to interact with plasmid DNA to form polyelectrolyte fiber through IPC with various morphologies (Figure 3.1B). The AR10 and AR20 peptides formed homogeneous straight fibers with clear edges, showing a relatively uniform dimension of ~10 μm in width and 2 to 5 cm in length. The LR10, its derivative, and LR16 peptides, however, formed homogeneous straight fibers with varying dimensions of 5 to 50 μm in width and 5 to 20 cm in length, due to the fact that the width varies depending on the length of the fiber drawn. For Tat peptide and its derivative, homogeneous straight fibers can also be assembled with a dimension of ~20 μm in width and 5 to 10 cm in length. Florescence microscopy images of the LR10 fibers resembled those visualized by light microscopy. The plasmid DNA were labeled with Hoechst blue, a fluorescent dye that binds to the minor groove of the DNA, and the fibers assembled using such plasmids were viewed under fluorescent microscopes to validate the constitution of the fiber. The results suggest that DNA molecules were evenly incorporated in the fibers as one of its components (Figure 3.1C). We further performed confocal scans by labeling the peptide with FITC green dye and plasmid DNA with PI at a 1:1 molar ratio to double confirm the constitution and explore the inner structure of the fiber. We found that both peptide and plasmid DNA were present in the fiber, as indicated by their respective colors, suggesting both ingredients are involved in the fiber formation process (Figure 3.1C). We also noticed several

consecutive yellow regions in the superimposed images (results not shown) where the DNA and peptide overlapped, indicating some binding and interaction between peptide and plasmid, although the scope and degree of such interactions were unclear.

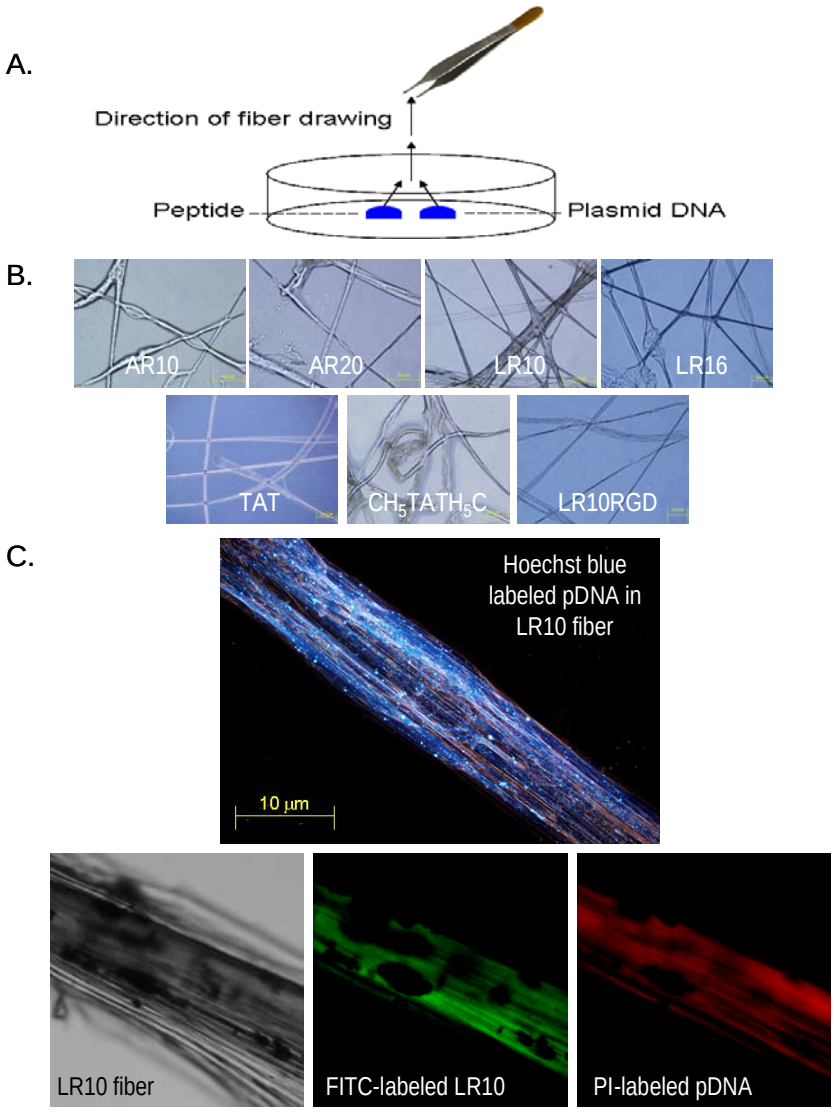

Figure 3.1 - Formation and characterization of peptide–DNA fibers. (a) Schematic of the fiber drawing process. For drawing one fiber, 5 µL droplets of the positive electrolyte and negative electrolyte were deposited on a plastic Petri dish in close proximity with each other. The interface of the droplets was then pulled together using a pair of tweezers, and the fiber was drawn in a continuous upward movement from the interface. (b) Morphology of the fibers formed using seven types of peptides drawn against plasmid DNA. Concentrations of 8 µg/µL were used for each of the peptides and for the plasmid DNA. Fibers were drawn between plasmid DNA and each of these peptides. Fibers were air dried for 5 minutes to a semi-dry state and laid on a cell culture disc. PBS was poured into the disc to submerge the fiber surface to mimic the cell culture condition. The fibers were viewed under a transmission microscope at 10x magnification. (c) Fluorescence microscope images of a LR10-DNA fiber with Hoechst blue labeled DNA at 10x magnification. Images show uniform incorporation of DNA in the fibers. All images were taken with the fiber in a wet state for better visualization. (d) Confocal scans of fiber with fluorescent-labeled peptide and DNA. The confocal microscopy images show LR10-DNA fiber made of FITC-labeled peptide and PI-labeled DNA using a 10x objective lens. The images show equal incorporation of the two biomolecules in the fiber. The excitation for FITC was 510 nm and emission was 530 nm. The excitation and emission for PI were 490 and 635 nm, respectively. FITC, fluorescein isothiocyanate; PBS, Phosphate Buffered Saline; PI, Propidium Iodide.

3.3.2 Encapsulation of Baculovirus with Fiber

Having confirmed the fiber-forming ability of peptide and plasmid, we attempted to encapsulate BV with such fibers with the purpose of protecting it from serum complement inactivation. Previous results from our studies have suggested that BVs have a net negative surface charge of ~20 mV at physiological pH. Therefore, we presumed that fibrous structures could potentially be formed through electrostatic interaction between a positively charged peptide and a negatively charged complex constituted from plasmid and BV particles. By combining concentrated plasmid solution and BV PBS solution, we demonstrated that it is possible to draw fibers against various peptide solutions using the fiber-forming approach described above. The BV particles were suspended in 0.1M PBS at a titer of 1 x 10^9 PFU per mL, using the previously optimized plasmid concentration of 8 μg/μL. We found the ratio of 3:1 between plasmid and BV solutions produced the best quality fibers. The BV containing fibers had similar dimensions as fibers without virus encapsulation, when observed under light microscope (Figure 3.2A). Fiber morphology analysis, however, revealed that the dimensions of BV-containing fibrous structures varied dramatically depending on the length of the fiber drawn, namely the longer fiber we have drawn, the diameter of the fibers becomes thinner given total amount of polyelectrolyte solutions is fixed. Field emission SEM (FESEM) was used to study the surface morphology of the fibers formed through self-assembly of the AR20 peptides and plasmid DNA, with and without BV encapsulation (Figure 3.2B), as it is capable of creating clearer, less electrostatically distorted images withspatial resolution down to

1.5 nm, which is 3 to 6 times better than conventional SEM. FESEM photographs of both types of fiber revealed the formation of fibrous assemblies of microfibers with similar morphology and dimensions as observed under light microscope. It was evident, however, that the surface appearance of these two fibers differed greatly. The fiber without BV incorporation displayed a smoother surface with very few ridges along the fiber axis. The fiber with BV incorporation, however, showed a much rougher surface morphology with clear ridges along the fiber axis, probably due to the encapsulation of nano-sized BV particles or aggregates of BVs inside the nuclear sub-microfibers composing the microfiber as a whole. Conventional SEM photographs of microfibers formed through self-assembly of AR20 peptide and plasmid DNA with BV incorporation (Figure 3.2B) once again showed the prominent indents and even clearly identified aggregates of BV particles. Fluorescence microscopy images of fiber consisting of BV labeled with Cy5 confirmed that the virus particles were successfully incorporated into the fiber (Figure 3.2B). We further characterized the charge property of the fiber by measuring the surface zeta potential of the AR20 and LR10 fiber. The results showed that peptide–DNA fiber has a general negative surface zeta potential at pH 7.4 and 25°C for both types of fiber, probably caused by the highly negatively charged DNA molecule. However, a significantly lower surface zeta potential was produced by introducing BV particles in the fiber-forming process due to the negatively charged surface of the virus particles (Figure 3.2C).

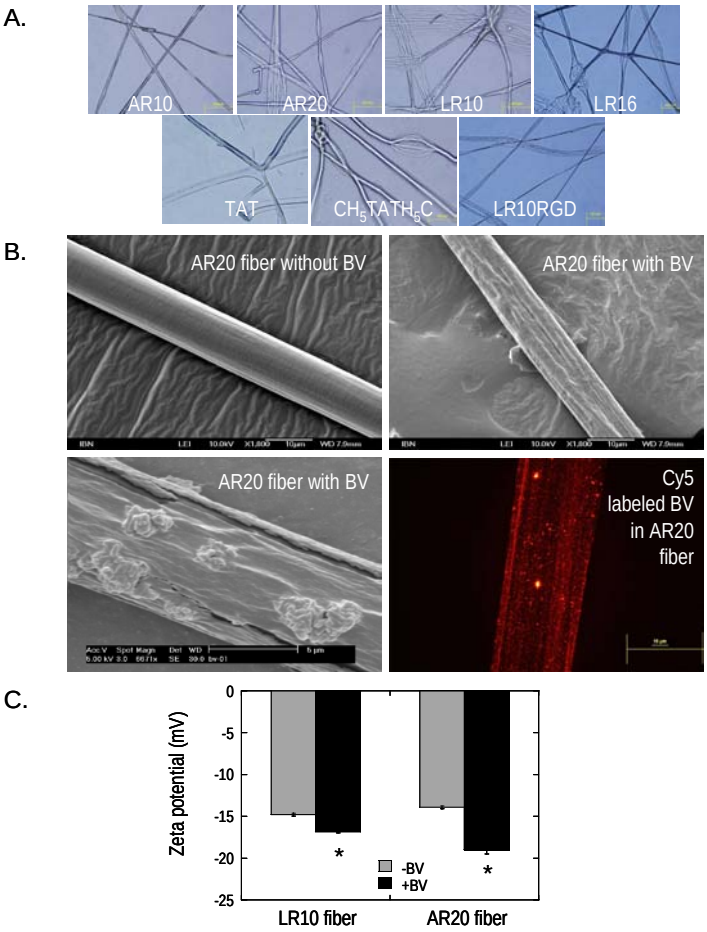

Figure 3.2 - Characterization of peptide–DNA fibers encapsulating BV. (a) Morphology of the fibers formed using seven types of peptides drawn against a plasmid DNA and BV mixture. Concentrations of 8 μg/μL were used for each of the peptides and for the plasmid DNA. BV and plasmid solution were mixed together with a 1:3 volume ratio. The titer of the BV solution was 10^9 PFU. Fiber was drawn using 5 μL droplets of both peptide solution and BV plus plasmid solution. Fibers were air-dried for 5 minutes to a semi-dry state and laid on a cell culture disc. PBS was poured into the disc to submerge the fiber surface to mimic the cell culture condition. The fibers were viewed under a transmission microscope at 10x magnification. (b) (upper panel) FESEM images of fibers without and with BV. Fiber morphology was determined using FESEM. (b) (lower panel left) A SEM micrograph of peptide–DNA fibers encapsulating BV, indicating floating BV on the fiber surface. (b) (lower panel right) Fluorescence microscopy of virus encapsulated in fibers. BV was labeled using Cy5. The virus was resuspended in sodium carbonate–sodium bicarbonate buffer, mixed, and incubated with dye for 30 minutes. The labeled virus was centrifuged at 28,000g for 60 minutes followed by thorough washing with 0.1M PBS. (c) The zeta potential of the peptide–DNA fiber without and with BV encapsulation. The measurement was performed at pH 6.5 and 26°C. A dilute electrolyte (0.1 mM KCl, pH 6.5) was circulated through the measuring cell containing the fiber sample, creating a pressure difference. The zeta potential value is the average of 5 measurements for each sample. The fiber was drawn using 5 μL droplets of both peptide solution and plasmid solution, with or without BV. The fiber containing BV was prepared with a BV and plasmid solution ratio of 1:3. BV, baculovirus; FESEM, field emission scanning electron microscopy; KCl, potassium chloride; PBS, Phosphate Buffered Saline; PFU, plaque-forming units; SEM, scanning electron microscopy.

3.3.3 Transduction Ability of Bio-microfiber

Having demonstrated the ability to encapsulate BV in the peptide–DNA fiber, we proceeded to test the *in vitro* transduction efficiency of BV released from fibers in U87 human glioma cell lines. Self-assembled polyelectrolyte fibers comprising AR20 peptide, DNA, and BV carrying an EGFP or luciferase reporter gene were produced and laid on the 24-well cell culture plate, followed by application of U87 cells suspended in media. Prior to the addition of cell suspensions, one group of the transduction reagents was treated with human serum complement, whereas the other control group was treated with PBS blank solution. Gene expression assessment was carried out 48 hours post-transduction. Results showed that a comparable number of cells can be transduced in the fiber group as compared with the naked BV group in the absence of human serum complement treatment. Though the intensity of fluorescence in the fiber group was slightly lower than the positive control, the number of green cells infected was at the same level (Figure 3.3A). On the other hand, the transduction efficiency of the fiber group was substantially higher than the naked BV group in the presence of human serum complement, suggesting that fiber encapsulation can effectively protect BV from inactivation by complement proteins (Figure 3.3A). Moreover, we found that in the presence of human serum complement treatment, the percentage of EGFP-positive cells in the fiber group was significantly higher than that of the mixture group, where the AR20 peptide was mixed together with plasmid and BV solution under the same conditions without forming fibrous structures, indicating that the protective effect is only functional when ordered microfiber

arrangements are formed (Figure 3.3A). The transgene expression pattern, and therefore the protective capability of fiber in the experimental groups, was also corroborated and verified by the luciferase expression profiles of BVs carrying a luciferase reporter gene, with or without serum inactivation in U87 cells (Figure 3.3B). We also demonstrated that of the seven types of peptide used for fiber formation, only AR20 is capable of effectively protecting BVs against serum complement inactivation (data not shown).

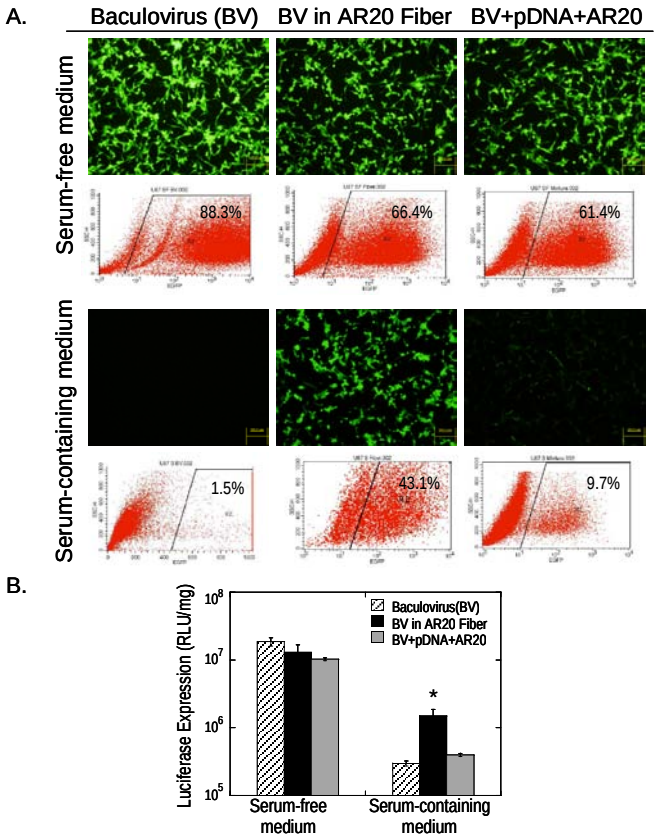

Figure 3.3 - Transduction efficiencies of peptide–DNA fiber with BV encapsulation and peptide, DNA, and BV mixture after human serum complement treatment. Human U87 glioblastoma cells were used. Cells were transduced at an MOI of 50 PFU per cell by BVs alone, BV encapsulated in peptide–DNA fiber, or BV simply mixed with the same amount of peptide and DNA used to form the fiber. The encapsulation was performed at a BV and DNA volume ratio of 1:3. Fiber was drawn using 5 μL droplets of both peptide solution and BV plus plasmid solution. Fibers were deposited on a 24-well cell culture plate. Naked, fiber-encapsulated, and mixed BVs were pre-treated with human serum complement at 37°C for 30 minutes. 100 μL of human serum complement was used to inactivate BV, fiber, and the mixture. After serum treatment, cell culture media containing U87 cells were added on top of the fiber solution, making the final volume in each well 2 mL and therefore the final serum complement concentration 5%, to minimize the cytotoxic effect of human serum complement on U87 cells. EGFP and luciferase reporter gene expression was detected 48 hours post-transduction with the BV construct CMV-EGFP and CMV-Luc, respectively. (a) Fluorescence microscope images and flow cytometric analysis of EGFP-positive U87 cells 2 days after transduction. The percentages of EGFP-positive cells are indicated. FACS analysis was used to quantify the transduction efficiency of BV vectors. After trypsinization to detach U87 cells from the cell culture plate, the cells were collected, washed in PBS, and resuspended in PBS before being analyzed with a FACSCalibur Flow Cytometer. (b) Luciferase expression profiles of U87 cells 2 days after transduction. Luciferase expression is expressed as RLU per mg of total protein and the standard deviation is indicated with error bars (n = 5). BV, baculovirus; CMV-EGFP, cytomegalovirus-enhanced green fluorescent protein; EGFP, enhanced green fluorescent protein; FACS, fluorescence-activated cell sorting; Luc, luciferase; MOI, multiplicity of infection; PBS, Phosphate Buffered Saline; PFU, plaque-forming units; RLU, relative light unit.

3.3.4 Therapeutic Efficiency of Bio-microfiber

We performed additional studies to evaluate the inhibitory effect on tumor cells of the fiber encapsulating a BV carrying therapeutic genes. Inspired by the finding of selective expression of the HSV-TK suicide gene in glioma cells under the control of the HMGB2 promoter, we set out to examine the cellular effects of BV transduction for a duration of 24 hours followed by prodrug GCV treatment on U87 cells for another 24 hours. We constructed HMGB2-TK-BV to determine whether introduction of the HSV-TK gene would render U87 cells susceptible to induced cell death by GCV. This recombinant BV was used to transduce U87 glioma cells in culture. Various transduction complexes were then fabricated, including AR20-plasmid fiber encapsulating HMGB2-TK-BV and designated combinations of the three components, followed by treatment with human serum complement or PBS control. We then carried out cell viability analysis of U87 glioma cells, transduced by the above prepared transduction reagents, and of naked BV, using quantitative MTS assays. We found no obvious difference in the reduced viability caused by the induced cell death in glioma cell lines following GCV treatment, or after transduction in the absence of treatment with human serum complement (Figure 3.4A). However, in the presence of human serum complement, transduction of tumor cells by HMGB2-TK-BV fiber significantly reduced the number of viable U87 glioma cells at a GCV concentration of 500 μmol/L, whereas transduction by naked BV vectors produced no observable effect on U87 glioma cells at the same GCV level, suggesting fiber formation provides a barrier preventing the inactivation of HMGB2-TK-BV by human serum complement (Figure 3.4A). Furthermore, the tests indicated that only by establishing fibrous structure can

BV become resistant to serum complement inhibition. In the presence of serum complement, other combinations of transduction reagents failed to drive sufficient transgene expression of HMGB2-TK genes to induce the corresponding cells death achieved by the fiber group (Figure 3.4A). Collectively, the protective effect of fiber on BV is applicable for reporter genes and also for therapeutic genes such as HSV-TK.

3.3.5 Tumor Suppressive Effect of Bio-microfiber

After substantiating the superior efficiency of BV-encapsulating fiber in eliminating U87 glioma cells *in vitro*, we then explored the *in vivo* efficacy of the bio-microfiber. We studied the therapeutic efficacy of BV-mediated HSV-TK gene delivery into U87 glioma cells followed by GCV administration in tumors generated on the backs of nude mice. We established glioma xenografts in nude mice using U87-Luc cells, followed by double injections of the designated gene transfer vectors into the xenografts on day 7 and day 14, respectively, post-tumor inoculation. Subsequently, GCV was administered by intraperitoneal injection daily for 2 consecutive weeks. During this period, we assessed tumor growth by determining the luciferase expression levels in tumor cells. Bioluminescence intensities from U87-Luc cells, indicative of tumor volume, were measured at 4-day intervals after tumor inoculation using a non-invasive *in vivo* imaging system. At days 11 and 19, there was an apparent slow-down in the speed of tumor growth in mice injected with fiber encapsulating HMGB2-TK-BV, probably due to the tumor suppression resulting from ample therapeutic gene expression. By contrast, an increase in tumor size was evident in the other control groups, suggesting that the tumor-

killing effect of BV encapsulated in fiber is much better than that of naked BV and other gene delivery vector combinations (Figure 3.4B,C). Although the TK-induced suicide gene expression did not completely eliminate tumors in the mice, the fiber group showed activity high enough to inhibit *in vivo* tumor growth compared with BV alone, BV-AR20-plasmid mixture, and PBS groups. The luciferase quantification result was also supported by tumor size measurement data, showing a smaller tumor size in the fiber-injected mice at day 60 (Figure 3.4D). More importantly, survival data showed that by the end of the study, more mice survived the tumor inoculation in the fiber group, suggesting that the therapeutic efficacy of fiber-encapsulating BV is much more significant than in the other three groups (Figure 3.4E). These results demonstrated that the recombinant BV vector encapsulated in IPC fiber can function as an efficient gene delivery vehicle for the treatment of gliomas by *in vivo* gene therapy.

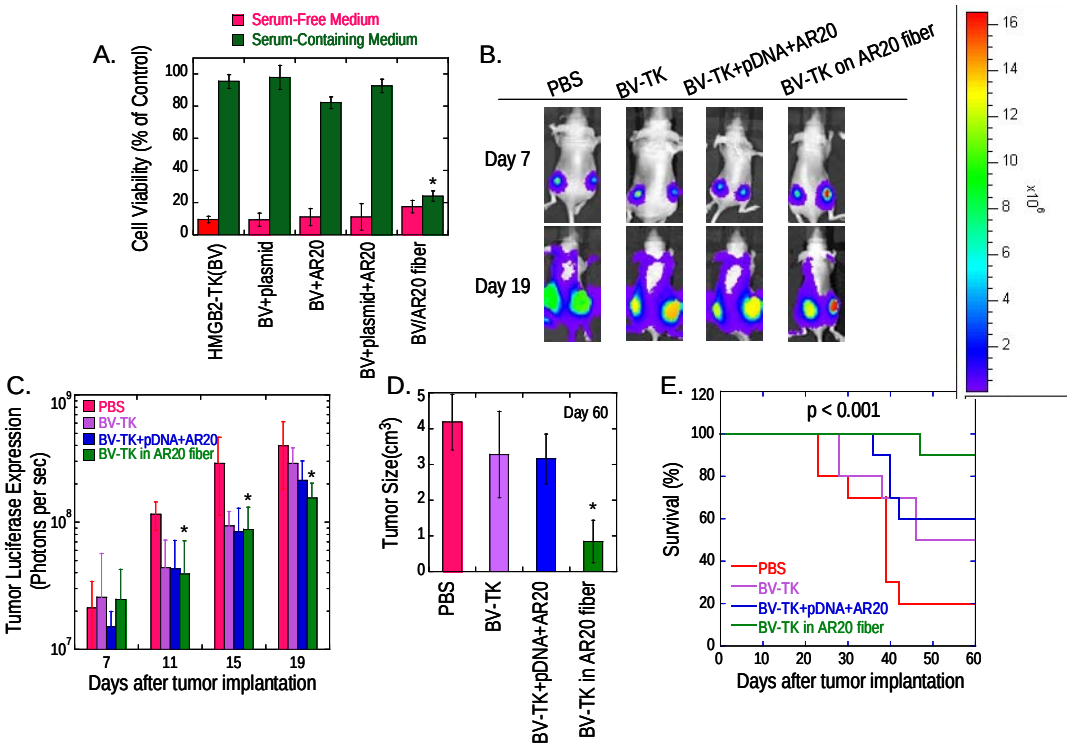

Figure 3.4 - Tumor inhibitory effect of bio-microfiber encapsulating HMGB2-TK-BV. (a) Cell viability analysis of HMGB2-TK-BV–transduced U87 glioblastoma cells using quantitative MTS assays. BV containing an HMGB2-TK construct were employed to form complex or fiber with plasmid DNA and AR20 peptide using the same ratio as previously described. Cells were transduced for 24 hours with BV-TK, BV-TK+pDNA, BV-TK+AR20, BV-TK+pDNA+AR20, and BV-TK in AR20 fiber at an MOI of 50, followed by treatment with the prodrug GCV 500 μmol/L for another 24 hours. Cell survival rates were then measured by MTS assay (Promega) following the manufacturer's instructions. Cells were seeded onto 96-well plates at 1 × 104 cells per well in DMEM supplemented with 10% FBS and infected with BVs. The spectrophotometric assay for cell proliferation was performed 24 and 48 hours later by measuring OD at 490 nm. For *in vivo* study, human glioma U87-Luc cells were inoculated into the back region of nude mice. After the tumor became visible, naked HMGB2-TK-BV, fiber encapsulating HMGB2-TK-BV, PBS, and a mixture containing HMGB2-TK-BV, plasmid DNA, and AR20 peptide, were injected into tumor xenografts on day 7 and day 14 post-tumor implantation, respectively. GCV (5 mg/mL) intraperitoneal injection was performed daily from day 8 to day 20. (b) IVIS bioluminescence images of tumors. Photos were taken non-invasively on day 7 and day 19 post-tumor cell inoculation, respectively, using the IVIS imaging system. (c) Quantitative analysis of tumor burden from IVIS bioluminescence images. The data are presented as the mean of tumor burden ± SD from 10 mice per group imaged 7 and 19 days post-tumor cell inoculation. (d) Tumor size measurements of nude mice treated with bio-microfiber. Tumor size was measured by a caliper and calculated as 0.5 x width^2 x length and shown as cm^3 at day 60. (e) Prolonged survival of mice treated with various gene delivery reagents containing HMGB2-TK-BV. The mice were observed until 60 days post-tumor inoculation. The significance was determined by the two-factor analysis of variance with replication followed by ANOVA analysis using SigmaStat 3.1 software. The statistical analysis of survival data was performed using the log rank test. A $P<0.05$ was considered statistically significant. BV, baculovirus; DMEM, Dulbecco's Modified Eagle's Medium; FBS, fetal bovine serum; GCV, ganciclovir; HMGB2, human high-mobility group box 2; Luc, luciferase; MOI, multiplicity of infection; PBS, Phosphate Buffered Saline; TK, thymidine kinase.

3.4 Discussion

Microfiber structure is one of the most extensively studied synthetic polymer biomaterials currently employed in tissue engineering and regenerative medicines (Sarkar *et al.*, 2006). Polymeric materials are often modified to advance their desired biological activities through chemical reactions, coating, or encapsulation with biologics. However, this approach is rarely applied in cancer therapy through gene delivery, which requires effective transgene expression to kill tumor cells, even though several groups have demonstrated the possibility of accomplishing tumor inhibition by co-delivery of various polymer structures and drugs. In terms of treating brain tumors， researchers have developed several promising pre-clinical combined drug–polymer implants, including biodegradable 5-flurouracil-loaded microspheres, carboplatin-loaded PLGA microspheres, biodegradable PLGA polymer sheets, and aclarubicin-loaded cationic-albumin pegylated nanoparticles (Lu *et al.*, 2007; Menei *et al.*, 1996; Chen and Lu, 1999). The development of drug resistance has been a major hindrance to the successful application of such drug delivery methods. This limitation, however, has led to the evolution of other polymer-mediated cancer therapies. For example, it was reported that paclitaxel-loaded biodegradable PLGA microfiber implants can effectively deliver paclitaxel for post-surgical chemotherapy against malignant glioma, and can mediate the sustained release of paclitaxel from fiber matrices (Ranganath and Wang, 2008). This discovery shed light on the application of microfiber in drug and gene delivery therapies for glioma, especially by means

of gene therapy where genetic composition can be tailored to fundamentally correct tumor pathogenicity.

This study has provided evidence for the first time that microfiber assembly can significantly improve the transduction and therapeutic efficiency of BV-based gene transfer vectors in glioma cells, both *in vitro* and *in vivo*. Effective gene delivery to tumor cells is essential for genetic treatment of CNS diseases such as glioma. It has been well established that BV as a novel gene transfer vector can transduce a number of mammalian cell lines, with satisfactory transduction efficiency and a bio-safety profile free from apparent viral replication or cytopathic effects (Boyce and Bucher, 1996). No viral replication or transcription of the BV genome has been detected in mammalian cells. Despite these encouraging advantages, however, one of the most challenging obstacles to the successful application of BV vectors has been its poor *in vivo* performance due to the vulnerability of BV to serum complement factors presented in the blood stream after systemic administration (Hofmann and Strauss, 1998). BV-mediated gene transfer has also been hampered by serum complement in organs in direct contact with complement components. This fact was corroborated by our *in vitro* transduction experiment in the presence of both human and mouse serum complement (Figure 3.5). In this study, we identified an innovative material engineering approach to overcome the problem of serum complement inactivation, thereby furthering the potential applications of BV vectors for genetic treatment of CNS diseases.

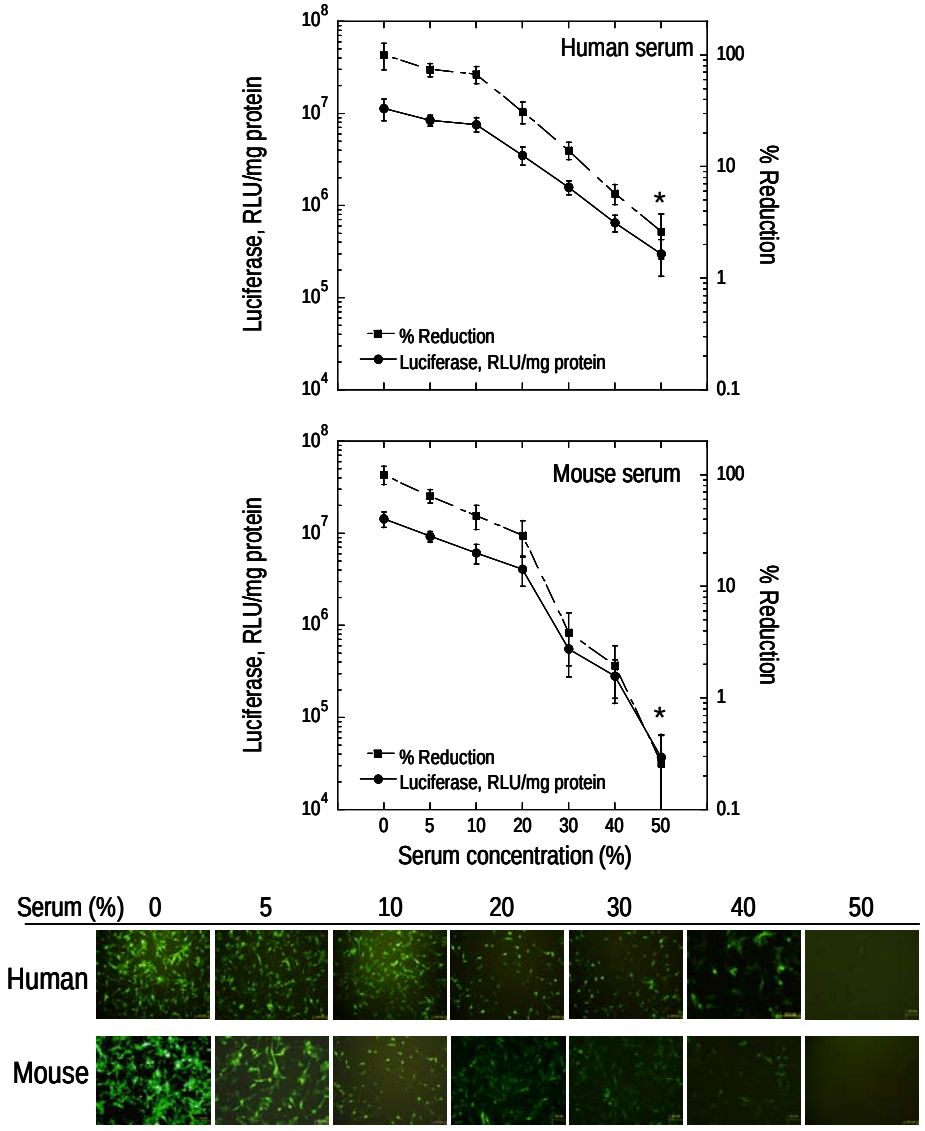

Figure 3.5 - Effect of human and mouse serum concentration on BV transduction efficiency. Human U87 glioblastoma cells were used. Cells were transduced by BVs at an MOI of 50 PFU per cell. Naked BVs were pre-treated with serum complement at 37°C for 30 minutes. 100 µL serum complement was used to inactivate BV, fiber, and the mixture. The serum complement concentration range from 0 to 50% was achieved by adjusting the BV solution volume while keeping the BV copy number constant. After serum treatment, cell culture media containing U87 cells were added on top of the BV and serum mixture, making the final volume in each well 2 mL and therefore the final serum complement concentration 5%, to minimize the cytotoxic effect of serum complement on U87 cells. (a) Luciferase expression profiles at various serum concentrations. Luciferase assay was performed 24 hours post-transduction on U87 cells transduced with CMV-Luc BV. The results are shown as mean RLU of luciferase activities per mg of cellular protein (mean ± SD, obtained from five replicate assays). Percentage of reduction in BV transduction efficiencies is indicated. (b) EGFP expression profiles at various serum concentrations. The cells transduced with CMV-EGFP BV were photographed under fluorescent microscope 24 hours after transduction. BV, baculovirus; CMV, cytomegalovirus; EGFP, enhanced green fluorescent protein; Luc, luciferase; MOI, multiplicity of infection; PFU, plaque-forming units; RLU, relative light unit.

We further examined the mechanism by which microfiber encapsulation can protect BV against serum complement inactivation, and achieved enhanced transduction efficiency with fiber-encapsulated BV. Since the size of most mammalian cells is comparable to these microfibers (10–100 μm), upon attachment to the microfibers the cells still exhibit a 3D topology with a curvature that depends on the compatibility of the dimensions of the cells and microfibers. Because of their microscale sizes, the mechanical strength of the fibers usually prevents further material structural alteration as a result of the forces exerted by cells during the adhesion, migration, and transduction processes. We incorporated BV particles in the microfiber assembled through charge attraction between condensed peptide and plasmid DNA electrolyte solutions, with an encapsulation efficiency of 68% (Table 3.1). Since fibers both with and without BV encapsulation dissolve slowly in cell culture medium (up to 10 hours) (Figure 3.6), we reasoned that the fibers would shield the virus for a certain period of time. Many peptides with a standard amphiphilic binary pattern easily aggregate to form bundles or gels of assembled structures displaying varying morphologies. The broad hydrophobic or charged faces of the peptides offered the possibility for varied interfacing and intermolecular arrangements with DNA, allowing the formation of a range of microfibers. The interactions appeared to form nanofiber intermediates, and further bundled and formed a network towards a microfiber architecture. Rheology measurements revealed that the viscosity of the peptide and plasmid mixture increased exponentially after being blended together, indicating the possible formation of polyelectrolyte complex and possibly nanofibers among these two components (Figure 3.7). This finding, coupled

with the fact that plasmid retains its functionality after forming fiber with peptide (Figure 3.8), further supports the supposition that the released virus may be still surrounded by peptide–DNA nanofibers or fragments assembled from the active DNA and peptide, which need to be degraded extracellularly or even intracellularly before gene expression can reach its peak. We illustrated that the virus does not show any significant loss in activity in the encapsulation process. In addition, we noticed that there was no new chemical bond formed during the fiber formation process (Figure 3.9), suggesting the main driving force behind fiber formation is electrostatic interaction. Based on these characterization studies, we speculate that the underlying mechanics of the protection of fibers against serum inactivation is that fibrous matrices not only mediate controlled and sustained release of BVs into the media as the fiber dissolves, but also provide greater surface area to volume ratio for effective BV release rates directly to the cells attached to the fiber. Even after being released into the serum-containing media, the BV particles may still be coated or bound by the peptide–DNA nanofibers or peptide molecules alone, which on their own have already shown some ability to protect BV from serum inactivation (data not shown). Conversely, free BV particles are completely exposed to the serum-containing media during the diffusion process, a major means by which BVs approach the cell surface, and transduction activity is easily inhibited by the complement factor unless a system of shielding, timed releasing, or protective tagging is employed.

Sample	Ct/Mean	SQ Mean	Total BV copy number
Original BV	15.52	1.12E+07	4.13E+08
Fiber	15.51	1.13E+07	2.81E+08
Leftover	16.70	5.30E+06	1.32E+08
Encapsulation efficiency	68%		

Table 3.1 - BV encapsulation efficiency of fiber. Fiber containing CMV-Luc-BV was produced as previously described. Immediately after the fiber was fabricated, both the fiber and the leftover mixture were dissolved in 200 µL cell culture media followed by copy number measurement by Real-Time quantitative PCR. Encapsulation efficiency is calculated as BV copy number in fiber divided by total BV copy number used to form fiber. BV, baculovirus; CMV, cytomegalovirus; Luc, luciferase; PCR, polymerase chain reaction.

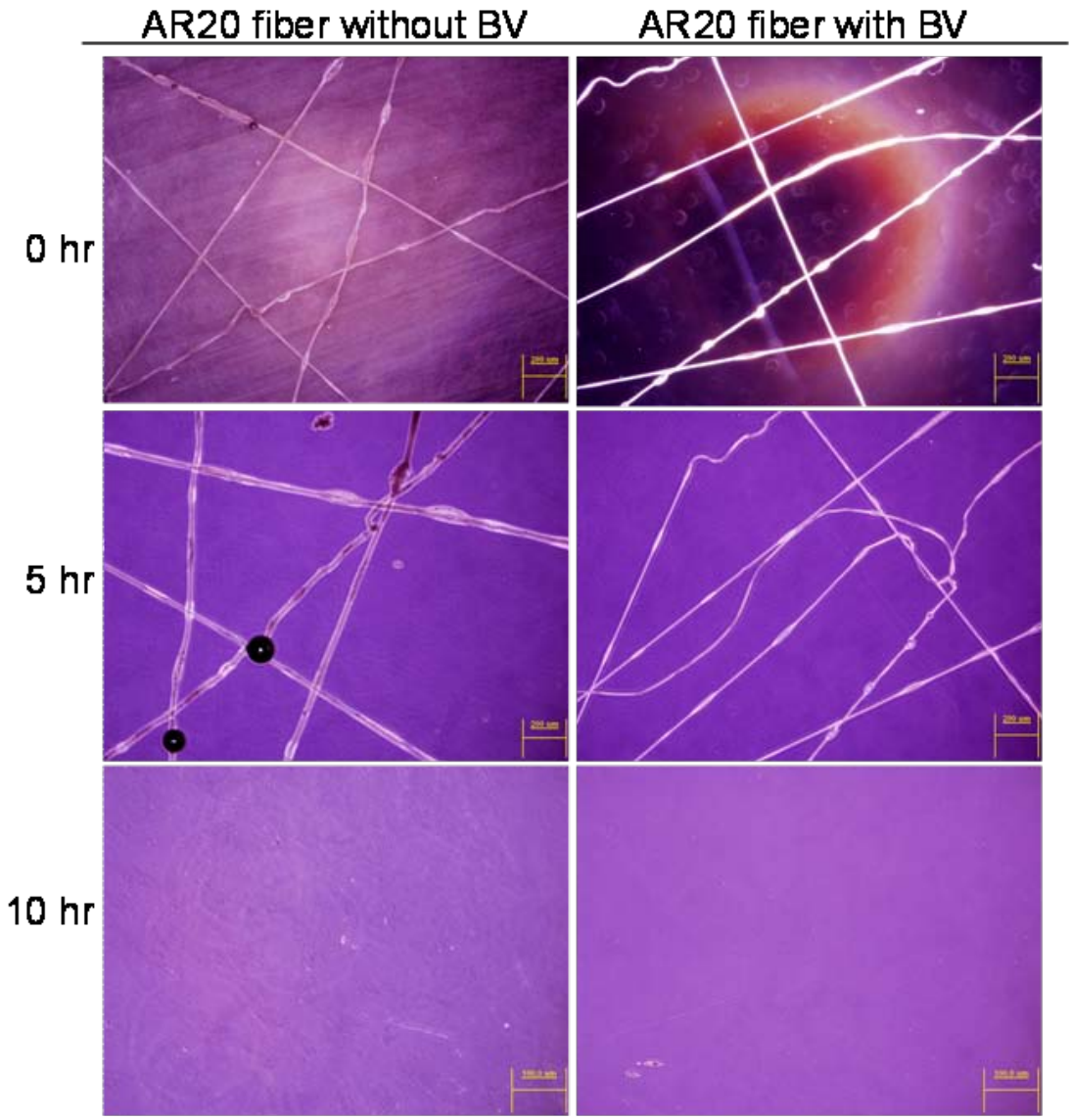

Figure 3.6 - Solubility of AR20 fibers without or with BV encapsulation. Photos were taken under light microscope showing AR20-DNA fiber morphology (left panel) in DMEM cell culture media containing 10% FBS and 1% penicillin-streptomycin at 0, 5, and 10 hours, respectively. Photos in the right panel show the morphology of AR20-DNA fibers encapsulating BV under the same conditions at 0, 5, and 10 hours, respectively, suggesting fibers both with and without BV encapsulation were degraded and dissolved within 10 hours. The fibers were viewed under a transmission microscope at 4x magnification. BV, baculovirus; DMEM, Dulbecco's Modified Eagle's Medium; FBS, fetal bovine serum.

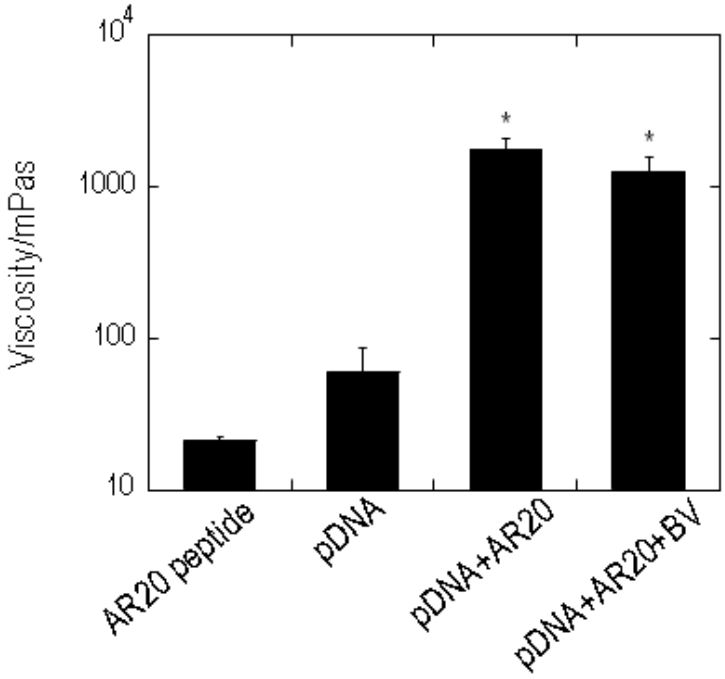

Figure 3.7 - Rheological properties of the raw materials used to form fiber. Fiber formation was performed using an 8 µg/µL AR20 peptide solution and 8 µg/µL plasmid DNA solution. The two solutions were mixed together with a 1:1 volume ratio to form the pDNA+AR20 mixture solution used for viscosity measurements. Meanwhile, a plasmid DNA solution was mixed with a concentrated BV PBS solution with the titer of 10^9 PFU per mL using a volume ratio of 3:1 to constitute the negatively charged polyelectrolyte solution. This mixture was then mixed with the AR20 peptide solution noted above with a 1:1 volume ratio, after which viscosity measurements were performed with a RheoScope 1 rheometer. BV, baculovirus; PBS, Phosphate Buffered Saline; PFU, plaque-forming units.

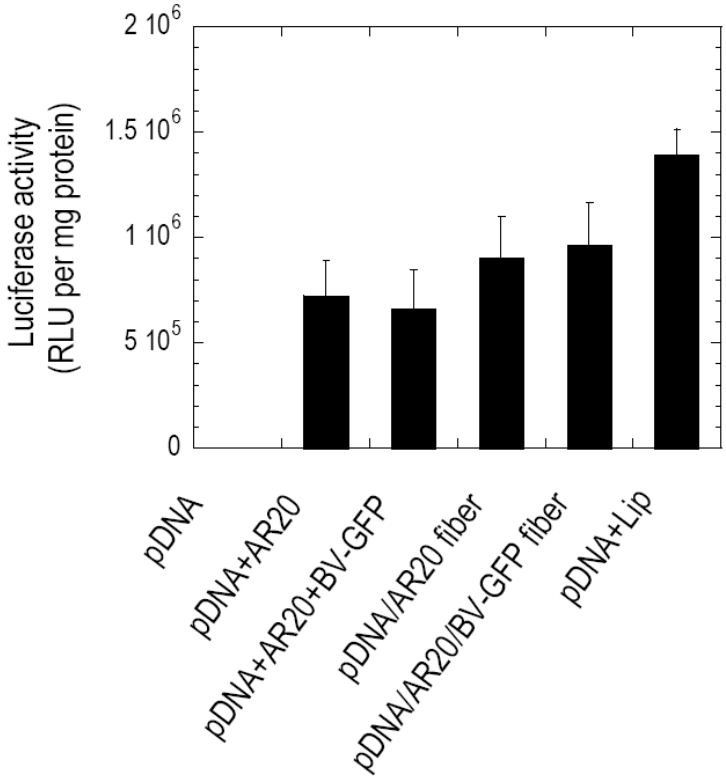

Figure 3.8 - Luciferase gene expression profiles of plasmid DNA in fibers and mixtures. Transfection efficiencies of plasmid DNA before and after the formation of fiber. Human U87 glioblastoma cells were used. For the lipofectin group, 10 μg of DNA was diluted in 100 μL of Opti-MEM I Reduced Serum Medium followed by the dilution of 10 μL of Lipofectin in 100 μL of Opti-MEM I Medium. The solutions were left to stand at room temperature for 40 minutes, after which the diluted DNA was combined with the diluted Lipofectin (total volume = 200 μL). The solution was mixed gently and incubated for 15 minutes at room temperature. For the fiber groups, 10 μg of DNA was used to form fiber with peptide or peptide and BV using the same ratio as previously described. For the mixture groups, the same amount of plasmid DNA was mixed with the amount of peptide or peptide and BV used previously to form the fiber. U87 cells were transfected into 24-well plates per cell by pDNA, pDNA+AR20, pDNA+AR20+BV-GFP, pDNA/AR20 fiber, pDNA/AR20/BV-GFP fiber, and pDNA+ Lipofectin. Cells were cultivated in the growth medium for 24 hours before the luciferase assay. The results are shown as the mean RLU of luciferase activities per mg of cellular protein (mean ± SD, obtained from five replicate assays). BV, baculovirus; GFP, green fluorescent protein; Lip, Lipofectin; RLU, relative light unit.

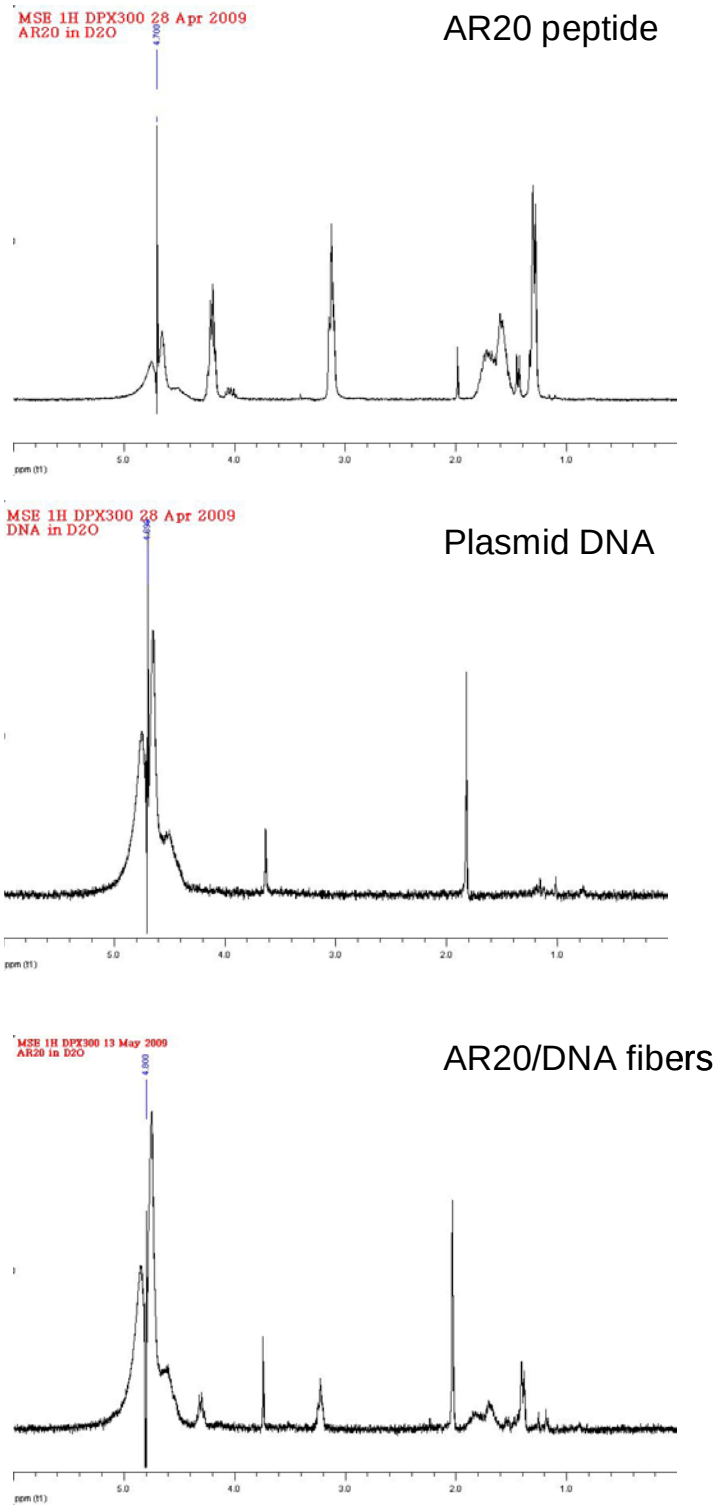

Figure 3.9 - NMR spectrum of peptide, plasmid DNA, and peptide–DNA fiber. Fiber was formed as previously described using 8 µg/µL AR20 peptide solution and 8 µg/µL plasmid DNA solution. The same solutions were used to carry out the NMR measurements. All samples were prepared by dissolving about 10 mg of materials in 1 mL D_2O. The 1 hour NMR was performed with a Bruker DPX-300 NMR Spectrometer. D_2O, deuterium oxide; NMR, nuclear magnetic resonance.

Another hallmark of our findings is the suppressive effect of HMGB2-TK-BV-containing microfiber on subcutaneously inoculated tumors compared with the naked BV in nude mice. Malignant glioma, known as glioblastoma multiforme, is characterized by aggressive ontogenesis of undifferentiated cells, pervasive invasion into nearby brain tissue, and a high percentage of recurrence, and is therefore one of the most refractory tumors. Although most glioma patients have access to state-of-the-art imaging, neurosurgery, radiotherapy, and chemotherapy, the median survival time is around 3 months and most patients fail to live more than 3 years post-diagnosis (Ohgaki *et al.*, 2004; Ohgaki and Kleihues, 2005). Recent advancements in molecular biology and gene therapy have provided the tools to treat patients with malignant brain tumors by modifying the gene expression profiles in tumor cells. Virus-mediated transfer of the HSV-TK gene has been commonly employed to present cytotoxic sensitivity to nucleoside analogues, such as GCV, in a wide spectrum of tumor cells both *in vitro* and *in vivo* (Moolten, 1986). HSV-TK protein functions by converting the prodrug GCV into a phosphorylated compound that selectively defeats dividing cells by acting as a chain terminator in DNA synthesis. This approach is particularly suitable for treatment of glioma tumors, which grow aggressively and invade normal brain tissue, consisting largely of non-proliferating cells. Recombinant retroviral vectors containing HSV-TK have been successfully generated and used to confer significant regression of tumors originated from inoculating glioma cells in rat brains (Culver *et al.*, 1992). Tumor development and progression engage alterations in a variety of genes; therefore, a variety of BV-based gene delivery approaches for malignant gliomas have been established. The

recombinant BV vector has been used extensively to achieve high levels of transduction efficiency and transgene expression in cultured mammalian cells and in experimental animal models. Attempts have been made to experimentally treat glioma by systemic injecting of PEI-coated BV vectors in a nude mice xenograft model, and the resulting binary complex is resistant to serum complement inactivation when compared with naked BV (Yang *et al.*, 2009). On the other hand, based on the observation that the HMGB2 promoter is capable of inducing glioma-specific gene expression, targeted cancer therapy has been realized by using a BV vector expressing the HSV-TK suicide gene driven by the HMGB2 promoter (Balani *et al.*, 2009).

Encouraged by the findings in previous studies, we hypothesized that the microfiber complexation methodology may offer the possibility of circumventing the serum inactivation problem faced by BV vectors *in vivo*. We investigated the capacity of a hybrid BV-fiber vector to produce a high level of transduction and gene expression of HSV-TK under the control of the HMGB2 promoter, and to render U87 glioma cells vulnerable to the cytotoxic effects of phosphorylated GCV. Polyelectrolyte fibers were formed by drawing two droplets of peptide and plasmid DNA plus therapeutic BV solution together, and glioma xenografts were established in nude mice using U87-Luc cells, followed by double injections of the designated vectors into the xenografts at a 1-week interval. As expected, there was an obvious lag in the speed of tumor growth in the mice injected with fiber-encapsulated HMGB2-TK-BV as compared to the naked HMGB2-TK-BV and other control groups. This suggests that local recurrence of the tumor is controlled and inhibited by the

sustained release of therapeutic BV vectors from the protective fiber, preventing them from being inactivated by serum complement factors being present in the vascularized tumor tissues. This finding is further confirmed by the smaller local glioma size observed is the groups treated with fiber-encapsulated BV, as well as an increased survival rate in the fiber group. Thus, by inhibiting local recurrence possibly induced by complement inactivating effect of the surrounding blood serum, improvement in patient survival seems achievable.

CHAPTER 4

CONCLUSION

4.1 Results and Indications

The objective of this study was to establish safe and efficient gene delivery systems with the objective of significantly improving the gene transfer performance for neurological disorders in the CNS, particularly glioma tumors. This study can be divided into two parts: establishing both DNA-based and BV-based bio-nanoparticles, and developing bio-microfibers for BV encapsulation.

4.1.1 Generation and Assessment of Bio-nanoparticles

While both magnetic field-mediated gene transfer and Tat peptide-assisted delivery offer attractive therapeutic features, this study has documented that the two methods combined provide additional advantages in improving targeted transgene expression. We believe this strategy holds potential for gene therapy applications, especially those that require targeting approaches for effective localized treatment. Gene delivery using PEI involves condensation of DNA into compact particles, uptake into the cells, release from the endosomal compartment into the cytoplasm, and uptake of the DNA into the nucleus. This multistep process indicates that there are many factors affecting the transfection efficiency of PEI-based gene delivery vectors, including particle size, molecular weight, shape (branch or linear), and surface charge. The magnetic nanoparticles used in this study were coated with PEI 25 kDa; therefore, the gene transfer route was expected to resemble that mediated solely by PEI. We intended to accelerate the cell uptake process by applying an external magnetic force during the transfection process and then expediting the endosomal escape step by tagging the vector with Tat peptide.

In this way, the traditional PEI vector was multifunctionalized to achieve enhanced transfection efficiencies.

Gene therapy holds promise in treating neurological disorders such as glioma, but is still in the pre-clinical trial phase. One of the most challenging obstacles to successful clinical application is the difficulty in achieving efficient gene delivery to the brain due to the blood–brain barrier. The bio-nanoparticle system developed in this study could potentially provide an innovative engineering approach to this problem. We used lumbar injection, a low invasive procedure, to circumvent the blood–brain barrier for efficient gene expression in the spinal cord. However, only limited distribution of gene expression can be observed in the CNS, probably due to CSF flow, which poses a restriction on the use of this technique for the treatment of CNS disorders.

One of the most promising features of bio-nanoparticles is their ability to target the genes in special organs or tissues in the presence of an external magnetic force. This study showed the potential of magnetofection to deliver genes to desired sites in the CNS using external magnetic fields. During the animal study, we found an external magnet could be used to manipulate the distribution of gene transfer vectors along the spinal cord. Under magnetic guidance, bio-nanoparticles were forced to accumulate in the cervical region of the spinal cord as indicated by the gene expression patterns, suggesting this modular approach can be practically used to overcome the blood–brain barrier. Future studies could focus on the in-depth development and

optimization of such retargeting platform technologies to circumvent current barriers to glioma gene therapy. In addition, new magnetic guiding systems need to be designed and optimized to produce suitable magnetic forces for use in human gene therapy.

We found that the transduction efficiency of BV-based bio-nanoparticles was substantially higher than that achieved by naked BV when magnetic force was applied, an indication that gene delivery performance in a serum-containing environment could be greatly improved by forming bio-nanoparticles with PolyMag. Moreover, our results suggested that the magnetic force played an important role in enhancing the luciferase expression of the PolyMag-BV complex. Results obtained in the absence and in the presence of external magnetic force during transduction in a serum-containing medium indicated the multifunctionality of the PolyMag-BV bio-nanoparticles to simultaneously achieve magnetically guided transduction and the protection of BV against serum complement inactivation.

We used human glioma cell lines and animal models of human gliomas to investigate the gene delivery efficiency and therapeutic efficacy of the developed bio-nanoparticles. We employed mainly reporter genes such as EGFP and luciferase to characterize our designated modular gene delivery systems. For future studies, it would be useful to customize the complex forming parameters and transfection or transduction conditions for the therapeutic genes when designing more complicated gene transfer vectors for clinical application. We expect the knowledge gleaned from this project could

be valuable in developing effective and potent delivery vectors not only for gene therapy of gliomas, but also for other types of tumors. In addition, when dealing with other relevant plasmid DNA or virus complex vectors, the production procedures and characterization methods should be optimized according to the unique features of specific vector constructs.

4.1.2 Assembly and Evaluation of Bio-microfibers

We established a method to form bio-microfibers through self-assembly of polyelectrolytes comprising plasmid DNA and amphiphilic and Tat peptides, and used the fibers to encapsulate BV particles to protect the viruses against serum complement inactivation. The suicide gene-mediated glioma therapy could be accomplished by BV carrying HSV-TK under the control of the glioma-specific HMGB2 promoter, followed by systemic administration of the prodrug GCV. However, the efficacy of this approach is often undermined by serum complement inactivation of the BV, resulting from angiogenesis and pre-existing blood vessels present in tumor tissues, which makes it extremely difficult to achieve sufficient suicide gene expressions within gliomas. We demonstrated that BVs retain their activity in the presence of human serum complement after being encapsulated in the fiber. More importantly, the incorporated BV vectors were found to be functional in suppressing the aggressive growth of human brain tumor xenografts in nude mice. The HMGB2-TK-BV–based bio-microfibers were shown to effectively induce cell death in the presence of GCV. A luciferase reporter gene expressing human glioma cell line (U87-Luc) in the xenograft animal model was established in this study, allowing for non-invasive monitoring of glioma growth *in vivo*. High

transduction efficiency was observed in U87 cells *in vitro*, when transduced by HMGB2-TK-BV–based bio-microfibers pre-treated with human serum complement. Thus, it is reasonable to expect a significant suppression of U87 cell growth in similar animal models. Even though the U87 cells were not completely eliminated by the HSV-TK gene expression, probably due to the poor diffusion of injected bio-microfibers within the tumor mass, the gene delivery efficiency of bio-microfibers was high enough to inhibit tumor growth when compared with naked BV and other unprotected viral vectors. To improve delivery efficiency, we attempted to implant the bio-microfiber inside the glioma xenografts in nude mice. The overall gene expression level in the entire tumor mass was not increased, although local expression along the implantation site appeared elevated. Therefore, it is necessary to further enhance the inhibitory effect of such bio-microfibers by either injecting fiber solutions into several sites of the glioma mass, or optimizing delivery protocols in the pre-clinical study. The current proof-of-principle study has provided gene therapeutic strategies to overcome one of the most challenging issues still outstanding for clinical application of BV-mediated gene therapy in malignant gliomas. In this study, the therapeutic efficacy of bio-microfibers was tested only in human glioma cell line xenograft models. Further research could also involve tumors generated by stereotaxic intracerebral injection of human glioma cells in nude mice for more clinically relevant results. Thus, the gene delivery systems developed in this study hold great potential for gene therapy of disorders in the CNS.

4.2 Conclusion

With hybrid non-viral and viral vectors, this study provides useful delivery systems for gene therapy of disorders in the CNS. In this study, to develop efficient gene delivery systems for CNS disorders, especially glioma, we investigated DNA and BV-mediated gene delivery systems by modification or combination with other materials such as nanoparticles and microfibers. We also tried to apply them in a CNS disease model—glioma tumors—both *in vitro* and *in vivo* to explore the possibility of their application in human gene therapy. Efficient and site-specific gene delivery to the CNS is critical for the success of gene therapy to achieve satisfactory therapeutic effects. We successfully generated the magnetic complexes for efficient gene transfer *in vitro* by incorporating Tat peptides with PolyMag/DNA. We also demonstrated the possibility of assembling bio-nanoparticles using BV and PolyMag, and their efficient *in vitro* gene delivery performance in preventing serum complement inactivation. This study documented that magnetically guided gene delivery can conquer the distribution confinement of gene agents intrathecally injected in the CNS. Therefore, the combination of magnetofection and the spinal fluid delivery technique hold significant potential to effectively delivery therapeutic genes to the CNS for the treatment of glioma, spinal cord injury, and other degenerative neurological illnesses. In addition, we illustrated that microfiber structures could be formed by self-assembly of concentrated peptide solutions and plasmid DNA solutions through electrostatic interaction. Numerous advantages highlight the newly emerged BV as one of the most promising gene delivery vectors. Such fibers could be used to encapsulate BV for the purpose of protecting it against

serum complement inactivation presented during systemic administration. The BVs incorporated in the microfiber were found to be resistant to serum complement inhibition. Moreover, bio-microfibers encapsulating therapeutic BVs were discovered to suppress tumor growth in human glioma cell line xenograft animal models, indicating the strong clinical application potential of such technology.

The procedures and findings presented in this thesis involve the preparation, characterization, and assessment of the transduction efficiency and therapeutic efficacy of two gene delivery systems: plasmid DNA or BV-based bio-nanoparticles and BV-based bio-microfibers. Our findings suggest these delivery systems are efficient both *in vitro* and *in vivo*, and their applications in glioma models indicate their promising future in clinical glioma therapy, although further improvements and modifications are needed for optimal therapeutic effect. To the best of our knowledge, this study is the first demonstration of the use of microfiber structures to protect BV against serum complement inactivation and the use of such vectors for cancer gene therapy in an animal model. We believe our results will provide important insights for potential human clinical trials. Due to the disappointing outcomes of clinical trials in current glioma gene therapy, it is crucial to establish efficient gene delivery vector systems that can be safely adopted in the clinical setting. The knowledge generated from these experimental results, such as the development of complex gene transfer vectors and the evaluation of relevant complexation methodologies, should greatly assist the exploration and

establishment of CNS gene therapies as well as the promotion of BV-related and gene therapy-related fields.

REFERENCES

Abdallah B, Hassan A, Benoist C, Goula D, Behr JP, Demeneix BA. A powerful non-viral vector for *in vivo* gene transfer into the adult mammalian brain: polyethylenimine. *Hum Gene Ther.* 1996;7:1947–1954.

Ayres MD, Howard SC, Kuzio J, Lopez-Ferber M, Possee RD. The complete DNA sequence of *Autographa californica* nuclear polyhedrosis virus. *Virology*. 1994 Aug 1;202(2):586–605.

Balagúe C, Kalla M, Zhang WW. Adeno-associated virus Rep78 protein and terminal repeats enhance integration of DNA sequences into the cellular genome. *J Virol.* 1997 Apr;71(4):3299–3306.

Balani P, Boulaire J, Zhao Y, Zeng J, Lin J, Wang S. High mobility group box2 promoter-controlled suicide gene expression enables targeted glioblastoma treatment. *Mol Ther.* 2009 Jun;17(6):1003–1011.

Barsoum J, Brown R, McKee M, Boyce FM. Efficient transduction of mammalian cells by a recombinant baculovirus having the vesicular stomatitis virus G glycoprotein. *Hum Gene Ther.* 1997 Nov 20;8(17):2011–2018.

Bearer EL, Schlief ML, Breakefield XO, Schuback DE, Reese TS, LaVail JH. Squid axoplasm supports the retrograde axonal transport of herpes simplex virus. *Biol Bull.* 1999 Oct;197(2):257–258.

Berry CC. Intracellular delivery of nanoparticles via the HIV-1 Tat peptide. *Nanomed.* 2008 Jun;3(3):357–365.

Boussif O, Lezoualc'h F, Zanta MA, Mergny MD, Scherman D, Demeneix B, Behr JP. A versatile vector for gene and oligonucleotide transfer into cells in culture and *in vivo*: polyethylenimine. *Proc Natl Acad Sci U S A.* 1995 Aug 1;92(16):7297–7301.

Boyce FM, Bucher NL. Baculovirus-mediated gene transfer into mammalian cells. *Proc Natl Acad Sci U S A.* 1996 Mar 19;93(6):2348–2352.

Bronich TK, Kabanov AV, Kabanov VA, Yu K, Eisenberg A. Soluble complexes from poly(ethylene oxide)-*block*-polymethacrylate anions and *N*-alkylpyridinium cations. *Macromol.* 1997;30:3519–3525.

Brooks H, Lebleu B, Vivès E. Tat peptide-mediated cellular delivery: back to basics. *Adv Drug Deliv Rev.* 2005 Feb 28;57(4):559–577.

Campeau P, Chapdelaine P, Seigneurin-Venin S, Massie B, Tremblay JP. Transfection of large plasmids in primary human myoblasts. *Gene Ther.* 2001 Sep;8(18):1387–1394.

Cepko CL, Ryder E, Austin C, Golden J, Fields-Berry S, Lin J. Lineage analysis with retroviral vectors. *Methods Enzymol.* 2000;327:118–145.

Chen W, Lu DR. Carboplatin-loaded PLGA microspheres for intracerebral injection: formulation and characterization. *J Microencapsul.* 1999 Sep-Oct;16(5):551–563.

Coffin J, Hughes Stephen H. Varmus Harold E.. *Retrovirus*. Plainview: Cold Spring Harbor Laboratory Press; 2000.

Condreay JP, Witherspoon SM, Clay WC, Kost TA. Transient and stable gene expression in mammalian cells transduced with a recombinant baculovirus vector. *Proc Natl Acad Sci U S A.* 1999 Jan 5;96(1):127–132.

Culver K, Ram Z, Wallbridge S, Ishii H, Oldfield EH, Blaese RM. *In vivo* gene transfer with retroviral vector-producer cells for treatment of experimental brain tumors. *Science.* 1992 Jun 12;256:1550–1552.

Dai Y, Schwarz EM, Gu D, Zhang WW, Sarvetnick N, Verma IM. Cellular and humoral immune responses to adenoviral vectors containing factor IX gene: tolerization of factor IX and vector antigens allows for long-term expression. *Proc Natl Acad Sci U S A.* 1995 Feb 28;92(5):1401–1405.

Davis ME. Non-viral gene delivery systems. *Curr Opin Biotechnol.* 2002;13:128–131.

Dobson J. Gene therapy progress and prospects: magnetic nanoparticle-based gene delivery. *Gene Ther.* 2006 Feb;13(4):283–287.

Factor P. Gene therapy for acute diseases. *Mol Ther.* 2001;4:515–524.

Fairman R, Åkerfeldt KS. Peptides as novel smart materials. *Curr Opin Struct Biol.* 2005;15:453–463.

Fischer D, Bieber T, Li Y, Elsässer HP, Kissel T. A novel non-viral vector for DNA delivery based on low molecular weight, branched polyethylenimine: effect of molecular weight on transfection efficiency and cytotoxicity. *Pharm Res.* 1999 Aug;16(8):1273–1279.

Fisher KJ, Choi H, Burda J, Chen SJ, Wilson JM. Recombinant adenovirus deleted of all viral genes for gene therapy of cystic fibrosis. *Virology.* 1996 Mar 1;217(1):11–22.

Ghosh S, Parvez MK, Banerjee K, Sarin SK, Hasnain SE. Baculovirus as mammalian cell expression vector for gene therapy: an emerging strategy. *Mol Ther.* 2002 Jul;6(1):5–11.

Godbey WT, Wu KK, Mikos AG. Poly(ethylenimine) and its role in gene delivery. *J Control Release.* 1999 Aug 5;60(2-3):149–160.

Goula D, Remy JS, Erbacher P, Wasowicz M, Levi G, Abdallah B, Demeneix BA. Size, diffusibility and transfection performance of linear PEI/DNA complexes in the mouse central nervous system. *Gene Ther.* 1998 May;5(5):712–717.

Guibinga GH, Friedmann T. Baculovirus GP64-pseudotyped HIV-based lentivirus vectors are stabilized against complement inactivation by codisplay of decay accelerating factor (DAF) or of a GP64-DAF fusion protein. *Mol Ther.* 2005 Apr;11(4):645–651.

Gupta B, Levchenko TS, Torchilin VP. Intracellular delivery of large molecules and small particles by cell-penetrating proteins and peptides. *Adv Drug Deliv Rev*. 2005 Feb 28;57(4):637–651.

Harada A, Kataoka K. Novel polyion complex micelles entrapping enzyme molecules in the core: preparation of narrowly distributed micelles from lysozyme and poly(ethylene glycol)-poly(aspartic acid) block copolymers in aqueous medium. *Macromol.* 1998;31(2):288–294.

Hardy S, Kitamura M, Harris-Stansil T, Dai Y, Phipps ML. Construction of adenovirus vectors through Cre-lox recombination. *J Virol.* 1997 Mar;71(3):1842–1849.

Hartgerink JD, Beniash E, Stupp SI. Peptide-amphiphile nanofibers: a versatile scaffold for the preparation of self-assembling materials. Proc Natl Acad Sci U S A. 2002 Apr 16;99(8):5133–5138.

Ho Y, Lin PH, Liu CY, Lee SP, Chao YC. Assembly of human severe acute respiratory syndrome coronavirus-like particles. *Biochem Biophys Res Commun.* 2004 Jun 11;318(4):833–838.

Hoare J, Waddington S, Thomas HC, Coutelle C, McGarvey MJ. Complement inhibition rescued mice allowing observation of transgene expression following intraportal delivery of baculovirus in mice. *J Gene Med.* 2005 Mar;7(3):325–333.

Hofmann C, Hüser A, Lehnert W, Strauss M. Protection of baculovirus-vectors against complement-mediated inactivation by recombinant soluble complement receptor type 1. *Biol Chem.* 1999 Mar;380(3):393–395.

Hofmann C, Strauss M. Baculovirus-mediated gene transfer in the presence of human serum or blood facilitated by inhibition of the complement system. *Gene Ther.* 1998 Apr;5(4):531–536.

Hüser A, Rudolph M, Hofmann C. Incorporation of decay-accelerating factor into the baculovirus envelope generates complement-resistant gene transfer vectors. *Nat Biotechnol.* 2001 May;19(5):451–455.

Jen,C.P., Chen,Y.H., Fan,C.S., Yeh,C.S., Lin,Y.C., Shieh,D.B., Wu,C.L., Chen,D.H., and Chou,C.H. A Nonviral Transfection Approach *in Vitro*: The Design of a Gold Nanoparticle Vector Joint with Microelectromechanical Systems. *Langmuir.* 2004 Jan; 20, 1369-1374.

Kim YK, Park IK, Jiang HL, *et al.* Regulation of transduction efficiency by pegylation of baculovirus vector *in vitro* and *in vivo*. *J Biotechnol.* 2006 Aug 20;125(1):104–109.

Kleemann E, Neu M, Jekel N, *et al.* Nano-carriers for DNA delivery to the lung based upon a TAT-derived peptide covalently coupled to PEG-PEI. *J Control Release.* 2005 Dec 5;109(1-3):299–316.

Kochanek S, Clemens PR, Mitani K, Chen HH, Chan S, Caskey CT. A new adenoviral vector: replacement of all viral coding sequences with 28 kb of DNA independently expressing both full-length dystrophin and beta-galactosidase. *Proc Natl Acad Sci U S A.* 1996 Jun 11;93(12):5731–5736.

Kost TA, Condreay JP. Recombinant baculoviruses as mammalian cell gene-delivery vectors. *Trends Biotechnol.* 2002 Apr;20(4):173–180.

Kotin RM, Siniscalco M, Samulski RJ, *et al.* Site-specific integration by adeno-associated virus. P*roc Natl Acad Sci U S A.* 1990;87:2211–2215.

Krupp H. Particle adhesion, theory and experiment. *H Adv Colloid Interface Sci.* 1967; 1:111–239.

Kumar-Singh R, Farber DB. Encapsidated adenovirus mini-chromosome-mediated delivery of genes to the retina: application to the rescue of photoreceptor degeneration. *Hum Mol Genet.* 1998 Nov;7(12):1893–1900.

Ladewig,K., Xu,Z.P., and Lu,G.Q. Layered double hydroxide nanoparticles in gene and drug delivery. *Expert Opinion on Drug Delivery.* 2009 Sep; 6, 907-922.

Lambert RC, Maulet Y, Dupont JL, Mykita S, Craig P, Volsen S, Feltz A. Polyethylenimine-mediated DNA transfection of peripheral and central neurons in primary culture: probing Ca2+ channel structure and function with antisense oligonucleotides. *Mol Cell Neurosci.* 1996 Mar;7(3):239–246.

Lehtolainen P, Tyynelä K, Kannasto J, Airenne KJ, Ylä-Herttuala S. Baculoviruses exhibit restricted cell type specificity in rat brain: a comparison of baculovirus- and adenovirus-mediated intracerebral gene transfer *in vivo*. *Gene Ther.* 2002 Dec;9(24):1693–1699.

Lewin M, Carlesso N, Tung CH, Tang XW, Cory D, Scadden DT, Weissleder R. Tat peptide-derivatized magnetic nanoparticles allow *in vivo* tracking and recovery of progenitor cells. *Nat Biotechnol*. 2000 Apr;18(4):410–414.

Li Y, Wang X, Guo H, Wang S. Axonal transport of recombinant baculovirus vectors. *Mol Ther.* 2004 Dec;10(6):1121–1129.

Li Y, Yang Y, Wang S. Neuronal gene transfer by baculovirus-derived vectors accommodating a neurone-specific promoter. *Exp Physiol*. 2005 Jan;90(1):39–44.

Liao IC, Wan AC, Yim EK, Leong KW. Controlled release from fibers of polyelectrolyte complexes. *J Control Release.* 2005 May 18;104(2):347–358.

Lieber A, He CY, Kay MA. Adenoviral preterminal protein stabilizes mini-adenoviral genomes *in vitro* and *in vivo*. *Nat Biotechnol.* 1997 Dec;15(13):1383–1387.

Lo SL, Wang S. An endosomolytic Tat peptide produced by incorporation of histidine and cysteine residues as a non-viral vector for DNA transfection. *Biomaterials.* 2008 May;29(15):2408–2414.

Lu W, Wang J, Zhang Q, She Z, Jiang X. Aclarubicin-loaded cationic albumin-conjugated pegylated nanoparticle for glioma chemotherapy in rats. *Int J Cancer.* 2007 Jan 15;120(2):420–431.

Lungwitz U, Breunig M, Blunk T, Göpferich A. Polyethylenimine-based non-viral gene delivery systems. *Eur J Pharm Biopharm.* 2005 Jul;60(2):247–266.

Lusky M, Christ M, Rittner K, *et al. In vitro* and *in vivo* biology of recombinant adenovirus vectors with E1, E1/E2A, or E1/E4 deleted. *J Virol.* 1998 Mar;72(3):2022–2032.

Maboudian R, Howe RT. Critical review: adhesion in surface micromechanical structures. *J Vac Sci Technol.* 1997 Jan;15(1):1–20.

Martin B, Sainlos M, Aissaoui A, *et al.* The design of cationic lipids for gene delivery. *Curr Pharm Des.* 2005;11:375–394.

Mathei C, Van Damme P, Meheus A. Hepatitis B vaccine administration: comparison between jet-gun and syringe and needle. *Vaccine.* 1997;15:402–404.

McBain SC, Yiu HH, Dobson J. Magnetic nanoparticles for gene and drug delivery. *Int J Nanomedicine.* 2008;3:169–180.

Menei P, Boisdron-Celle M, Croué A, Guy G, Benoit J. Effect of stereotactic implantation of biodegradable 5-fluorouracil-loaded microspheres in healthy and C6 glioma-bearing rats. *Neurosurgery.* 1996 Jul;39(1):117–123.

Merrihew RV, Clay WC, Condreay JP, Witherspoon SM, Dallas WS, Kost TA. Chromosomal integration of transduced recombinant baculovirus DNA in mammalian cells. *J Virol.* 2001;75:903–909.

Merrihew RV, Kost TA, Condreay JP. Baculovirus-mediated gene delivery into mammalian cells. *Methods Mol Biol.* 2004;246:355–365.

Moolten FL. Tumor chemosensitivity conferred by inserted herpes thymidine kinase genes: paradigm for a prospective cancer control strategy. *Cancer Res.* 1986;46: 5276–5281.

Morgan PW, Kwolek SL. The nylon rope trick: demonstration of condensation polymerization. *J Chem Ed.* 1959;36:182.

Morsy MA, Gu M, Motzel S, *et al.* An adenoviral vector deleted for all viral coding sequences results in enhanced safety and extended expression of a leptin transgene. *Proc Natl Acad Sci U S A.* 1998;95:7866–7871.

Mountain A. Gene therapy: the first decade. *Trends Biotechnol.* 2000;18:119–128.

Mulligan RC. The basic science of gene therapy. *Science.* 1993;260:926–932.

Muzyczka N. Use of adeno-associated virus as a general transduction vector for mammalian cells. *Curr Top Microbiol Immunol.* 1992;158:97–129.

Mykhaylyk O, Antequera YS, Vlaskou D, Plank C. Generation of magnetic non-viral gene transfer agents and magnetofection *in vitro*. *Nat Protocols.* 2007;2:2391–2411.

Naldini L, Blomer U, Gallay P, *et al. In vivo* gene delivery and stable transduction of nondividing cells by a lentiviral vector. *Science.* 1996;272:263–267.

Nguyen J, Xie X, Dumitrascu R, *et al.* Effects of cell-penetrating peptides and pegylation on transfection efficiency of polyethylenimine in mouse lungs. *J Gene Med.* 2008;10:1236–1246.

Ohgaki H, Dessen P, Jourde B, *et al.* Genetic pathways to glioblastoma: a population-based study. *Cancer Res.* 2004;64:6892–6899.

Ohgaki HP, Kleihues PM. Population-based studies on incidence, survival rates, and genetic alterations in astrocytic and oligodendroglial gliomas. *J Neuropathol Exp Neurol.* 2005 Jun;64(6):479–489. Review.

Papapostolou D, Smith AM, Atkins EDT, Oliver SJ, Ryadnov MG, Serpell LC, Woolfson DN. Engineering nanoscale order into a designed protein fiber. *Proc Natl Acad Sci U S A.* 2007;104:10853–10858.

Payne GF. Biopolymer-based materials: the nanoscale components and their hierarchical assembly. *Curr Opin Chem Biol.* 2007;11:214–219.

Plank C, Anton M, Rudolph C, Rosenecker J, Krotz F. Enhancing and targeting nucleic acid delivery by magnetic force. *Expert Opin Biol Ther.* 2003;3:745–758.

Rabinowtz JE, Samulski J. Adeno-associated virus expression system for gene transfer. *Curr Opin Biotechnol.* 1998;9(5):470–475.

Rakotondradany F, Palmer A, Toader V, Chen B, Whitehead MA, Sleiman HF. Hydrogen-bond self-assembly of DNA-analogues into hexameric rosettes. *Chem Commun.* 2005 Nov 21;43;5441–5443.

Ranganath SH, Wang CH. Biodegradable microfiber implants delivering paclitaxel for post-surgical chemotherapy against malignant glioma. *Biomaterials.* 2008;29:2996–3003.

Raper SE, Chirmule N, Lee FS, *et al.* Fatal systemic inflammatory response syndrome in a ornithine transcarbamylase deficient patient following adenoviral gene transfer. *Mol Gen Metab.* 2003;80:148–158.

Russell SJ. Science, medicine, and the future: gene therapy. *BMJ.* 1997;315:1289–1292.

Sandig V, Hofmann C, Steinert S, Jennings G, Schlag P, Strauss M. Gene transfer into hepatocytes and human liver tissue by baculovirus vectors. *Hum Gene Ther.* 1996;7:1937–1945.

Sarkar S, Lee GY, Wong JY, Desai TA. Development and characterization of a porous micro-patterned scaffold for vascular tissue engineering applications. *Biomaterials.* 2006;27:4775–4782.

Sarkis C, Serguera C, Petres S, Buchet D, Ridet JL, Edelman L, Mallet J. Efficient transduction of neural cells *in vitro* and *in vivo* by a baculovirus-derived vector. *Proc Natl Acad Sci U S A.* 2000;97:14638–14643.

Schiedner G, Morral N, Parks RJ, *et al.* Genomic DNA transfer with a high-capacity adenovirus vector results in improved *in vivo* gene expression and decreased toxicity. *Nat Genet.* 1998;18:180–183.

Shi L, Tang GP, Gao SJ, *et al.* Repeated intrathecal administration of plasmid DNA complexed with polyethylene glycol-grafted polyethylenimine led to prolonged transgene expression in the spinal cord. *Gene Ther.* 2003;10:1179–1188.

Sodeik B, Ebersold MW, Helenius A. Microtubule-mediated transport of incoming herpes simplex virus 1 capsids to the nucleus. *J Cell Biol*. 1997;136:1007–1021.

Tacket CO, Roy MJ, Widera G, Swain WF, Broome S, Edelman R. Phase 1 safety and immune response studies of a DNA vaccine encoding hepatitis B surface antigen delivered by a gene delivery device. *Vaccine.* 1999;17:2826–2829.

Tu RS, Tirrell M. Bottom-up design of biomimetic assemblies. *Adv Drug Del Rev.* 2004;56:1537–1563.

T.Welzel, I.Radtke, W.Meyer-Zaika, R.Heumann, M.Epple. Transfection of cells with custom-made calcium phosphate nanoparticles coated with DNA. *J. Mater. Chem.* 2004;14,2213-2217.

van den Beucken JJ, Vos MR, Thüne PC, *et al.* Fabrication, characterization, and biological assessment of multilayered DNA-coatings for biomaterial purposes. *Biomaterials.* 2006;27:691–701.

VandenDriessche T, Collen D, Chuah MK. Biosafety of onco-retroviral vectors. *Curr Gene Ther.* 2003;3:501–515.

van Loo ND, Fortunati E, Ehlert E, Rabelink M, Grosveld F, Scholte BJ. Baculovirus infection of nondividing mammalian cells: mechanisms of entry and nuclear transport of capsids. *J Virol.* 2001;75:961–970.

Verma IM, Somia N. Gene therapy—promises, problems and prospects. *Nature.* 1997;389:239–242.

Wadia JS, Stan RV, Dowdy SF. Transducible TAT-HA fusogenic peptide enhances escape of TAT-fusion proteins after lipid raft macropinocytosis. *Nat Med.* 2004;10:310–315.

Walther W, Stein U. Viral vectors for gene transfer: a review of their use in the treatment of human diseases. *Drugs.* 2000;60:249–271.

Wan AC, Liao I-C, Yim EK, Leong KW. Mechanism of fiber formation by interfacial polyelectrolyte complexation. *Macromol.* 2004a;37:7019–7025.

Wan AC, Yim EK, Liao IC, Le Visage C, Leong KW. Encapsulation of biologics in self-assembled fibers as biostructural units for tissue engineering. *J Biomed Mater Res A*. 2004b;71A:586–595.

Wang CY, Guo HY, Lim TM, *et al.* Improved neuronal transgene expression from an AAV-2 vector with a hybrid CMV enhancer/PDGF-beta promoter. *J Gene Med.* 2005a;7:945–955.

Wang CY, Li F, Yang Y, Guo HY, Wu CX, Wang S. Recombinant baculovirus containing the diphtheria toxin A gene for malignant glioma therapy. *Cancer Res.* 2006a;66:5798–5806.

Wang CY, Wang S. Astrocytic expression of transgene in the rat brain mediated by baculovirus vectors containing an astrocyte-specific promoter. *Gene Ther.* 2006b;13:1447–1456.

Wang X, Wang C, Zeng J, *et al.* Gene transfer to dorsal root ganglia by intrathecal injection: effects on regeneration of peripheral nerves. *Mol Ther.* 2005b;12:314–320.

Weitzman MD, Kyostio SR, Kotin RM, Owens RA. Adeno-associated virus (AAV) Rep proteins mediate complex formation between AAV DNA and its integration site in human DNA. *Proc Natl Acad Sci U S A.* 1994;91:5808–5812.

Xenariou S, Griesenbach U, Ferrari S, *et al.* Using magnetic forces to enhance non-viral gene transfer to airway epithelium *in vivo*. *Gene Ther*. 2006;13:1545–1552.

Xiao X, Li J, McCown TJ, Samulski RJ. Gene transfer by adeno-associated virus vectors into the central nervous system. *Exp Neurol.* 1997;144:113–124.

Yang CC, Xiao X, Zhu X, *et al.* Cellular recombination pathways and viral terminal repeat hairpin structures are sufficient for adeno-associated virus integration *in vivo* and *in vitro*. *J Virol.* 1997;71:9231–9247.

Yang Y, Lo SL, Yang J, *et al.* Polyethylenimine coating to produce serum-resistant baculoviral vectors for *in vivo* gene delivery. *Biomaterials.* 2009;30:5767–5774.

Yang Y, Nunes FA, Berencsi K, Furth EE, Gonczol E, Wilson JM. Cellular immunity to viral antigens limits E1-deleted adenoviruses for gene therapy. *Proc Natl Acad Sci U S A.* 1994;91:4407–4411.

Yim EK, Wan AC, Le Visage C, Liao IC, Leong KW. Proliferation and differentiation of human mesenchymal stem cell encapsulated in polyelectrolyte complexation fibrous scaffold. *Biomaterials*. 2006;27:6111–6122.

Zeng J, Du J, Zhao Y, Palanisamy N, Wang S. Baculoviral vector-mediated transient and stable transgene expression in human embryonic stem cells. *Stem Cells.* 2007a;25:1055–1061.

Zeng J, Wang X, Wang S. Self-assembled ternary complexes of plasmid DNA, low molecular weight polyethylenimine and targeting peptide for non-viral gene delivery into neurons. *Biomaterials.* 2007b;28:1443–1451.

Zhang S. Fabrication of novel biomaterials through molecular self-assembly. *Nat Biotech.* 2003;21:1171–1178.